

## ABSTRACT

Title of Thesis: DEVELOPMENT OF HIGH TEMPERATURE (3400°F) AND HIGH PRESSURE (27,000 PSI) GAS VENTING PROCESS FOR NITROGEN BATCH HEATER

Parth Navinchandra Kathrotiya,  
Master of Science in Mechanical Engineering,  
2017

Thesis Directed By: Professor Ashwani K. Gupta,  
Department of Mechanical Engineering

This thesis discusses a venting process for nitrogen gas heated up to 3,400°F and 27,000 psi. Nitrogen at similar temperatures and pressures have successfully been vented in hot isostatic pressing (HIP) manufacturing processes, but to date no further applications are known for Heater Vessels used in hypersonic wind tunnels. The thesis first focuses on the instrumentation and experimental setup to test venting nitrogen gas up to 1550°F and 22,000 psi and to measure thermal stratification in the Heater Vessel. The results of the experiment show the current Heater Vessel is capable of venting nitrogen gas up to 1550°F and 22,000 psi by instrumenting critical locations and leveraging passive cooling. The thesis then focuses on using data from the experiment to design a system that is capable of venting nitrogen gas heated up to 3,400°F and 27,000 psi through the bottom closure of the Heater Vessel.

DEVELOPMENT OF HIGH TEMPERATURE (3,400°F) AND HIGH PRESSURE  
(27,000 PSI) GAS VENTING PROCESS FOR NITROGEN BATCH HEATER

by

Parth Navinchandra Kathrotiya

Thesis submitted to the Faculty of the Graduate School of the  
University of Maryland, College Park, in partial fulfillment  
of the requirements for the degree of  
Master of Science  
2017

Advisory Committee:  
Professor Ashwani K. Gupta, Chair  
Professor Gary A. Pertmer  
Professor Bao Yang

Department of Defense  
United States Air Force – Arnold Engineering Development Complex  
Distribution Statement A. Approved for public release; distribution is unlimited.  
PA # AEDC 2017-067

## Dedication

This thesis is dedicated to my parents, and sister for their love and support.

To my late grandfather, for inspiring me to become an engineer.

## Acknowledgements

I would like to thank my advisor Professor Ashwani K. Gupta for his support during my studies and research at University of Maryland. Also I would like to thank the rest of my thesis committee; Professor Gary A. Pertmer, and Professor Bao Yang for their time and patience.

My sincere thanks also goes to Daniel Marren, John Lafferty, Nicholas Fredrick, Jeffery Waldo, Michael Metzger, and the rest of the team at Arnold Engineering Development Complex Hypervelocity Wind Tunnel No. 9, who provided me an opportunity to join their team as undergraduate researcher and funded this research as a graduate researcher.

This work is funded through contract # FA9101-10-D-0001-0010 at Arnold Engineering Development Complex Hypervelocity Wind Tunnel No. 9 in White Oak, Maryland. All images used with permission from Arnold Engineering Development Complex Hypervelocity Wind Tunnel No. 9.

## Table of Contents

DEDICATION .....	II
ACKNOWLEDGEMENTS .....	III
TABLE OF CONTENTS.....	IV
LIST OF TABLES .....	VI
LIST OF FIGURES .....	VII
LIST OF ABBREVIATIONS.....	X
CHAPTER 1: INTRODUCTION .....	1
1.1: Background on AEDC Hypervelocity Wind Tunnel No. 9 .....	1
1.2: Statement of the Problem.....	4
CHAPTER 2: LITERATURE REVIEW .....	5
2.1: Introduction & Search Description .....	5
2.2: Hot Isostatic Pressing (HIP) .....	5
CHAPTER 3: HEATER VENTING TEST .....	7
3.1: Introduction and Research Question.....	7
3.2: Test Setup and Plan.....	7
3.3: Data Analysis .....	12
3.4: Conclusion .....	16
CHAPTER 4: HEATER THERMAL STRATIFICATION TEST .....	17
4.1: Introduction and Research Question.....	17
4.2: Test Setup and Plan.....	18
4.3: Thermocouple Rig Design .....	19
4.4: Data Analysis .....	23
4.5: Conclusion .....	27
CHAPTER 5: DESIGN OF VENTING SYSTEM.....	28
5.1: Introduction.....	28
5.2: Design .....	29
5.3: Thermal Analysis & Results .....	37
5.4: Structural Analyses & Results – Closure Plug .....	49
5.5: Structural Analyses & Results – Seal Head.....	77
5.6: Summary .....	91
CHAPTER 6: CONCLUSIONS, AND FUTURE RESEARCH .....	92
6.1: Summary of Findings.....	92
6.2: Conclusions.....	92
6.3: Research Contributions.....	93
6.4: Suggestions for Future Research .....	94
APPENDICES .....	96
A.1: Stand Pipe Mixing Calculations.....	96
A.2: Additional Views of Design.....	98
A.3: Material Properties.....	100
A.4: Choked Flow Equation and Heat Transfer Correlations.....	108
A.5: Gas Heating Convective Heat Transfer Coefficient Calculation .....	109
A.6: Water Cooling Convective Heat Transfer Coefficient Calculation .....	111
A.7: Static Structural – Closure Plug Boundary Conditions.....	112

BIBLIOGRAPHY..... 114

## List of Tables

Table 3.1: Heater Venting Test Conditions .....	9
Table 3.2: Thermocouple Replacements for Heater Venting Test .....	10
Table 3.3: Thermocouple Abort Limits for Heater Venting Test .....	12
Table 4.1: Heater Thermal Stratification Test Conditions.....	18
Table 4.2: Thermocouple Replacements for Heater Thermal Stratification Test.....	19
Table 4.3: Thermocouple Abort Limits for Heater Thermal Stratification Test.....	19
Table 5.1: Structural Analyses Setup Summary – Closure Plug .....	51
Table 5.2: Structural Analyses Setup Summary – Seal Head.....	77
Table A.1: Stand Pipe Mixing Calculation based on Temperature .....	96
Table A.2: Stand Pipe Mixing Calculation based on Density .....	97
Table A.3: AISI 4340 Alloy Steel – Material Properties.....	100
Table A.4: C-103 Niobium – Material Properties .....	101
Table A.5: Glidcop AL-60 (UNS C15760) – Material Properties.....	102
Table A.6: Inconel 625 – Material Properties.....	104
Table A.7: Inconel 718 – Material Properties.....	106
Table A.8: Nitrogen (Thermal Conductivity) – Material Properties .....	107
Table A.9: Choked Flow Equation and Heat Transfer Correlations.....	108
Table A.10: Gas Heating Convective Heat Transfer Coefficient Calculation.....	110
Table A.11: Water Cooling Convective Heat Transfer Coefficient Calculation .....	111
Table A.12: Blow-Off Force and Elastic Foundation Stiffness Calculation .....	112
Table A.13: Seal Head Bearing Pressure Calculation .....	113



## List of Figures

Figure 1.1: Hypervelocity Wind Tunnel No. 9 Facility Layout .....	2
Figure 1.2: Hypervelocity Wind Tunnel No. 9 Heater Vessel.....	3
Figure 1.3: Broken Test Cell Window .....	4
Figure 3.1: Heater Vessel Vent Path for Heater Venting Test.....	8
Figure 3.2: Nominal Heater Vessel Thermocouples.....	9
Figure 3.3: Special Thermocouples for Heater Venting Test .....	11
Figure 3.4: Vent of Heater Vessel at Mach 10 Condition (22,000 psi & 1550°F) .....	14
Figure 3.5: Temperature Melting Paint before Test Program.....	15
Figure 3.6: Temperature Melting Paint after Test Program.....	15
Figure 3.7: Thermocouple Gamma ( $\gamma$ ) added as Nominal Thermocouple for Mach 10 Main Can Package .....	16
Figure 4.1: Unknown Gas Temperature Region in Heater Vessel.....	17
Figure 4.2: Thermocouple Rig CAD Model .....	21
Figure 4.3: Thermocouple Rig Built and Wrapped with Nextel Insulation.....	22
Figure 4.4: Run 3 – Vent of Heater Vessel for Thermal Stratification Test at 14,500 psi & 750°F .....	24
Figure 4.5: Run 4 – Vent of Heater Vessel for Thermal Stratification Test at 4,750 psi & 750°F.....	25
Figure 4.6: Run 5 – Vent of Heater Vessel for Thermal Stratification Test at 10,500 psi & 750°F .....	26
Figure 4.7: Realistic Thermal Stratification in Heater Vessel .....	27
Figure 5.1: Bottom Closure Plug in Heater Vessel.....	28
Figure 5.2: Closure Plug Cross-Sectional View .....	29
Figure 5.3: Modified Closure Plug .....	30
Figure 5.4: Modified Closure Plug with Stand Pipe, Seal Head & Commercial Piping .....	31
Figure 5.5: Gas Mixing Process.....	33
Figure 5.6: Bottom View of Closure Plug with Cooling System Setup .....	34
Figure 5.7: Cross-Sectional View of Cooling Ports.....	35
Figure 5.8: Cooling Water Flow Path.....	36
Figure 5.9: Boundary Conditions Cross-Sectional View – Steady-State Thermal.....	41
Figure 5.10: Assembly Temperature Results – Steady-State Thermal .....	42
Figure 5.11: Close-Up View of Assembly Temperature Results – Steady-State Thermal .....	43
Figure 5.12: Closure Plug Temperature Results – Steady-State Thermal .....	44
Figure 5.13: Vent Port in Closure Plug Temperature Results – Steady-State Thermal .....	45
Figure 5.14: Corrosion Barriers & Closure Plug Temperature Results Cross-Sectional View – Steady-State Thermal .....	46
Figure 5.15: Corrosion Barriers in Cooling Port Temperature Results Cross-Sectional View – Steady-State Thermal .....	47
Figure 5.16: Seal Head Temperature Results – Steady-State Thermal.....	48
Figure 5.17: Closure Plug – Boundary Condition Simplifications .....	50

Figure 5.18: Current Closure Plug at 80°F (Case 1) – Blow Off Force & Elastic Support (B.C.s) – Static Structural .....	54
Figure 5.19: Current Closure Plug at 80°F (Case 1) – Gas Pressure (B.C.) – Static Structural.....	55
Figure 5.20: Current Closure Plug at 80°F (Case 1) – Seal Ring Bearing Pressure (B.C.) – Static Structural.....	56
Figure 5.21: Current Closure Plug at 80°F (Case 1) – von-Mises Stress – Static Structural.....	57
Figure 5.22: Current Closure Plug at 80°F (Case 1) Fillet Area View – von-Mises Stress – Static Structural .....	58
Figure 5.23: Current Closure Plug at 80°F (Case 1) – Safety Factor – Static Structural .....	59
Figure 5.24: Current Closure Plug at 80°F (Case 1) Fillet Area View – Safety Factor – Static Structural.....	60
Figure 5.25: Modified Closure Plug (Case 2 & Case 3) – Blow Off Force & Elastic Support (B.C.s) – Static Structural .....	61
Figure 5.26: Modified Closure Plug (Case 2 & Case 3) – Gas Pressure (B.C.) – Static Structural.....	62
Figure 5.27: Modified Closure Plug (Case 2 & Case 3) – Seal Ring Bearing Pressure (B.C.) – Static Structural.....	63
Figure 5.28: Modified Closure Plug (Case 2 & Case 3) – Seal Head Bearing Pressure (B.C.) – Static Structural.....	64
Figure 5.29: Modified Closure Plug (Case 2 & Case 3) – Water Pressure (B.C.) – Static Structural.....	65
Figure 5.30: Modified Closure Plug with Thermal Load (Case 2) – Body Temp. (Imported S.S. Thermal) (B.C.) – Static Structural .....	66
Figure 5.31: Modified Closure Plug with Thermal Load (Case 2) – von-Mises Stress – Static Structural.....	67
Figure 5.32: Modified Closure Plug with Thermal Load (Case 2) Fillet Area View – von-Mises Stress – Static Structural .....	68
Figure 5.33: Modified Closure Plug with Thermal Load (Case 2) – Safety Factor – Static Structural.....	69
Figure 5.34: Modified Closure Plug with Thermal Load (Case 2) Fillet Area View – Safety Factor – Static Structural .....	70
Figure 5.35: Modified Closure Plug with Thermal Load (Case 2) Vent Port View – Safety Factor at 250°F – Static Structural .....	71
Figure 5.36: Modified Closure Plug with Thermal Load (Case 2) Cooling Port Cross Sect. View – Safety Factor – Static Structural.....	72
Figure 5.37: Modified Closure Plug with Thermal Load (Case 2) – Corrosion Barriers – Safety Factor – Static Structural .....	73
Figure 5.38: Modified Closure Plug at 80°F (Case 3) – Safety Factor – Static Structural.....	74
Figure 5.39: Modified Closure Plug at 80°F (Case 3) Fillet Area View – Safety Factor – Static Structural.....	75
Figure 5.40: Closure Plug Comparison – Safety Factor – Static Structural .....	76

Figure 5.41: Seal Head (Case 1 & Case 2) – Frictionless Support - Seal Head Bearing Pressure (B.C.) – Static Structural .....	79
Figure 5.42: Seal Head (Case 1 & Case 2) – Atmospheric Pressure (B.C.) – Static Structural.....	80
Figure 5.43: Seal Head (Case 1 & Case 2) – Gas Pressure (B.C.) – Static Structural	81
Figure 5.44: Seal Head with Thermal Load (Case 1) – Body Temperature (Imported S.S. Thermal) (B.C.) – Static Structural .....	82
Figure 5.45: Seal Head with Thermal Load (Case 1) – von-Mises Stress – Static Structural.....	83
Figure 5.46: Seal Head with Thermal Load (Case 1) – Minimum Principal Stress – Static Structural.....	84
Figure 5.47: Seal Head with Thermal Load (Case 1) – Maximum Principal Stress – Static Structural.....	85
Figure 5.48: Seal Head with Thermal Load (Case 1) – Safety Factor – Static Structural.....	86
Figure 5.49: Seal Head with Thermal Load (Case 1) – Safety Factor at 1200°F – Static Structural.....	87
Figure 5.50: Seal Head at 80°F (Case 2) – von-Mises Stress – Static Structural .....	88
Figure 5.51: Seal Head at 80°F (Case 2) – Safety Factor – Static Structural .....	89
Figure 5.52: Seal Head at 80°F (Case 2) O-Ring Groove – Safety Factor – Static Structural.....	90
Figure A.1: Close-Up of Modified Clouse Plug with Stand Pipe, Seal Head, and Hold Down Plates .....	98
Figure A.2: View of Modified Clouse Plug from Outside of Spool.....	98
Figure A.3: Top View of Modified Clouse Plug with Stand Pipe and Seal Head.....	99
Figure A.4: Seal Head Bearing Pressure Diagram.....	113

## List of Abbreviations

AEDC	Arnold Engineering Development Complex
CAD	Computer Aided Design
HIP	Hot Isostatic Pressing
T/C	Thermocouple
Tunnel 9	Hypervelocity Wind Tunnel No. 9

## Chapter 1: Introduction

### 1.1: Background on AEDC Hypervelocity Wind Tunnel No. 9

Hypervelocity Wind Tunnel No. 9 (Tunnel 9) is located in White Oak, Maryland and is part of Arnold Engineering Development Complex (AEDC). It is a unique world class ground-test facility with a blowdown capability that uses gaseous nitrogen as the working fluid and operates at Mach numbers of 7, 8, 10, and 14.

Tunnel 9 is used for hypersonic ground testing and the validation of computational fluid dynamics (CFD) simulations [1]. Figure 1.1 has an overview of Hypervelocity Wind Tunnel No. 9.

Tunnel 9 has a unique batch Heater Vessel, which can heat nitrogen gas up to 3,400°F and 27,000 psi. The Tunnel 9 nitrogen flow path is shown in Fig. 1.2. The Heater is charged with an initial amount of nitrogen, which is then heated by a graphite Heating Element using Joule heating. The nitrogen is heated to the desired temperature and pressure needed to create the test condition downstream in the Test Cell. The Test Cell and Vacuum Sphere are also pulled down to a vacuum condition. Two diaphragm plates are ruptured allowing the gas to leave the Heater Vessel. Driver Vessels push the gas through the Heater Vessel to the Test Cell to maintain a constant a hypersonic test condition in the Test Cell. Currently there is only one safe pathway for high temperature gas to exit the Heater Vessel, shown in Fig. 1.2. It also shows the temperature of the gas in the high pressure environment.

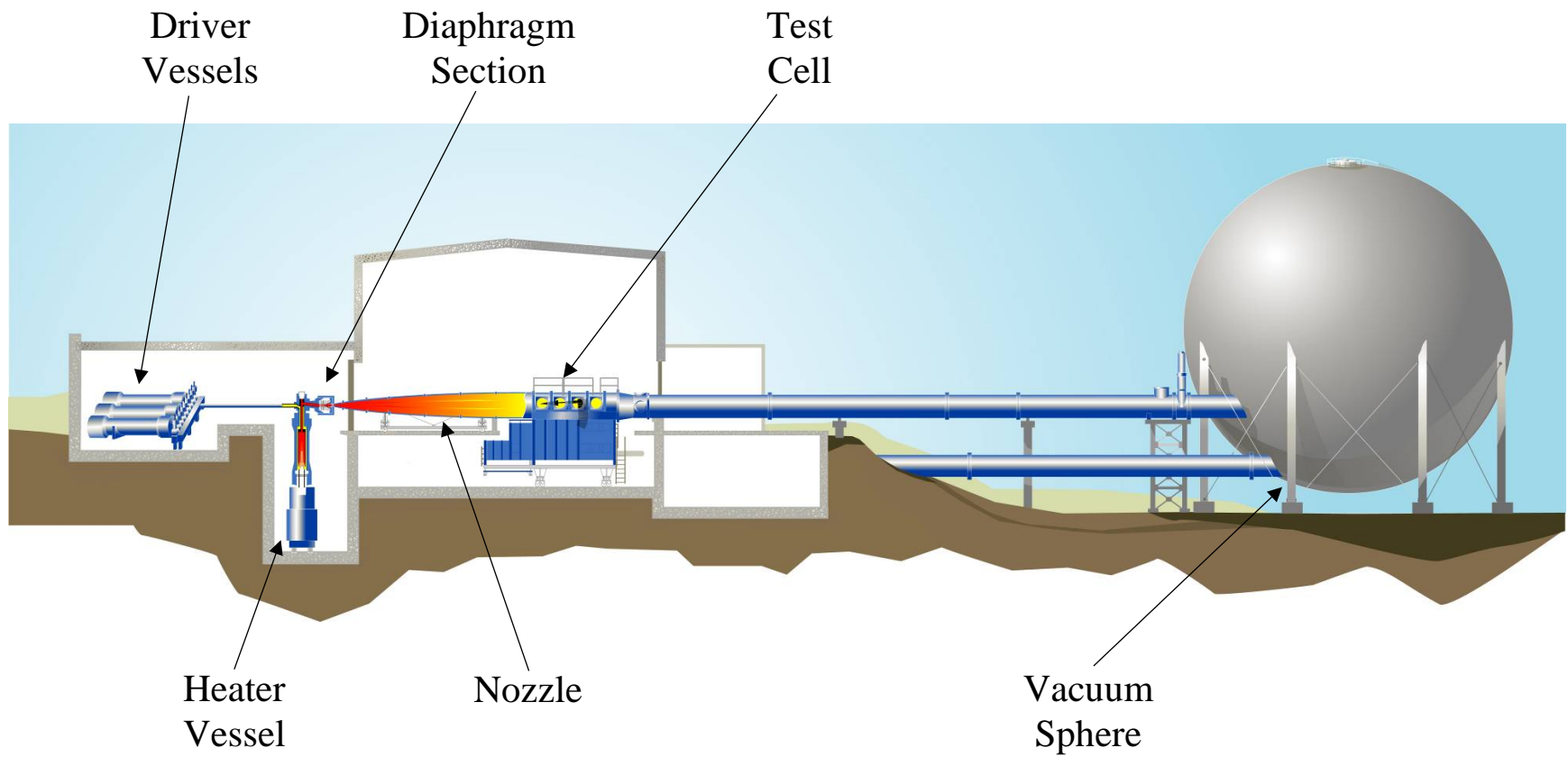


*Figure 1.1: Hypervelocity Wind Tunnel No. 9 Facility Layout*

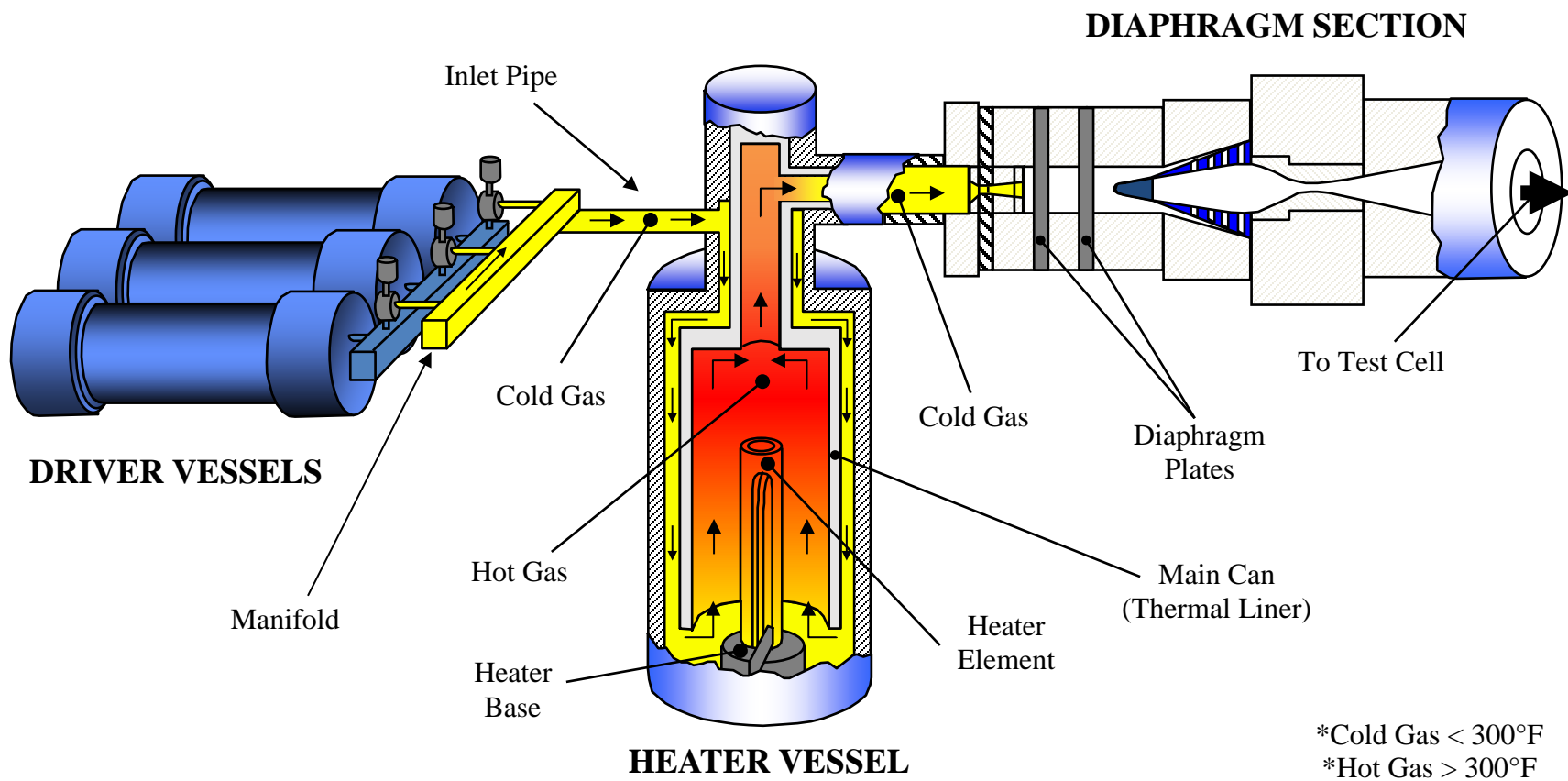


Figure 1.2: Hypervelocity Wind Tunnel No. 9 Heater Vessel

## 1.2: Statement of the Problem

The Heater Vessel has only one outlet for hot gas, which can pose a dangerous situation. During the heating phase there could be an unplanned event such as a broken Test Cell window or a vacuum leak in the Test Cell and vacuum piping. These conditions could lead to a situation where the high temperature and high pressure gas cannot be safely expelled from the Heater and has to be held. Figure 1.3 shows a broken Test Cell window, which happened prior to heating the gas in the Heater Vessel. Another situation that could occur is if debris becomes stuck in the Diaphragm Section leading to a blockage, trapping the high temperature and high pressure gas in the Heater Vessel. Either one of these situations can lead to loss of multi-million dollar systems in Tunnel 9. This has created a need to design an alternate hot gas vent path out of the Heater Vessel to vent nitrogen gas up to 3,400°F and 27,000 psi to reduce risk associated with testing in Tunnel 9.



*Figure 1.3: Broken Test Cell Window*



## Chapter 2: Literature Review

### 2.1: Introduction & Search Description

The need to vent large volumes of high temperature and high pressure gas is unique to a small number of industries. The search for high temperature and high pressure piping and valves for batch heater venting was limited. Industries that use high pressure valves and piping, but they do not subject these materials to the high temperature that are experienced at Tunnel 9. There are also industries that subject the materials to the high temperature but not to such high pressures. The one industry with similar requirements was the hot isostatic pressing (HIP) industry, which has pressure vessels that operate at similar temperatures and pressures.

### 2.2: Hot Isostatic Pressing (HIP)

Hot isostatic pressing vessels are similar in volume, pressure, and temperature as the Tunnel 9 Heater Vessel. One HIP vessel used for densifying boron carbide (B<sub>4</sub>C) has an operating temperature of 3,632°F and an operating pressure of 29,007.5 psi [2], compared to the Tunnel 9 Heater Vessel which operates at 3,400°F and 27,000 psi. The Tunnel 9 Heater Vessel uses nitrogen, while the hot isostatic pressing vessels use nitrogen as well as argon. HIP vessels operate differently from the Tunnel 9 Heater Vessel. They use the vessel to densify powders or cast and sintered parts which removes voids and pores to improve material properties. HIP vessels require more uniform thermal conditions for manufacturing processes, so the densified part has uniform material properties. To retrieve the parts after the HIP process, the vessels must be vented after each usage. HIP vessels are equipped with vent lines

through the bottom closure plug that leverage the stratification of gas temperature inside the vessel to vent low temperature gas first. This allows the remaining gas in the vessel to expand, which cools down and can be vented. HIP vessels also have the ability add cooling gas to lower the bulk temperature of the gas. The HIP venting process provides a great starting point for a test to better understand the Tunnel 9 Heater Vessel vent capability.

## Chapter 3: Heater Venting Test

### 3.1: Introduction and Research Question

The Tunnel 9 standard operating procedures allow venting gas heated to temperatures as high as 750°F from the Heater Vessel through the inlet pipe to a piping system that vents to atmosphere through the roof. The maximum temperature limit is based on the temperature reading in the hot gas region of the Heater Vessel. There is not maximum limit on the gas pressure. The Tunnel 9 vent procedure is based on the maximum temperature the material of the inlet pipe can reach before its metallurgical properties are permanently degraded. As shown in Fig. 1.2, the Heater Vessel has regions of gas that are much cooler than the 750°F limit. This leads to the question: What is the maximum at which hot gas can be vented through the existing back vent flow path? A test was proposed to determine this limit by installing additional instrumentation in critical locations.

### 3.2: Test Setup and Plan

Table 3.1 shows the conditions and runs for this test program. Run 5 corresponds to a full temperature, full pressure Mach 10 condition. Instead of running the tunnel, the gas was vented from the inlet pipe to give more insight into temperature of various areas of the Heater Vessel and vent path. The path used for venting through the inlet pipe is shown in Fig. 3.1. The Hot Gas thermocouples are read at the top of the Main Can and are used as the limit for venting to less than 750°F. The Heater Vessel is also instrumented with a nominal set of thermocouples, which were used for this test program and are shown in Fig. 3.2.

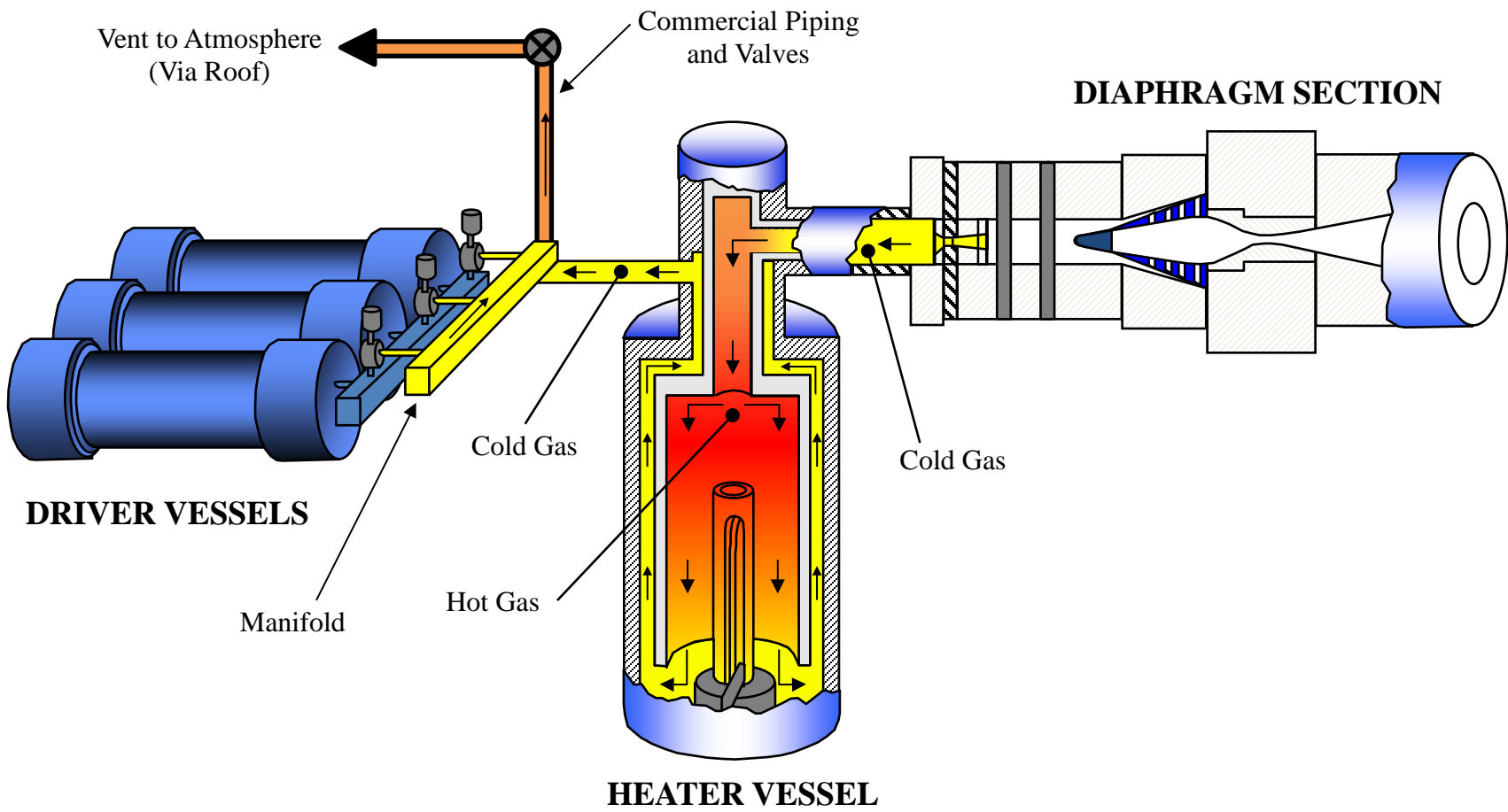


Figure 3.1: Heater Vessel Vent Path for Heater Venting Test

Run	Final Pressure (psia)	Hot Gas Temperature Limit (°F)
1	4750	750
2	14500	750
3	15500	1000
4	19000	1300
5	22000	1550

Table 3.1: Heater Venting Test Conditions

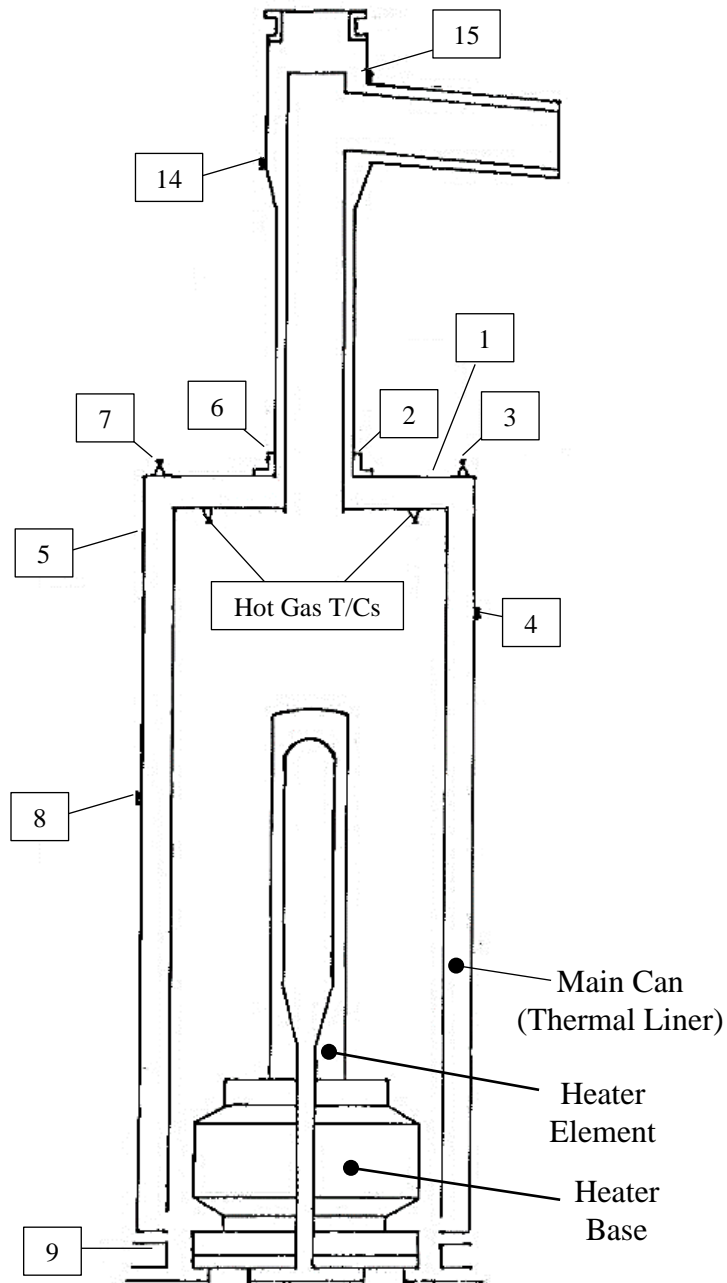


Figure 3.2: Nominal Heater Vessel Thermocouples

For this test program, the back vent flow path was instrumented with special thermocouples and temperature paints to better understand localized gas and hardware temperatures during venting. Since the heated gas will be moving past the Closure Plug, two thermocouples were added to monitor the Closure Plug’s main seal temperature, designated as thermocouples “A” and “B”. One skin temperature thermocouple was installed on the outer diameter surface of the Main Can’s support spool flange just above one of the flow windows, designated as thermocouple “Gamma” ( $\gamma$ ). Two hot gas thermocouples were installed in the flow windows of the Main Can’s support spool, designated as thermocouples “D” and “E”. Figure 3.3 shows the thermocouples A, B, Gamma ( $\gamma$ ), and E installed on the Main Can. Two additional thermocouples were used to monitor the temperature of the vent pipe to the roof designated as thermocouples “F” and “G”. To account for these additional thermocouples, some nominal thermocouples were replaced, shown in Table 3.2.

During the Heater Venting Test, data was recorded on the Tunnel 9 control system data system at a sample rate of 1 Hz. Temperature melting paints were also applied to various Heater Vessel system components in order to validate thermocouple skin temperature measurements. Each thermocouple was given a limit for each test condition, which is shown in Table 3.3. These safe limits were determined based on the material limits near the respective thermocouples.

<b>Thermocouple Designator</b>	<b>Nominal Thermocouple Replaced</b>
A (Seal 1 on Closure Plug)	3
B (Seal 2 on Closure Plug)	4
Gamma ( $\gamma$ ) (Main Can Spool)	1
D (Main Can Window – South)	9
E (Main Can Window – North)	14

*Table 3.2: Thermocouple Replacements for Heater Venting Test*

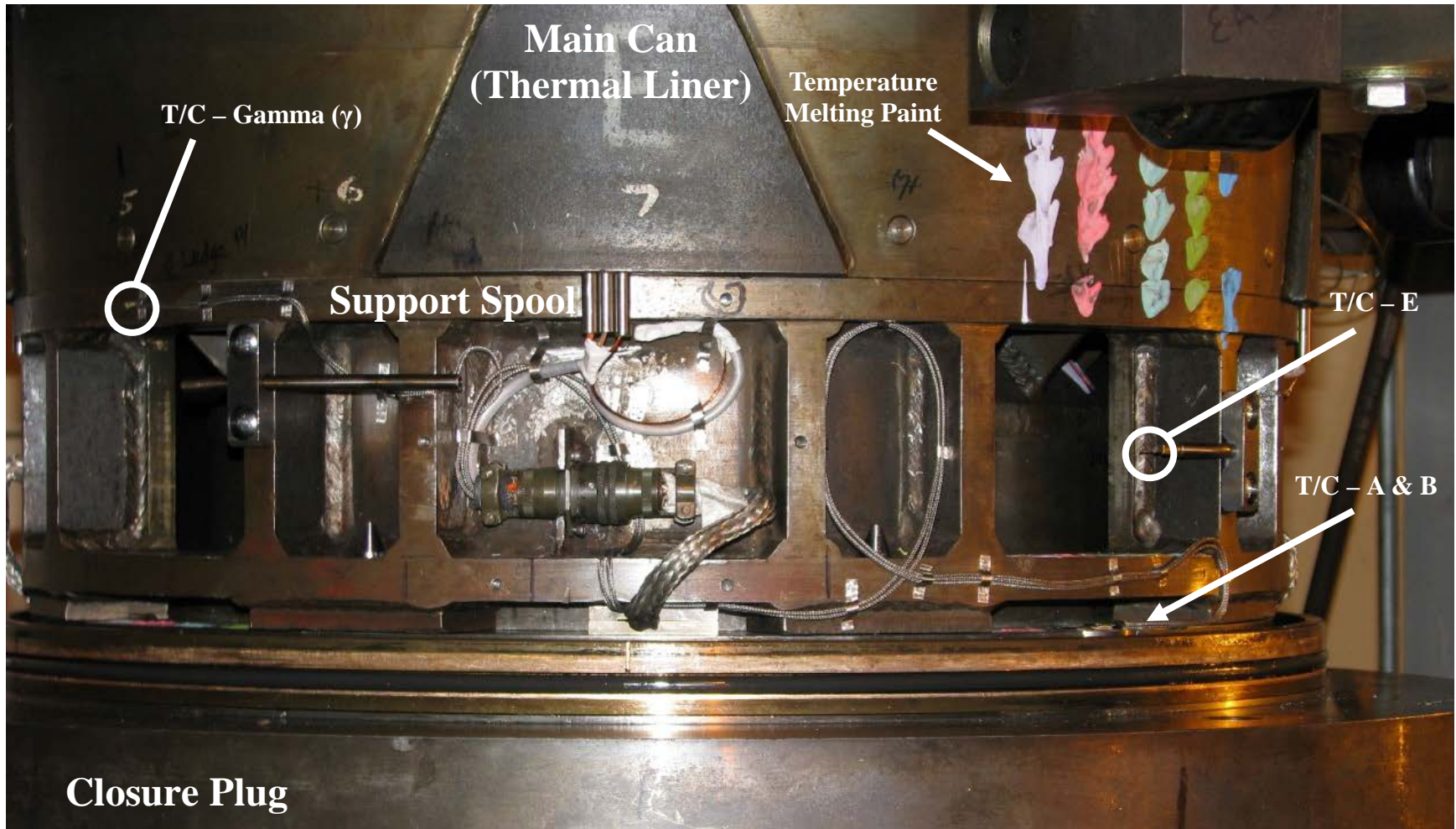


*Figure 3.3: Special Thermocouples for Heater Venting Test*

<b>Thermocouple Abort Limits for Each Test Condition</b>				
<b>Thermocouple Designator</b>	<b>Test Conditions</b>			
	<b>750°F</b>	<b>1000°F</b>	<b>1300°F</b>	<b>1550°F</b>
Hot Gas Thermocouples	750°F	1000°F	1300°F	1550°F
A (Seal 1 on Closure Plug)	300°F	300°F	300°F	300°F
B (Seal 2 on Closure Plug)	300°F	300°F	300°F	300°F
Gamma ( $\gamma$ ) (Main Can Spool)	400°F	400°F	400°F	400°F
D (Main Can Window – South)	500°F	500°F	500°F	500°F
E (Main Can Window – North)	500°F	500°F	500°F	500°F
F (Vent Pipe at Manifold)	450°F	450°F	450°F	450°F
G (Vent Pipe in Compressor Room)	300°F	300°F	300°F	300°F

*Table 3.3: Thermocouple Abort Limits for Heater Venting Test*

### 3.3: Data Analysis

Runs 1 to 4 were successful in venting the gas from the Heater Vessel by combination of venting and cooling passively. They were used to work up to venting a full Mach 10 condition for the Heater Vessel in run 5. This section discusses run 5 since it is a worst case scenario for a Mach 10 condition for the Heater Vessel. During run 5, gas was vented from the heater until one of the thermocouples reached within 50°F of the abort temperature limit. Venting was then halted and the heater vessel was allowed to cool. This was repeated until the gas was under 1000 psi at which point more venting paths could be utilized. During this run all nominal thermocouples and most special thermocouples read well below abort limits. It took about 67 minutes to vent down to 1,000 psi, which includes about 9 minutes of heating time. Figure 3.4 shows the temperature versus time of the various special thermocouples for run 5. The highest reading thermocouple was Gamma ( $\gamma$ ) (metal temperature on support spool above window), which was the only thermocouple to approach its abort temperature and limited the ability to continuously vent.



Gamma ( $\gamma$ ) peaked at 350°F (abort limit = 400°F) around 3 minutes into venting. This stopped the venting, to allow the area to passively cool down to 260°F at which time venting was resumed. Thermocouple Gamma ( $\gamma$ ) peaked at 350°F again around 5 minutes into venting, which stopped venting. In this case cooling gas was added from the compressors to cool down to 250°F at which time venting was continued. Gamma ( $\gamma$ ) peaked at 350°F again around 8 minutes into venting, which stopped venting. This time cooling gas was added from the compressors and Driver Vessels to cool down Gamma ( $\gamma$ ) to 250°F. Since the pressure is much higher in the Driver Vessels than the Heater Vessel the mass added lead to compression heating of the nitrogen in the Heater which is seen in the temperature increase in the hot gas thermocouple. Adding cooling gas from the compressor and Driver Vessels did not help cool the area down any faster than passive cooling. Gamma ( $\gamma$ ) peaked at 350°F again around 14, 18, and 25 minutes into venting, which stopped venting to allow for passive cooling down to 250°F at which time venting was resumed. Passive cooling was used without adding cooling gas for the last three stops, since the cooling gas was not directly cooling the location of Gamma ( $\gamma$ ) due to injection points of the gas.

The thermocouple data was shown to be consistent with temperature melting paint that was used near the thermocouples. The temperature melting paint applied before the test program near thermocouple Gamma ( $\gamma$ ) is shown in Fig. 3.5. This is compared to temperature melting paint near thermocouple Gamma ( $\gamma$ ) after the test program was completed, which is shown in Fig. 3.6. It clearly shows that the area remained under the 400°F limit and reached 350°F which correlates to the readings of thermocouple Gamma ( $\gamma$ ).

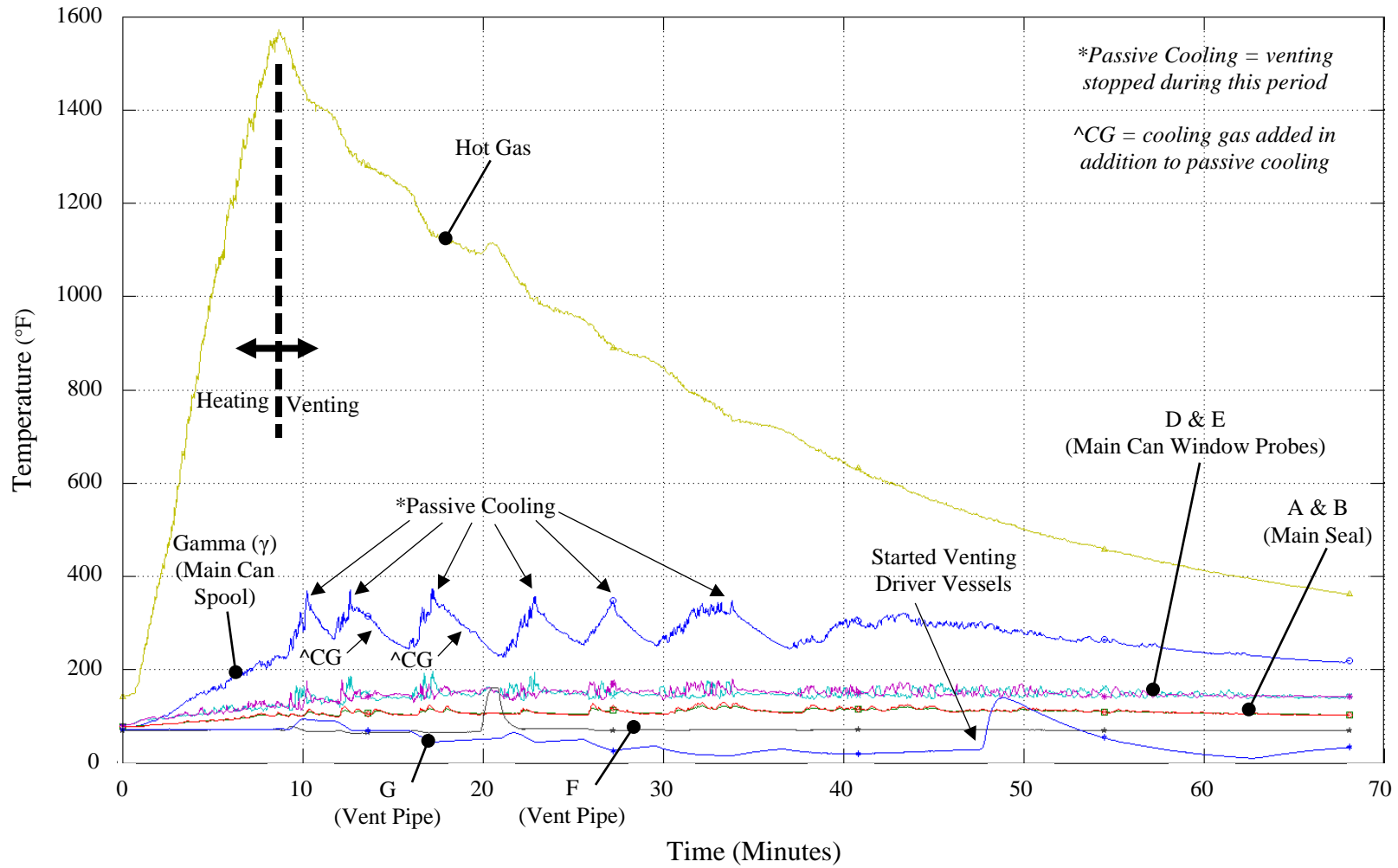
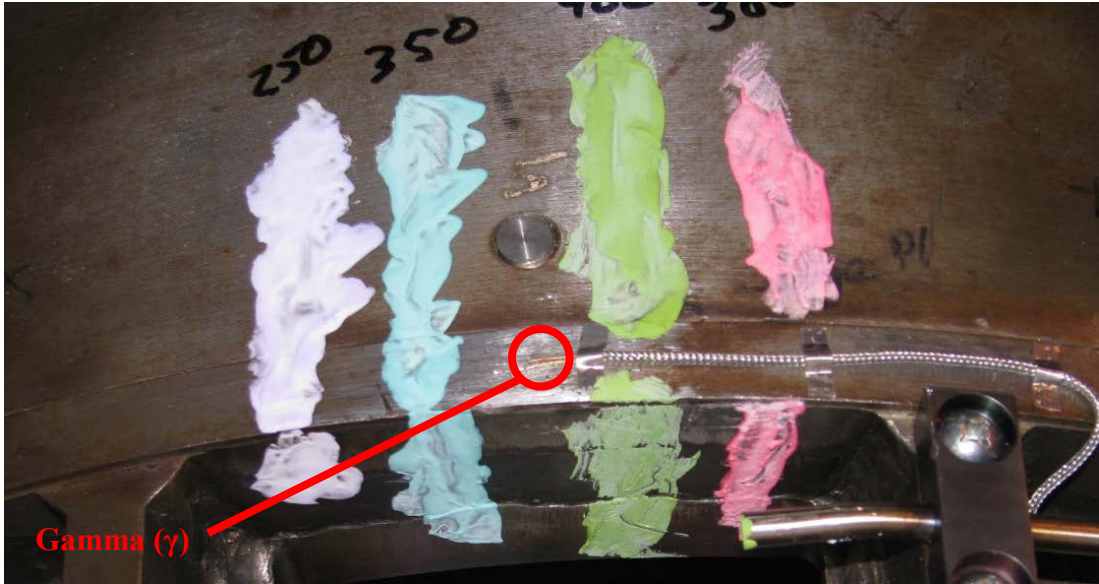


Figure 3.4: Vent of Heater Vessel at Mach 10 Condition (22,000 psi & 1550°F)



*Figure 3.5: Temperature Melting Paint before Test Program*



*Figure 3.6: Temperature Melting Paint after Test Program*

### 3.4: Conclusion

The results of the venting experiment at Mach 10 conditions in the Heater Vessel, demonstrated the feasibility of venting nitrogen gas at conditions up to 1550°F and 22,000 psi by instrumenting critical locations with thermocouples and leveraging passive cooling. A new venting capability is achieved with the current nominal thermocouple setup by adding a permanent thermocouple in the location that thermocouple Gamma ( $\gamma$ ) was for this test program to monitor the metal temperature during a Mach 10 vent. Figure 3.7 shows a mock-up of thermocouple Gamma ( $\gamma$ ) added to the Mach 10 Main Can. This solution will work for Mach 10 package, but will not work for the Mach 14 package which operates at 3400°F and 27,000 psi. The vent time using this method would be longer than an hour for Mach 14 possibly degrading seals ability to contain pressure due to exposure to high temperatures. A different solution for Mach 14 case will be discussed later in this paper.

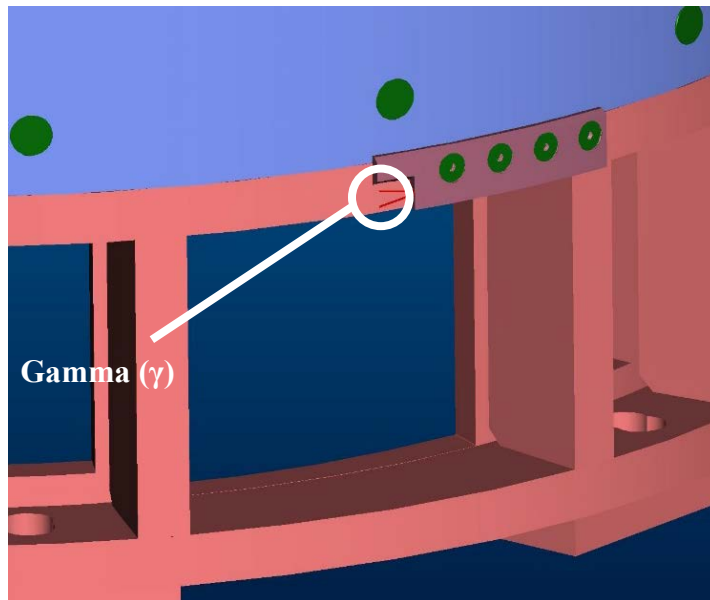


*Figure 3.7: Thermocouple Gamma ( $\gamma$ ) added as Nominal Thermocouple for Mach 10*

*Main Can Package*

## Chapter 4: Heater Thermal Stratification Test

### 4.1: Introduction and Research Question

The Heater Vessel is instrumented with a range of thermocouples in strategic locations, but it does not give a complete temperature profile for all locations in the Heater. The gas temperature is unknown in the region between the Heater Base to the Hot Gas Thermocouples, shown in Fig. 4.1. In order to design a vent system, the amount of hot gas versus cold gas in the Heater must be known. This means that any thermal stratification in the Heater must be determined. The purpose of this test was to measure the thermal stratification in Heater Vessel during a heating cycle.

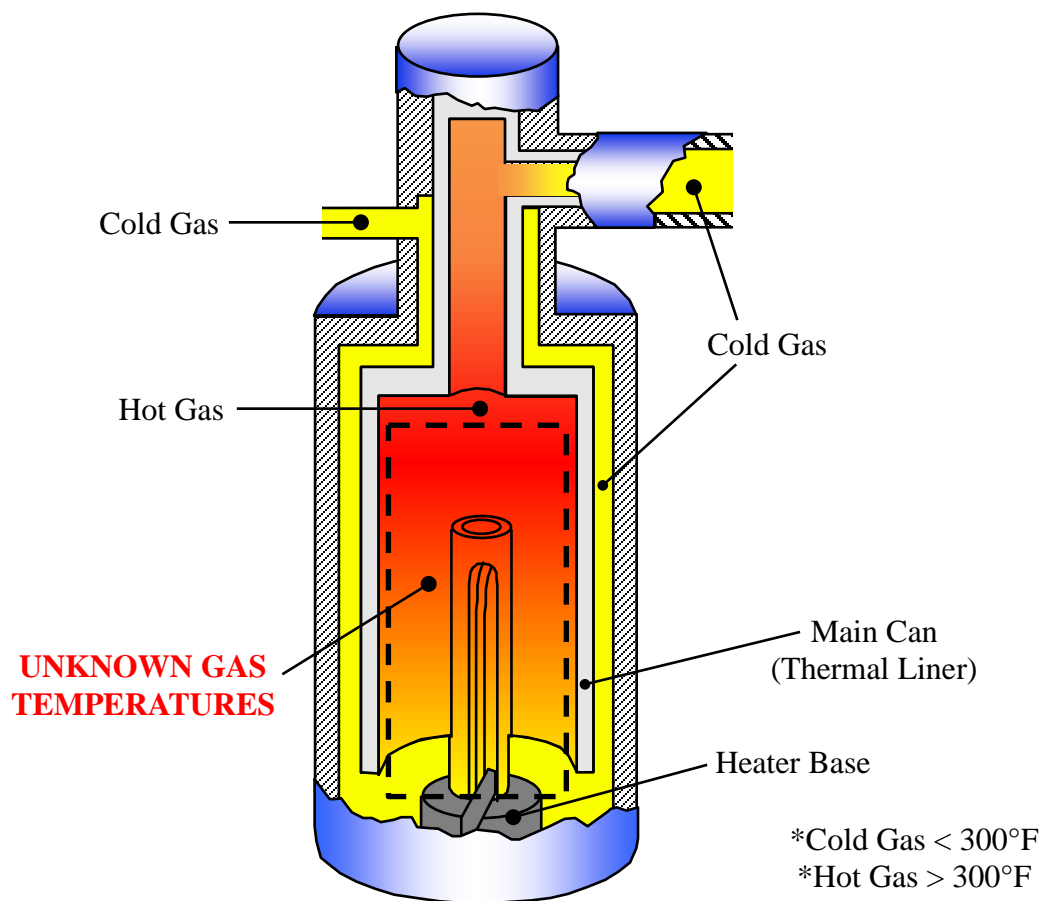


*Figure 4.1: Unknown Gas Temperature Region in Heater Vessel*

#### 4.2: Test Setup and Plan

The gas temperature inside the core of the Heater is only measured at the top of the Main Can, via the Hot Gas thermocouples, during standard runs. Thus gas temperature variations in other parts of the Heater core are unknown. For this test program, the same vent path was used as in the Heater Venting Test, shown in Fig. 3.1. The conditions and runs for this test program are shown in Table 4.1. Runs 1 and 2 with a Hot Gas temperature limit of 550°F were used to check the design of Thermocouple Rig (discussed later). The following runs, 3 to 5 were used to test the effect of heating the gas to the same temperature while varying the pressure. The Hot Gas temperature limit of 750°F was used since it was a known safe condition to vent hot gas prior to the data available from the Heater Venting test. For this test program the nominal set of thermocouples for the Heater Vessel were used, shown in Fig. 3.2.

<b>Run</b>	<b>Final Pressure (psia)</b>	<b>Hot Gas Temperature Limit (°F)</b>
1	12000	550
2	4250	550
3	14500	750
4	4750	750
5	10500	750

*Table 4.1: Heater Thermal Stratification Test Conditions*

For this experiment an apparatus (Thermocouple Rig, or “Rig”) was designed and built to add two more critically positioned gas thermocouples designated as “A” and “C”. In addition to one metal thermocouple designated as “B” to monitor the metal temperature of Thermocouple Rig. The Thermocouple Rig was installed inside the Heater near the Heater Base and Element. The two temperature backflow probes used in the Heater Venting Test were also used, designated as thermocouples “D” and “E”. Two additional thermocouples were used to monitor the temperature of the vent

pipe to the roof designated as thermocouples “F” and “G”. To account for these additional thermocouples, some nominal thermocouples were replaced, which is shown in Table 4.2. During the Heater Thermal Stratification Test, data was recorded on the Tunnel 9 control system data system at a sample rate of 1 Hz. Each thermocouple was given a limit for each test condition, which is shown in Table 4.3. These safe limits were determined based on the material limits near the respective thermocouples.

<b>Thermocouple Designator</b>	<b>Nominal Thermocouple Replaced</b>
A (Gas Temperature)	3
B (Rig Surface)	4
C (Gas Temperature)	1
D (Main Can Window – South)	9
E (Main Can Window – North)	14

*Table 4.2: Thermocouple Replacements for Heater Thermal Stratification Test*

<b>Thermocouple Abort Limits for Each Test Condition</b>		
<b>Thermocouple Designator</b>	<b>Test Conditions</b>	
	<b>550°F</b>	<b>750°F</b>
Hot Gas Thermocouples	550°F	750°F
A (Gas Temperature)	1600°F	1600°F
B (Thermocouple Rig Surface)	1600°F	1600°F
C (Gas Temperature)	1600°F	1600°F
D (Main Can Window – South)	500°F	500°F
E (Main Can Window – North)	500°F	500°F
F (Vent Pipe at Manifold)	450°F	450°F
G (Vent Pipe in Compressor Room)	300°F	300°F

*Table 4.3: Thermocouple Abort Limits for Heater Thermal Stratification Test*

#### 4.3: Thermocouple Rig Design

The Thermocouple Rig was designed to measure the gas temperature at certain locations near the Heating Element and Base. The Thermocouple Rig was

configured to have three upright probes at heights of approximately 2 feet, 3 feet, and 4 feet from the bottom Closure Plug's top surface. The probes are labeled A, B, and C from highest to lowest. Probes A and C took Heater core gas temperature measurements. Probe B was configured to have a thermocouple tacked to the outside of the probe tube, on the side facing the Heater Element, to measure the Thermocouple Rig's actual metal temperature during heating cycles and venting.

The Thermocouple Rig has a mounting flange that was used to affix the Thermocouple Rig to the bottom Closure Plug. The mounting flange supported the three upright probes made of 304L stainless steel tubes going directly up into the Heater core. The tubes carried Type K 24-AWG thermocouple wire with Nextel ceramic fiber insulation and Inconel 600 overbraid (Omega # XC-K-24-IB-500) which had a 1,600°F continuous max use temperature rating. Each thermocouple cable used as a gas temperature sensor was crimped to a 304 stainless steel sleeve at the top of the probe which was then inserted into a counter-bore in the larger tube. The tubes were clamped to the mounting flange using custom clamps. The mounting flange also had three terminal blocks to transition the high temperature Nextel insulated thermocouple wire to a lower temperature fiberglass insulated wire that did not have a conducting outer braid to electrical isolate the Thermocouple Rig. The mounting flange had a cover to protect all the terminal blocks and wiring in that area. The three probe tubes had two tube shield support ribs welded to cross brace them to increase rigidity of the overall structure.

Since we were interested in measuring gas temperatures, we needed to shield the gas thermocouple beads from direct radiation from the Heater Element. A



radiation shield made from 304L stainless steel was attached to the tubing with a bracket. An upper radiation plate was attached with screws to the top of the radiation shield to allow for an additional radiation protection from the top of the Heater thermal liner. It was designed to allow gas to freely flow vertically up and down through the radiation shield to ensure the Thermocouple bead sensed the gas temperature. The CAD Model of the Thermocouple Rig is shown in Fig. 4.2.

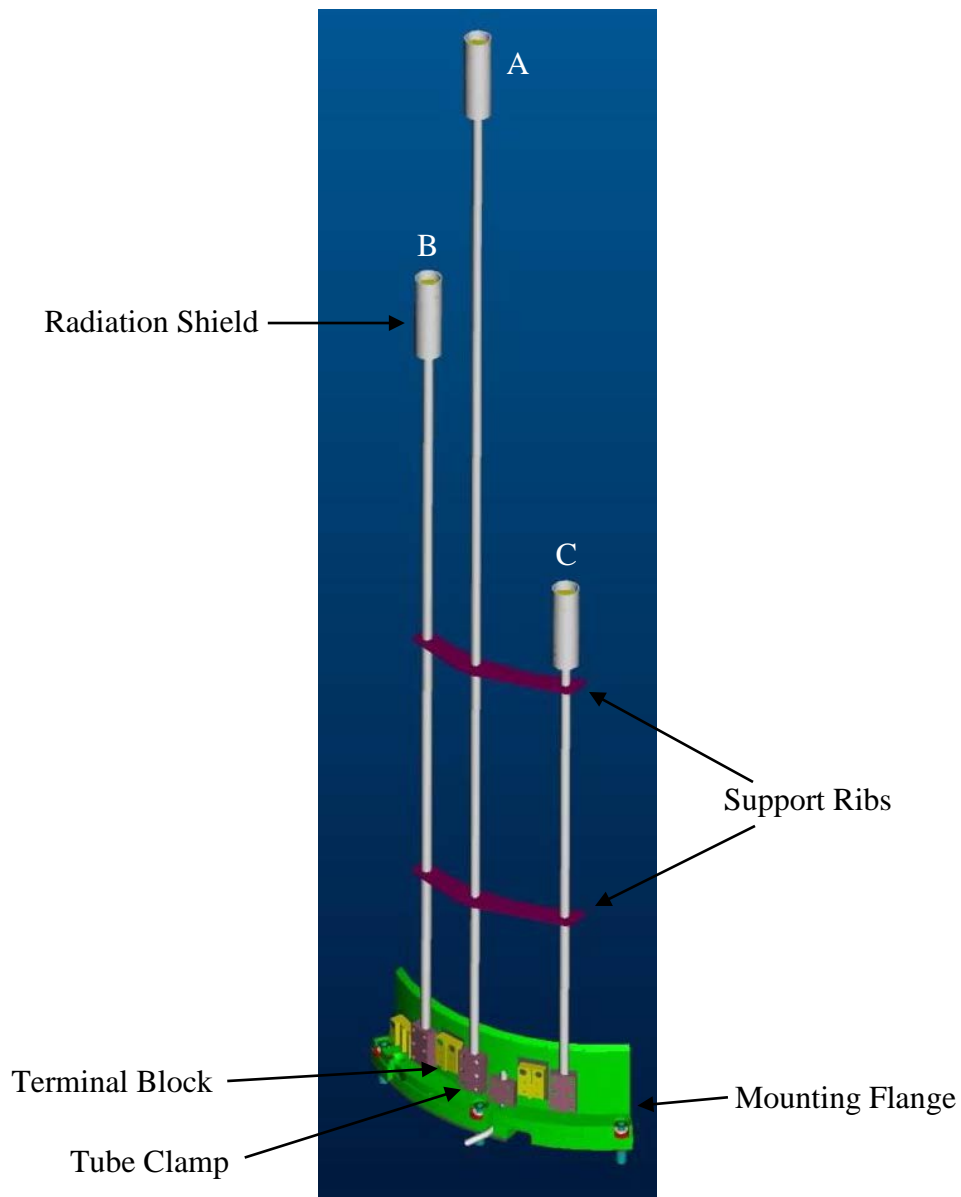
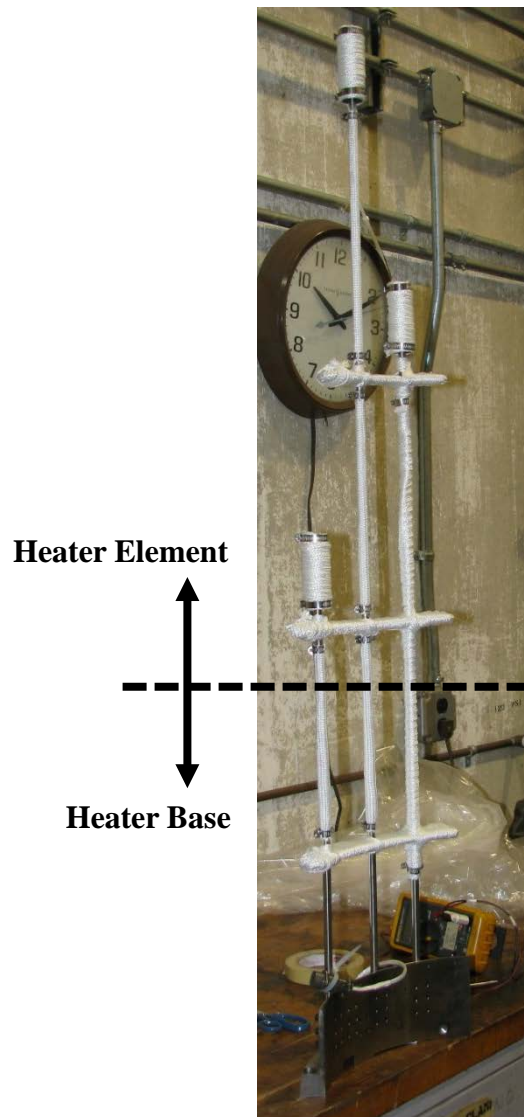


Figure 4.2: Thermocouple Rig CAD Model

The Thermocouple Rig was wrapped in Nextel ceramic fiber sleeving held in place with band clamps, shown in Fig. 4.3. This Nextel insulation was used to help lower the thermal gradients and thermal shock that the Thermocouple Rig saw during the heating cycle. It was also used as an electrical insulator if any part of the Thermocouple Rig structure contacted an electrically live Heater part. After each run the Thermocouple Rig was inspected using borescope taken from the open diaphragm area to check for any visible change in shape.



*Figure 4.3: Thermocouple Rig Built and Wrapped with Nextel Insulation*

#### 4.4: Data Analysis

The first 2 runs for the Heater Thermal Stratification Test were successful in showing that the Thermocouple Rig Design worked as expected and did not distort in shape, which allowed testing during runs 3 to 5. For runs 3 to 5, the final gas pressure was varied, while the final gas temperature was held constant. It was found that the thermal gradient in the Heater Core was the identical for all 3 runs. Run 3 and 4 are shown in Fig. 4.4 and Fig 4.5, respectively. Run 5 with a Heater at 10,500 psi and 750°F is discussed in this section as an example for all the runs and is shown in Fig. 4.6. Run 5 took about 35 minutes to vent down to 1,000 psi, which includes about 4 minutes of heating time. Probe A gas temperature tracked Hot Gas thermocouples during heating and was about 10°F hotter than Hot Gas thermocouples during venting. Probe C gas temperature was about 20°F cooler than Hot Gas thermocouples and probe A during heating, but tracked probe A during venting. Probe B metal temperature was cooler than Hot Gas thermocouples during heating and was slower to cool down during venting. The window probes D and E did not exceed 110 F and vent pipe probes F and G were room temperature or lower due to the throttling process occurring at the vent valve leading to the Joule-Thomson effect. The test showed that probes A and C gas temperatures tracked with the Hot Gas thermocouples at the top of the Main Can, which was evident in all 5 runs meaning the temperature is uniform in the Heater core. While probe B was slower to increase and decrease in temperature than the gas temperatures, since it was the metal temperature of the Thermocouple Rig which poses more thermal mass than the gas. During all the runs all nominal and special thermocouples read well below safe limits.

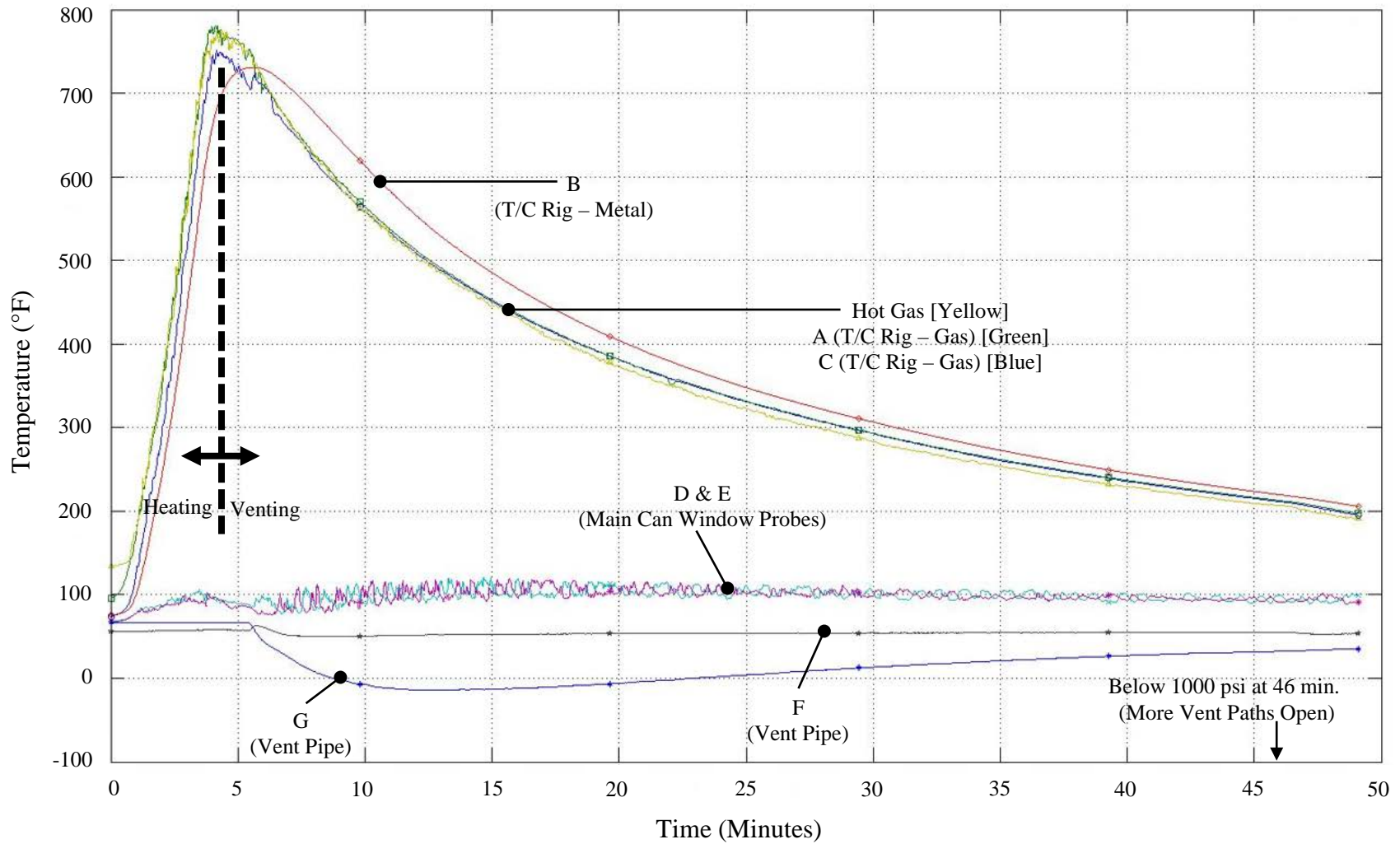


Figure 4.4: Run 3 – Vent of Heater Vessel for Thermal Stratification Test at 14,500 psi & 750°F

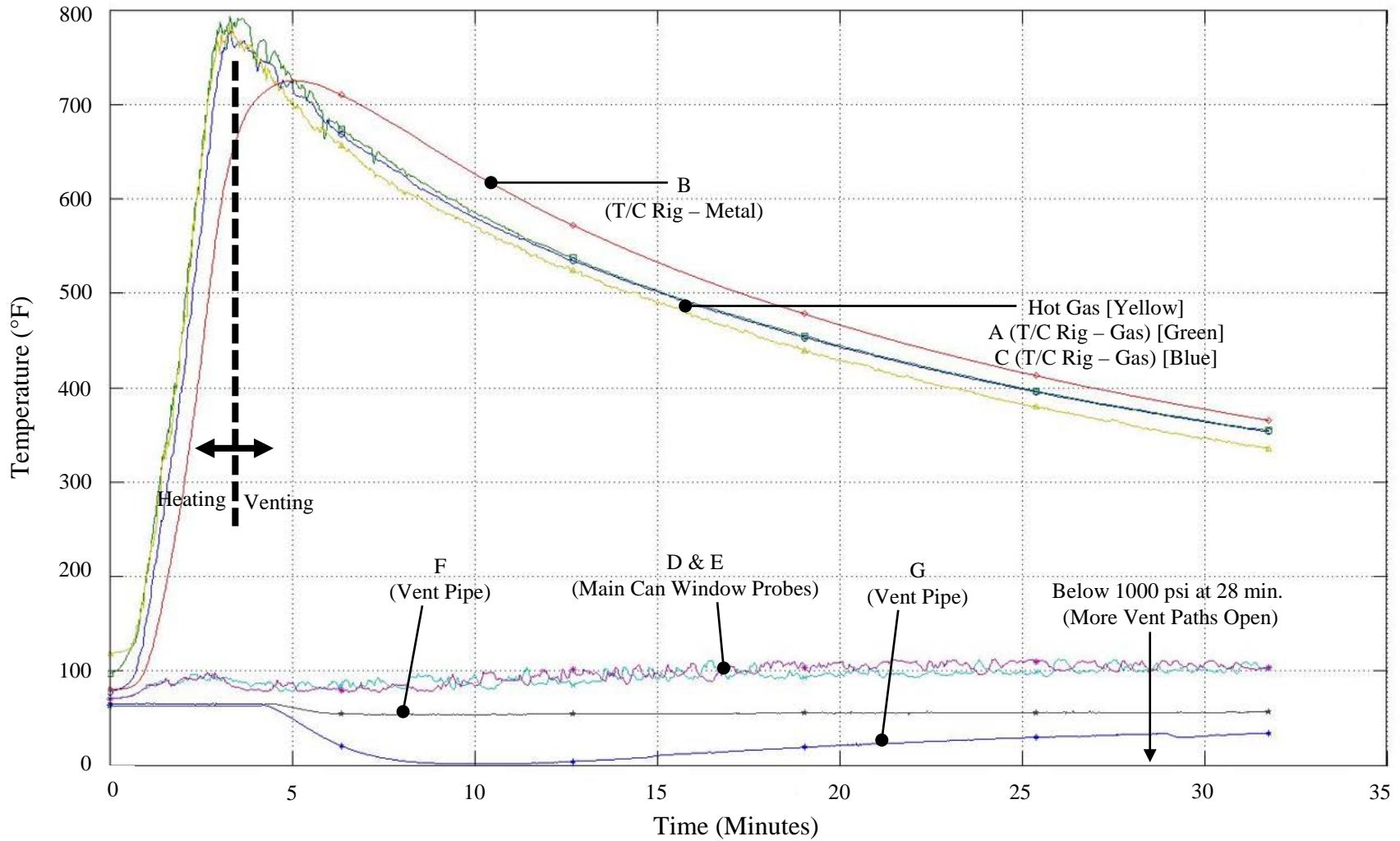


Figure 4.5: Run 4 – Vent of Heater Vessel for Thermal Stratification Test at 4,750 psi & 750°F

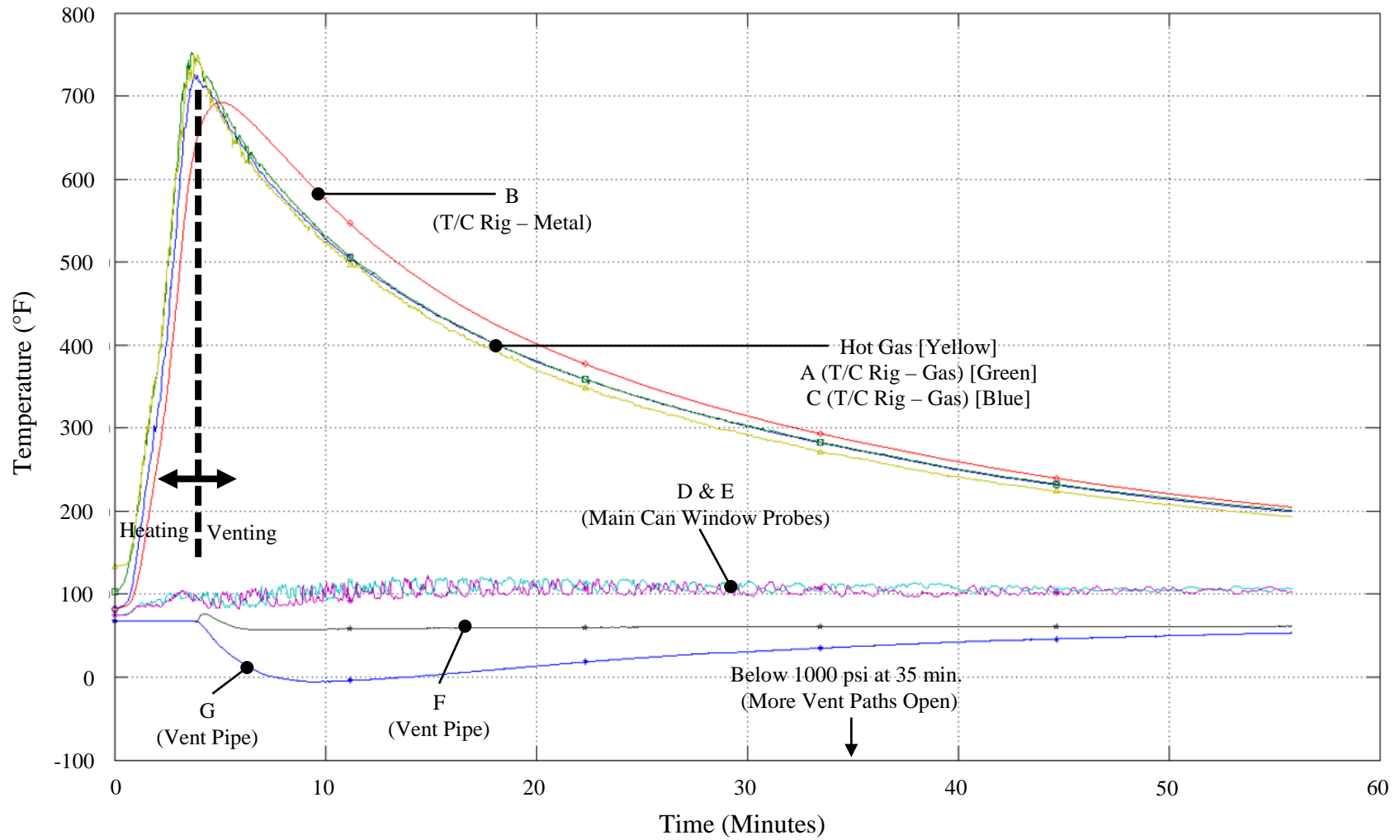
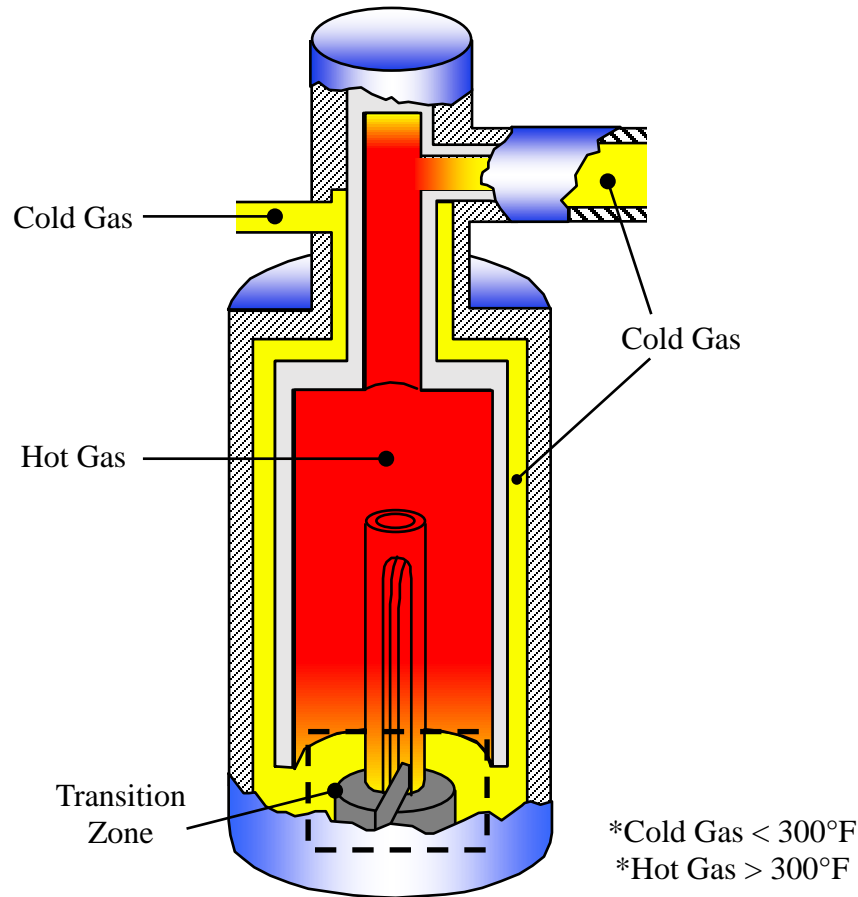


Figure 4.6: Run 5 – Vent of Heater Vessel for Thermal Stratification Test at 10,500 psi & 750°F

#### 4.5: Conclusion

The Heater Thermal Stratification Test showed that thermal stratification layers are located in a small region between the Closure Plug and top of the Heater Base. The transition in the temperature from cold gas to hot gas occurs abruptly in this small region. The result from this test extrapolated to higher temperatures means that the gas goes from 300°F to 3400°F gas in about 2 feet of height. Figure 4.7 shows a realistic view of the thermal stratification in the Heater Vessel. If the small transition zone is considered as hot gas to give the worst case scenario, the gas volume in the Heater Vessel can be treated as cold gas at 300°F (31% of the volume) and hot gas at 3400°F (69% of the volume).



*Figure 4.7: Realistic Thermal Stratification in Heater Vessel*

## Chapter 5: Design of Venting System

### 5.1: Introduction

The venting system for hot gas at 3400°F and 27,000 psi was designed using the results from the Heater Thermal Stratification Test. The nitrogen gas that is pressurized can be idealized and split into two different regions and analyzed as a worst case scenario. One region contains cold gas at 300°F (31% of the volume) and the other region contains hot gas at 3400°F (69% of the volume). This information was leveraged for the vent system design by devising a system that would mix the cold gas and hot gas, thus reducing the bulk temperature of the gas prior to venting through the bottom Closure Plug of the Heater Vessel. Figure 5.1 shows the placement of the bottom Closure Plug with respect to the entire Heater Vessel.

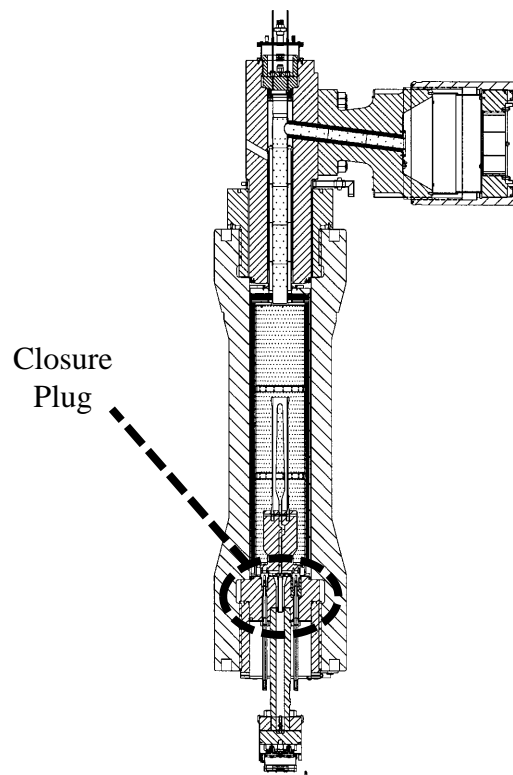


*Figure 5.1: Bottom Closure Plug in Heater Vessel*



## 5.2: Design

The Closure Plug is cylindrical in shape and measures about 17” tall with a 30.5” outer diameter. The Closure Plug is made from special low alloy steel similar to ASTM A723 and AISI 4340 and is limited to 300°F stamped maximum operating temperature rating. The Closure Plug has four existing instrumentation ports in it, only one of which is in use to cool the Heater Vessel after runs by introducing cooling gas into the vessel. Figure 5.2 shows the cross-sectional view of the ports and the one port in use.

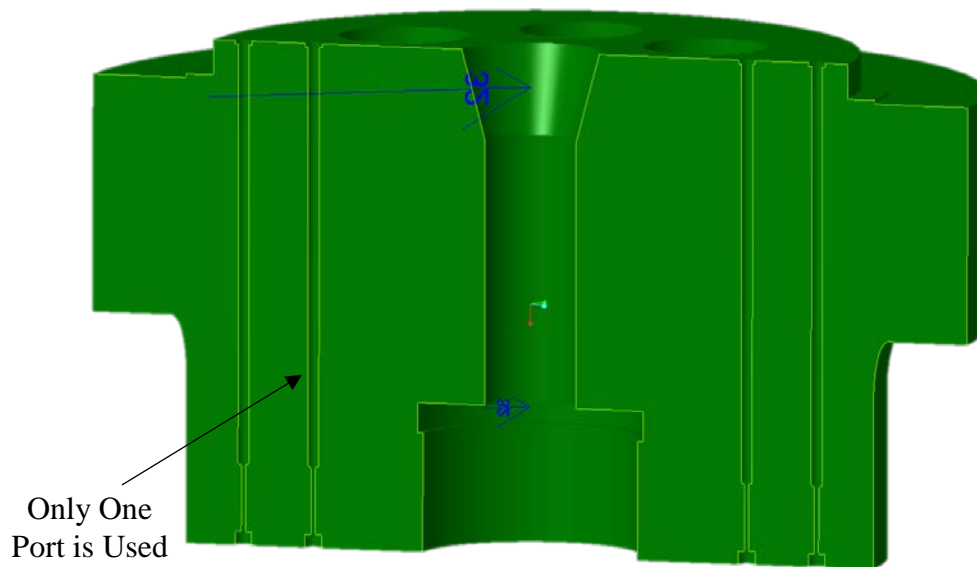


*Figure 5.2: Closure Plug Cross-Sectional View*

The proposed hot gas venting system proposes two modifications to the existing Closure Plug. The first proposed change to the Closure Plug is to make the two inboard ports larger to accommodate a thermal Seal Head. The second change is to add two ports inboard of the modified ports. One of the new ports will be used to introduce cooling gas from the Drivers. Figure 5.3 shows the modified Closure Plug with the Main Can’s support spool to help differentiate the hot gas region and cold

gas region. The hot gas at 3400°F is contained inside the inner diameter of the spool and the outer diameter is considered to be cold gas at 300°F.

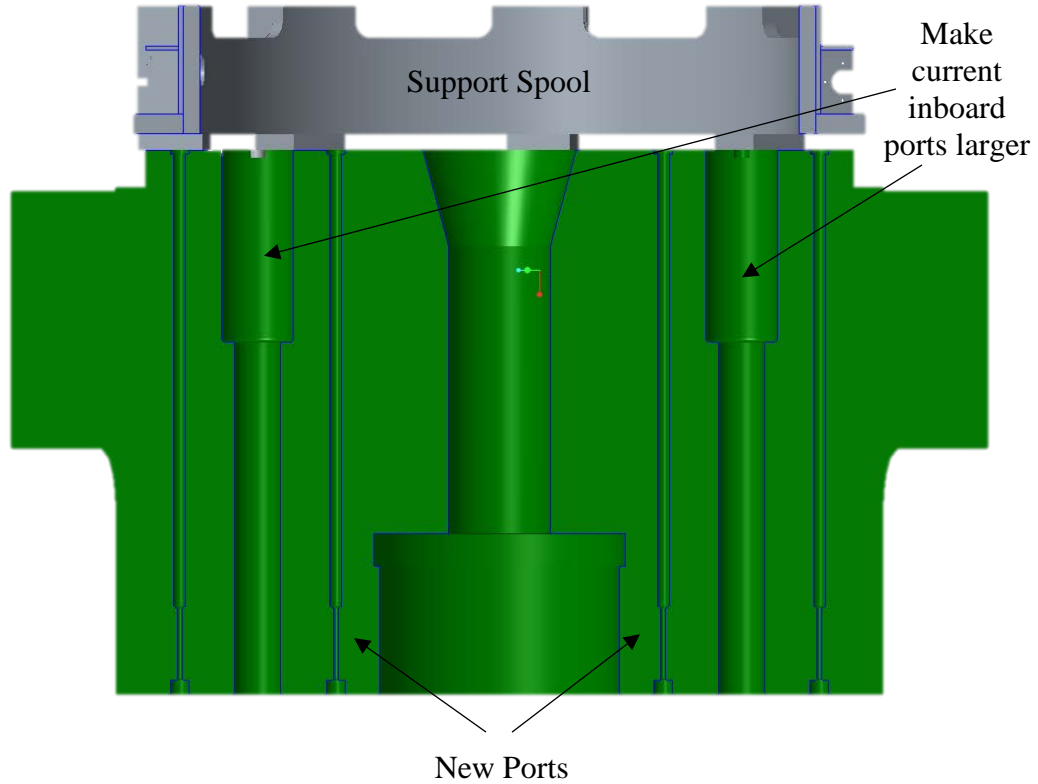


*Figure 5.3: Modified Closure Plug*

The new vent path design is shown in Fig. 5.4. The Stand Pipe is the inlet of the vent path, located inside the pressurized Heater Vessel at the top surface of the Closure Plug and is designed to mix the cold and hot gas. The Stand Pipe is made from C-103 Niobium alloy so it will survive the hot gas that are expected to reach 3400°F. This mixed gas then flows to the Seal Head, which is used to isolate the gas heating from the Closure Plug and Heater Vessel and to contain pressure. The larger port size is designed to accommodate the Seal Head. The Seal Head is made from Inconel 718 and uses a Parker O-Ring made from Perfluoroelastomer (FF352-75 2-031), which is rated to 608°F. The gas being vented then travels from the Seal Head

to Parker Autoclave high pressure piping made from Inconel 625 pressure rated for 60,000 psi at room temperature and 29,800 psi at 1100°F. The piping has a 0.5625” outer diameter and 0.1875” inner diameter. The piping is connected to a Parker Autoclave high pressure valve 60VM9081(HT) also made from Inconel 625 that has the same pressure rating as the piping with an extended stuffing box valve with graphite braided yarn packing. This valve can be controlled remotely by employing any one of various control options from Parker Autoclave to interface with the control system at Tunnel 9. The Stand Pipe, Seal Head, piping, and valve will be mirrored in the Closure Plug, so there is two of each part. This was done to match the venting time achieved in the 1550°F and 22,000 psi Heater Venting Test.

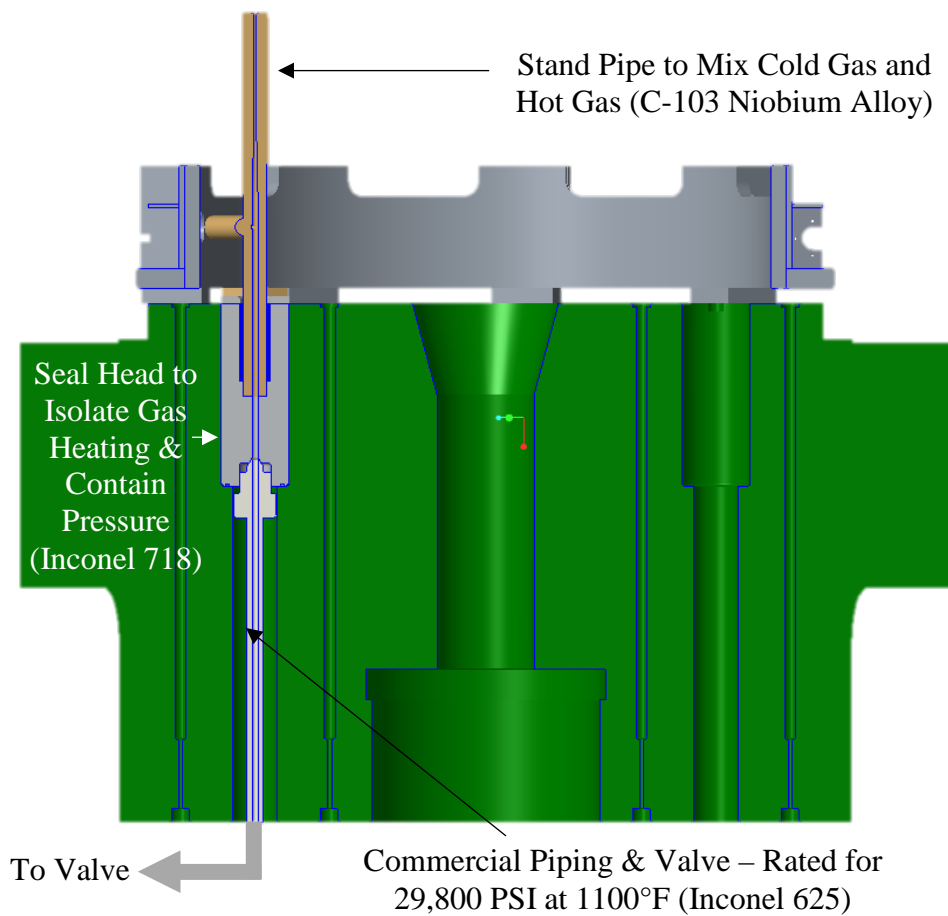
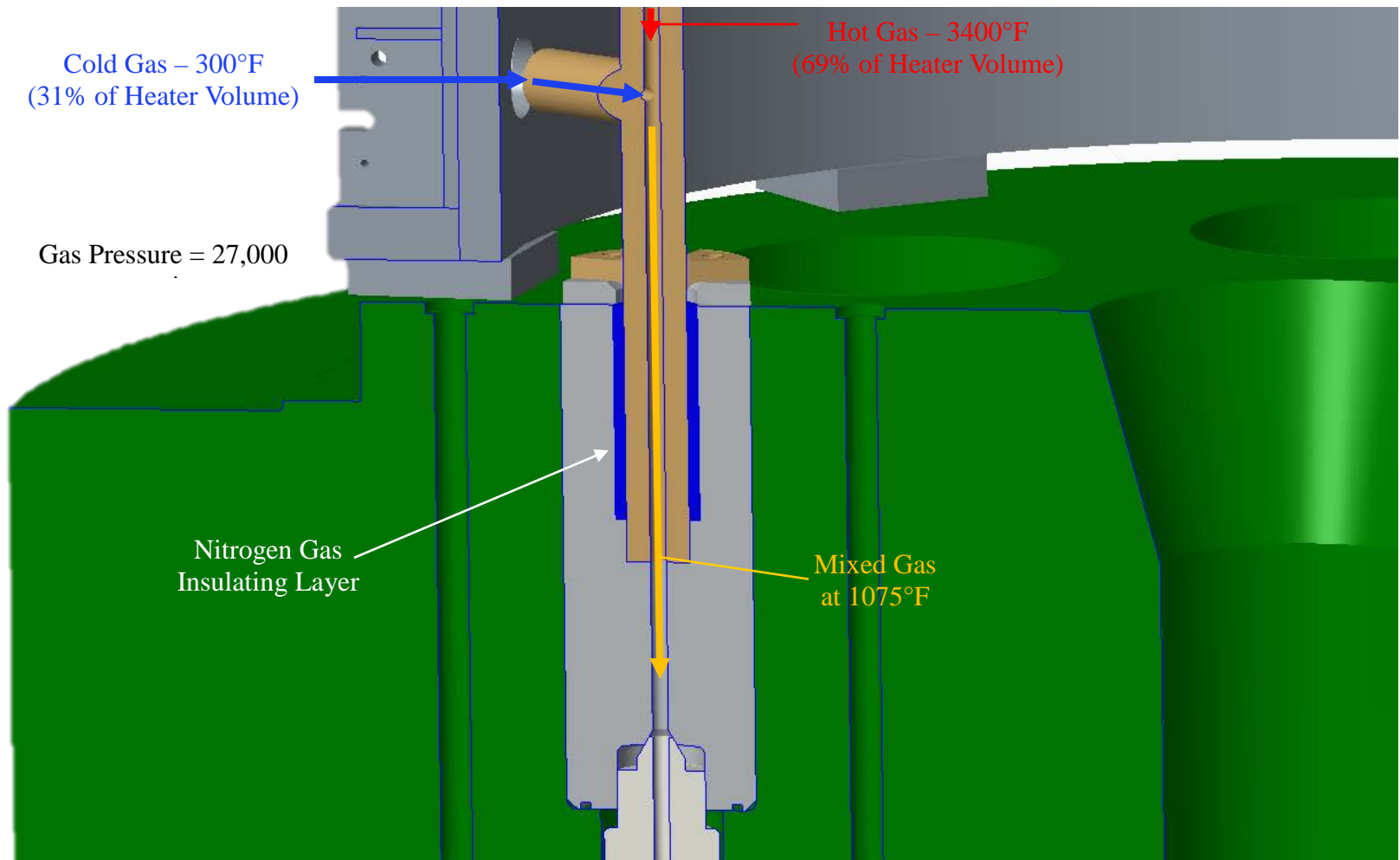


Figure 5.4: Modified Closure Plug with Stand Pipe, Seal Head & Commercial Piping

The Stand Pipe is key to the design because it allows the mixing of the cold and hot gas in the pressurized environment of up to 27,000 psi. Cold gas from the outer area of the spool enters the standpipe and mixes with the hot gas to get a mixed gas at 1075°F, which is a safe temperature for the commercial piping. The mixing is accomplished by sizing the area openings to allow 75 percent cold gas to 25 percent hot gas ratio. The inner diameter of the mixed section was fixed to 0.1875” to match the commercial piping. The result is that the inner diameter of the cold gas branch is 0.1625” and the inner diameter of the hot gas branch is 0.09375”. Additional information is included in Appendix A.1: Stand Pipe Mixing Calculations. Since the cold gas region will be using more gas for mixing the ability to replenish the cold gas region may be necessary. This will be achieved by adding gas from the Driver Vessels. The mixing process is shown in Fig. 5.5. The Stand Pipe is bolted to the Seal Head which transitions the mixed gas from Stand Pipe to commercial piping. The contact area between the Stand Pipe and Seal Head is minimized by introducing a nitrogen gas insulating layer which presents a lower thermal conductivity. The C-103 Niobium alloy used in the Stand Pipe and the Inconel 718 used in the Seal Head were subjected to thermal testing in an oven to ensure no eutectic reactions occurred up to 1400°F.



*Figure 5.5: Gas Mixing Process*

Since the gas venting process will be heating the Seal Head and Closure Plug, there is a need for a cooling system. The cooling system was designed using city water to lower the maintenance needed for the system in place of a closed loop cooling system with pump, chiller, plumbing, etc. Each vent path will have four cooling ports which are centered around the large vent port. The city water will be first connected to a manifold to split the water equally to the eight ports. The cooling ports will also have Corrosion Barriers to isolate the cooling water from the steel of the Closure Plug. The Corrosion Barriers are made from Glidcop AL-60 (UNS C15760), which is a copper base with high alumina content. It designed for high temperature applications where high thermal conductivities are needed, which is the case here to quickly transfer heat from the Closure Plug to the water. Figure 5.6 shows the bottom view of the Closure Plug with the cooling system setup.

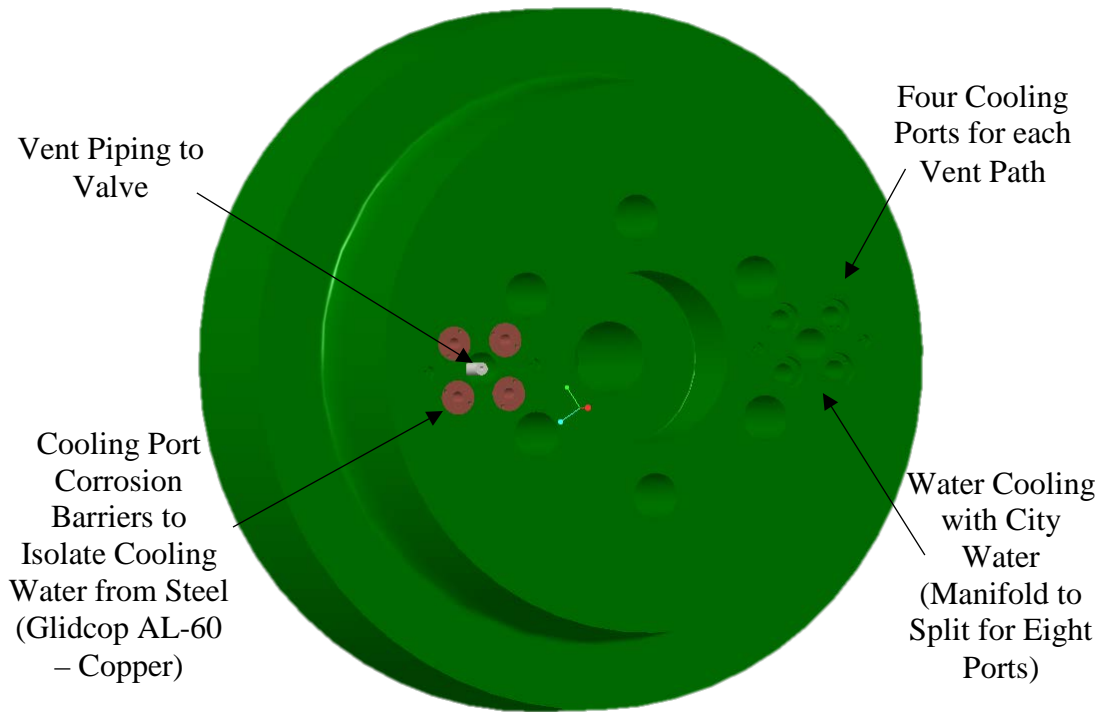


*Figure 5.6: Bottom View of Closure Plug with Cooling System Setup*

The Corrosion Barriers are bolted to the Closure Plug and have a tube inserted into them for water flow. The openings on the Corrosion Barriers are designed to match a current system in use at Tunnel 9, which is the Electrode Head Cooling assembly. The water will flow inside that tube and is deadened inside the Corrosion Barriers. Then the water returns between the outer diameter of the tube and the inner diameter of Corrosion Barriers. Figure 5.7 shows a closer look at the cooling ports in a Cross-Sectional view. Figure 5.8 shows the cooling water flow path.

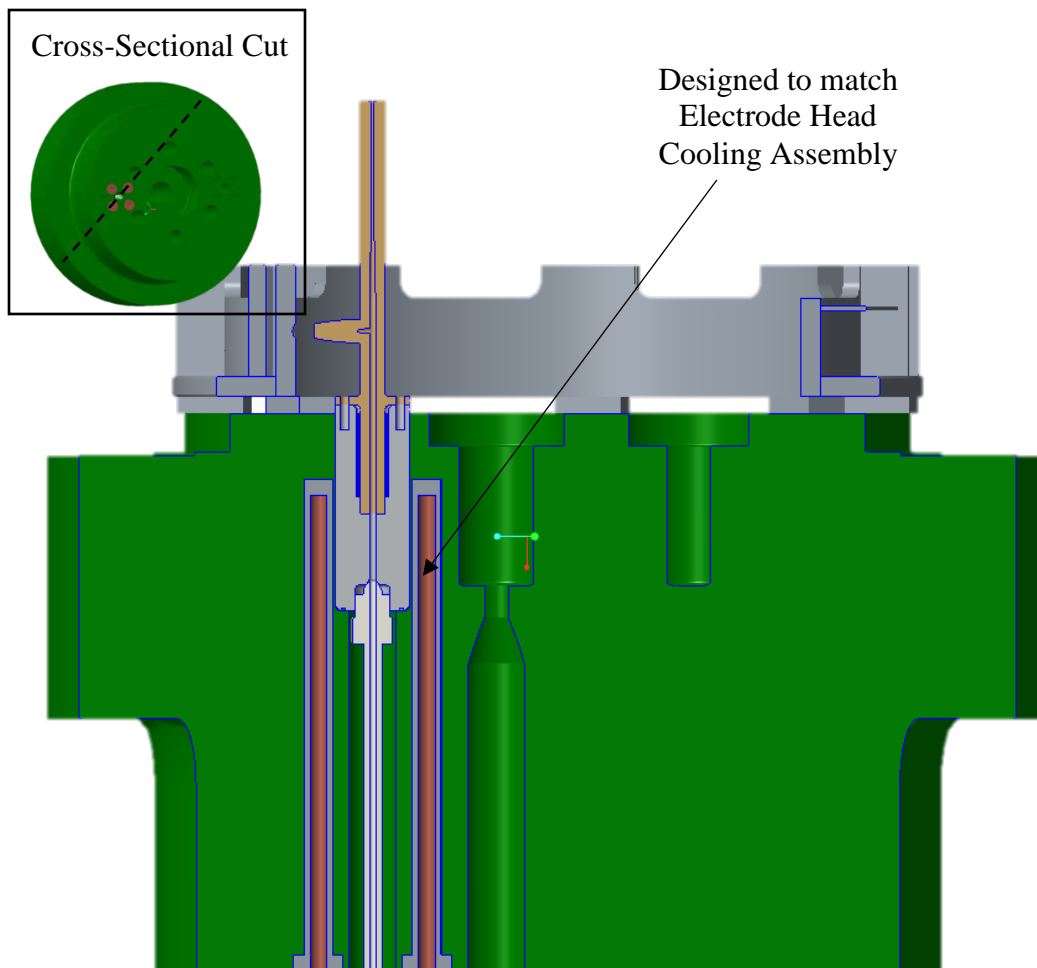


*Figure 5.7: Cross-Sectional View of Cooling Ports*

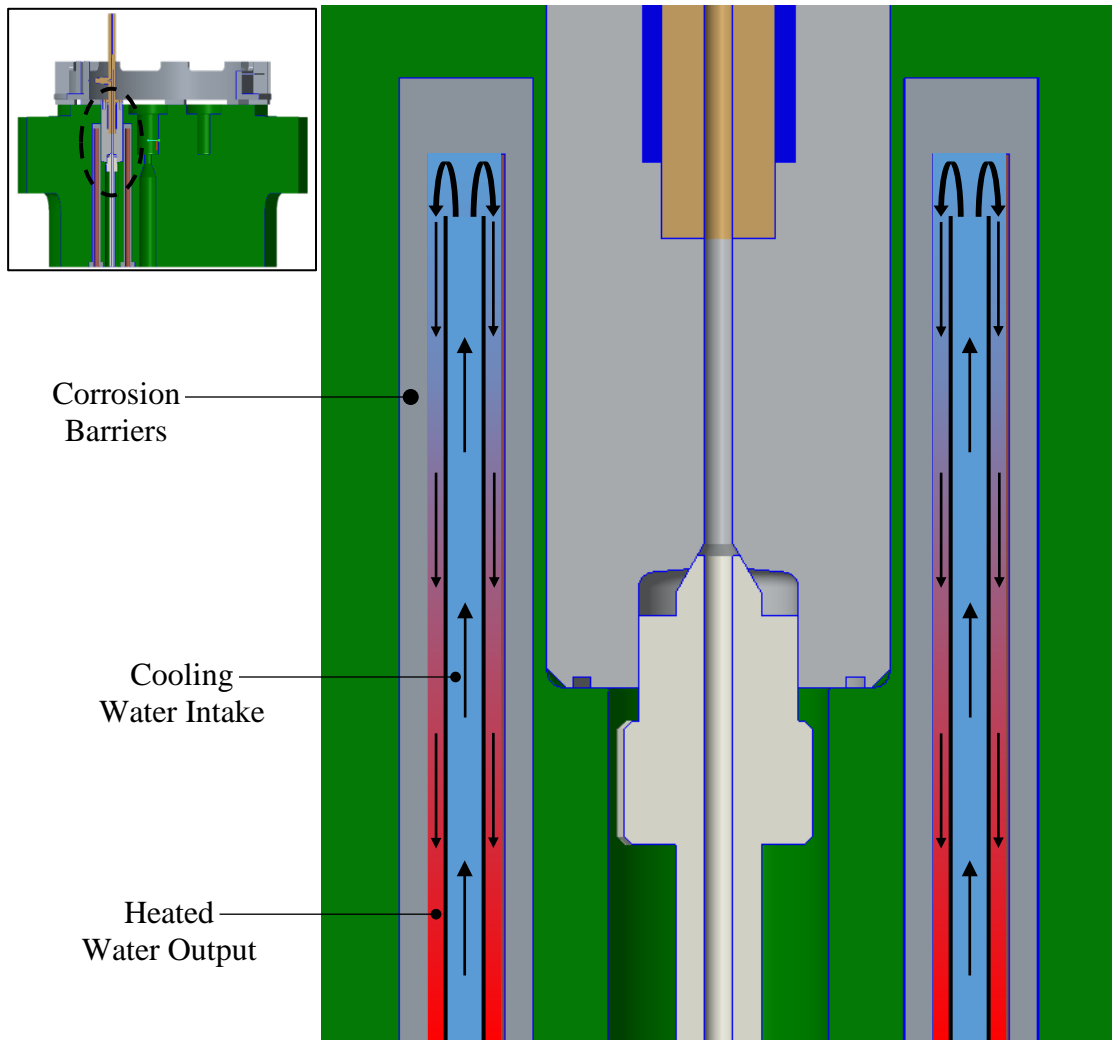


*Figure 5.8: Cooling Water Flow Path*

The venting system is designed to save other systems in Tunnel 9 in case of emergency and certain parts were design to be sacrificial. The Stand Pipe, Seal Head, piping, and valves are considered one use parts, so they can exceed their yield strengths if needed. Additional figures of the vent system design are included in Appendix A.2: Additional Views of Design. The material properties for each material used in the design and analyses are available in Appendix A.3: Material Properties.



### 5.3: Thermal Analysis & Results

A thermal analysis was completed in ANSYS Steady-State Thermal on the modified Closure Plug. The thermal analysis was then imported into a stress analysis. The results of the stress analysis on the modified Closure Plug were compared to the results from a stress analysis on the current Closure Plug. The stress analysis is discussed in the next sub-section.

The first step for the thermal analysis was to develop the thermal boundary conditions posed by heating due to venting gas and the cooling from the water. The natural convection on the Closure Plug is insignificant compared to gas heating and water cooling, which was evident in the Heater Venting Test of the Heater Vessel at 1550°F and 22,000 psi. All surfaces without a specified boundary condition were conservatively treated as adiabatic, which will yield a worst case result.

The boundary condition for gas heating was generated by assuming that there is choked flow at the valve orifice, since the Heater Vessel pressure is much higher than the atmospheric pressure. The mass flow rate at the valve orifice is expressed by the mass flow through a choked nozzle, which is shown in Eq. 5.1 [3]. See Appendix A.4: Choked Flow Equation and Heat Transfer Correlations for more details.

$$\dot{m} = \frac{p_0 A^*}{\sqrt{T_0}} \sqrt{\frac{\gamma}{R} \left( \frac{2}{\gamma + 1} \right)^{(\gamma+1)/(\gamma-1)}} \quad (\text{Eq. 5.1})$$

$\dot{m}$  = mass flow rate at choked valve

$p_0$  = pressure at valve entrance

$T_0$  = temperature valve entrance

$A^*$  = area of valve orifice

$\gamma$  = ratio of specific heats

$R$  = gas constant

The pressure at the valve entrance was set equal to the Heater Vessel pressure of 27,000 psi. The temperature at the valve entrance was set to the mixed gas temperature of 1075°F, and here it is assumed the gas in the piping to the valve undergoes an adiabatic process, giving the worst case scenario. The mass flow for one Parker Autoclave high pressure valve 60VM9081(HT) with these conditions is 1.711 lbm/s. The mass flow rate can be used to find the velocity at any point in the piping system through a conservation of mass analysis. This was used to find the velocity of the gas in the Stand Pipe and Seal Head which was then used to estimate convective heat transfer coefficients at the same locations. The convective heat transfer coefficient was determined using the Sieder-Tate correlation for forced convection in turbulent pipe flow, since it gave the highest rate of heating of any applicable correlation [4]. The gas heating convective heat transfer coefficient is 0.02831 BTU/s-in<sup>2</sup>-F. The complete calculations can be found in Appendix A.5: Gas Heating Convective Heat Transfer Coefficient Calculation.

The heat transfer coefficient should fall rapidly with time since the pressure and temperature decreases, which decreases the mass flow rate as gas is vented off to atmosphere. For this ANSYS Steady-State Thermal analysis the worst case convective heat transfer coefficient used corresponded to the highest mass flow rate. Since the pressure decrease and temperature decrease in the Heater Vessel could not be modeled using this new vent path design.

The boundary condition used for simulating the cooling water was similar. The volumetric flow rate of the city water is known to be a minimum of 10 gallons per minute. This is split between the eight cooling ports via a manifold. The city

water pressure and temperature were assumed to be 50 psi and 78°F, respectively. The conservation of mass principal was used to calculate the water velocity in the annulus where the water comes in contact with the Corrosion Barrier. This flow velocity was used to find the applicable correlation for forced convection in turbulent pipe flow, which in this case was the Gnielinski correlation [4]. The water cooling convective heat transfer coefficient is 0.002557 BTU/s-in<sup>2</sup>-F. The complete calculations can be found in Appendix A.6: Water Cooling Convective Heat Transfer Coefficient Calculation.

A quarter symmetry Finite Element ANSYS model of the modified Closure Plug was used in this analysis to minimize computational time. The gas heating and cooling water boundary conditions were applied to the ANSYS model of the modified Closure Plug. This is shown in Fig. 5.9 with a cross-sectional view of the modified Closure Plug. The initial material temperature for the simulation was 100°F for the entire assembly. Mesh convergence was performed manually to ensure a converged mesh was used, so the results would be independent of mesh size. ANSYS adaptive convergence feature was not supported in this study because the results from the Steady-State Thermal analysis were imported directly into Static Structural analysis. The mesh had 3,952,858 nodes and 2,712,843 elements. Tetrahedral and hexahedral element types were used, and the program optimized the mesh element quality. Since a high thermal gradient was expected in the areas of the Seal Head, Corrosion Barriers and the areas where they come in contact with the Closure Plug manual meshing was refined in these area using body sizing, face sizing, and sphere of influence since a high thermal gradient was expected in this area.

The results of the analysis are shown in Fig. 5.10 to Fig. 5.16. The bulk of the heat is retained in the Seal Head, Stand Pipe, and piping, which can be seen in both Fig. 5.10 and Fig. 5.11. Most of the heating is localized to the sacrificial parts. This heat is slowly conducted to the Closure Plug, which remains under the 300°F limit, as shown in Fig. 5.12. In fact, a significant portion of the Closure Plug is under 135°F, as shown in Fig. 5.13. The Corrosion Barriers also do not exceed 135°F, which will come in contact with the cooling water, shown in Fig. 5.14 and Fig. 5.15. This temperature is below the boiling point of water, which is at 212°F at atmospheric pressure and is at 281°F at 50 psi. The ability to keep the cooling water under the boiling point and slow the heating of the closure plug is due to the low thermal conductivity of the Seal Head which is made from Inconel 718, which is shown in Fig. 5.16. The low thermal conductivity of the Inconel 625 also results in a large thermal gradient in the Seal Head which is shown to be detrimental in the Static Structural analysis. The thermal results were imported into the ANSYS Static Structural analysis, which is discussed in the next section.

**A: Steady-State Thermal - Quarter Model**  
Steady-State Thermal  
Time: 1. s

- A** Gas Heating Convection: 1075. °F, 2.8305e-002 BTU/s-in<sup>2</sup>·°F
- B** Cooling Water Convection: 78. °F, 2.5568e-003 BTU/s-in<sup>2</sup>·°F

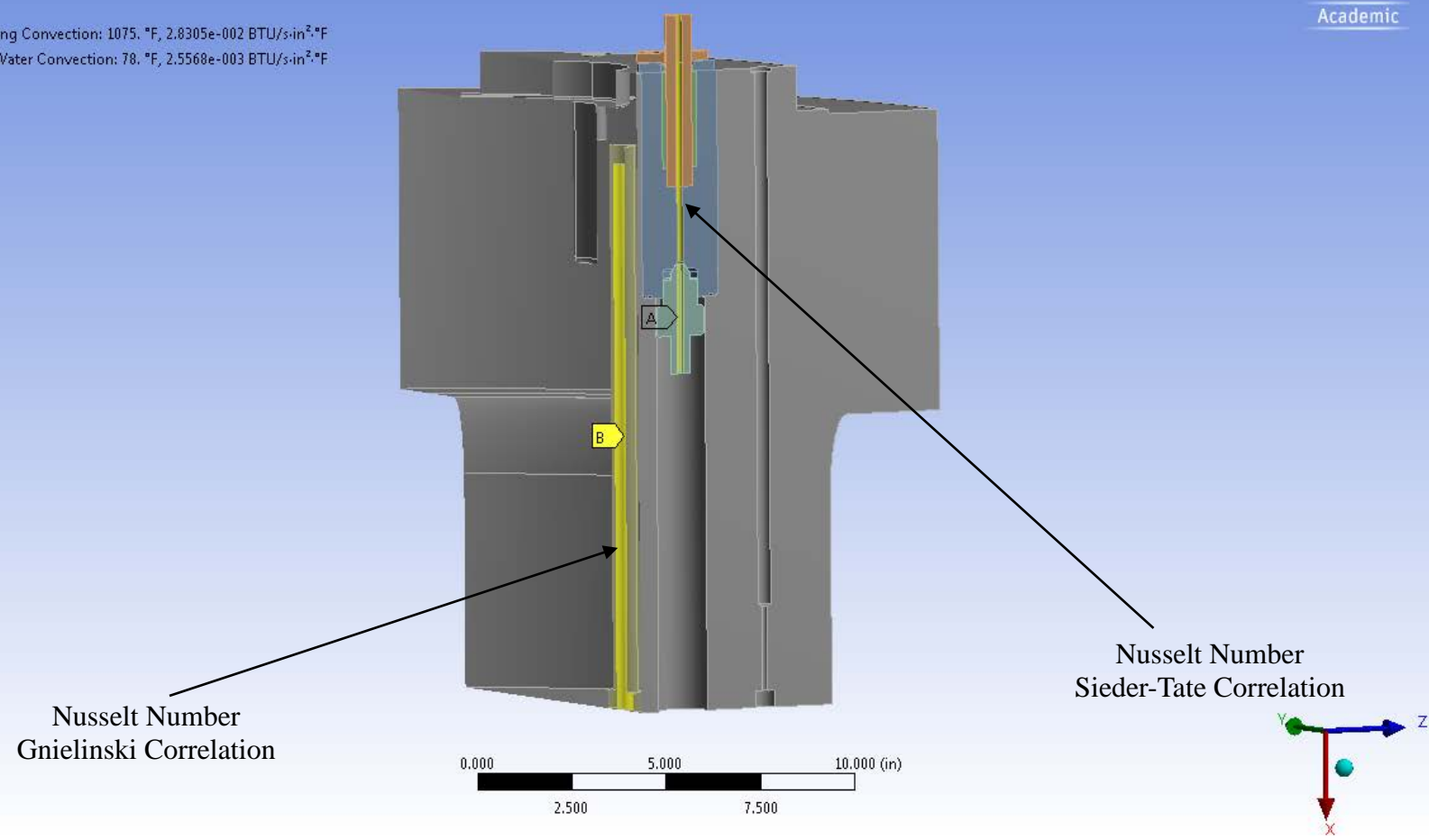
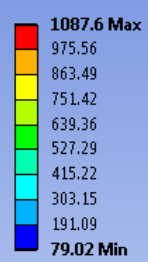


Figure 5.9: Boundary Conditions Cross-Sectional View – Steady-State Thermal

A: Steady-State Thermal - Quarter Model  
Temperature  
Type: Temperature  
Unit: °F  
Time: 1



Temperature (°F)

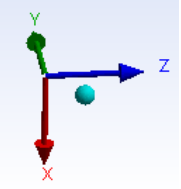
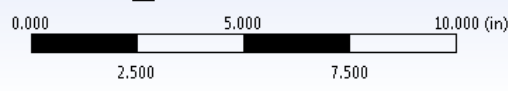
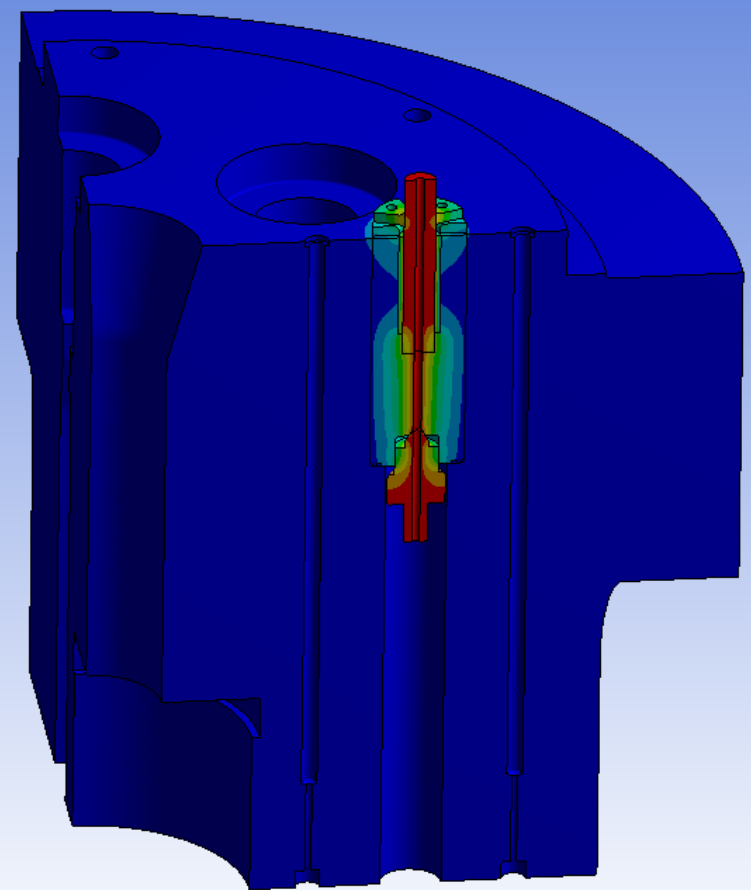


Figure 5.10: Assembly Temperature Results – Steady-State Thermal

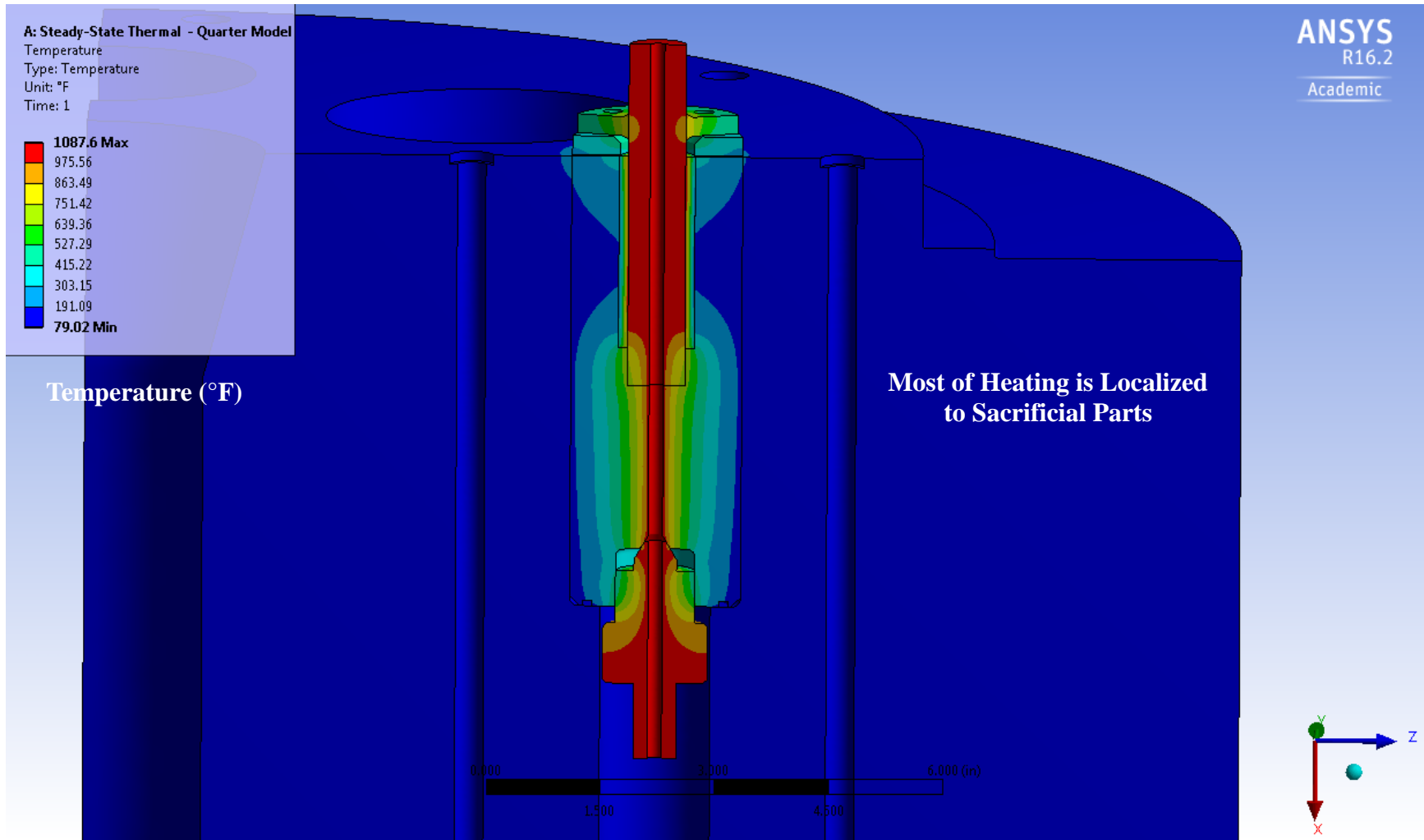
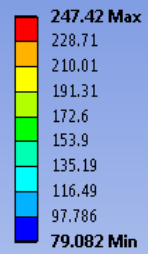
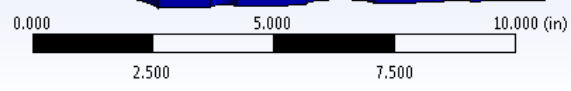
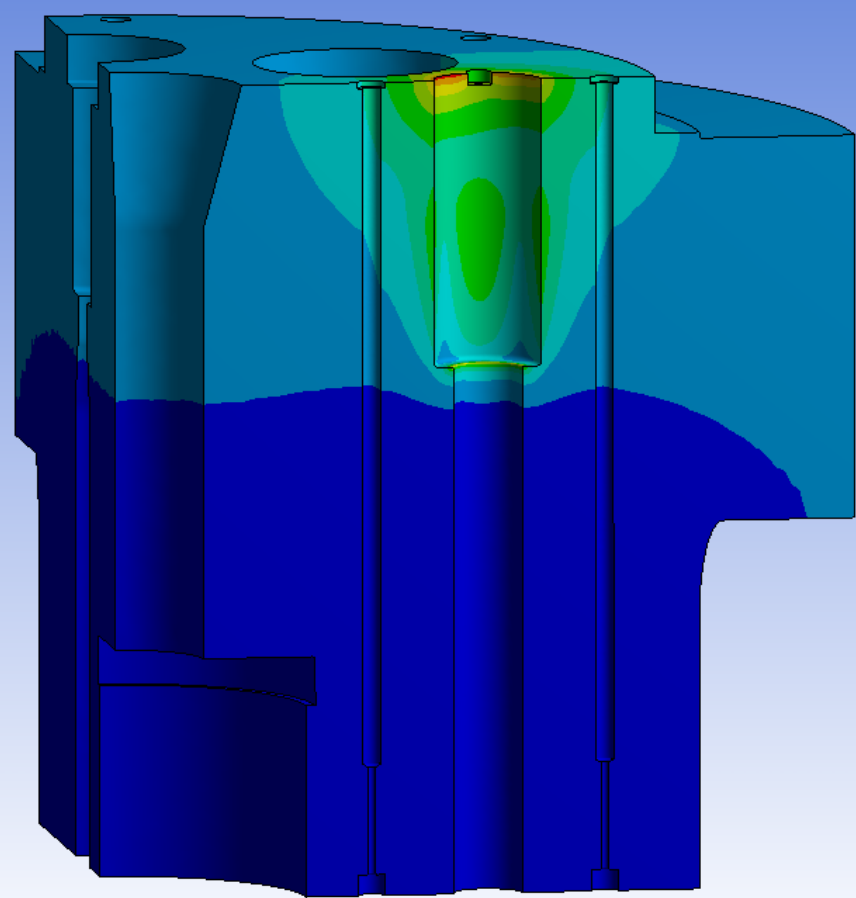


Figure 5.11: Close-Up View of Assembly Temperature Results – Steady-State Thermal

A: Steady-State Thermal - Quarter Model  
Temperature - 81-F-1646\_MOD\_ISD\Solid  
Type: Temperature  
Unit: °F  
Time: 1



Temperature (°F)



Closure Plug under  
300°F Limit

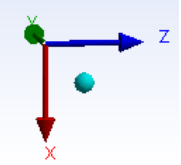


Figure 5.12: Closure Plug Temperature Results – Steady-State Thermal



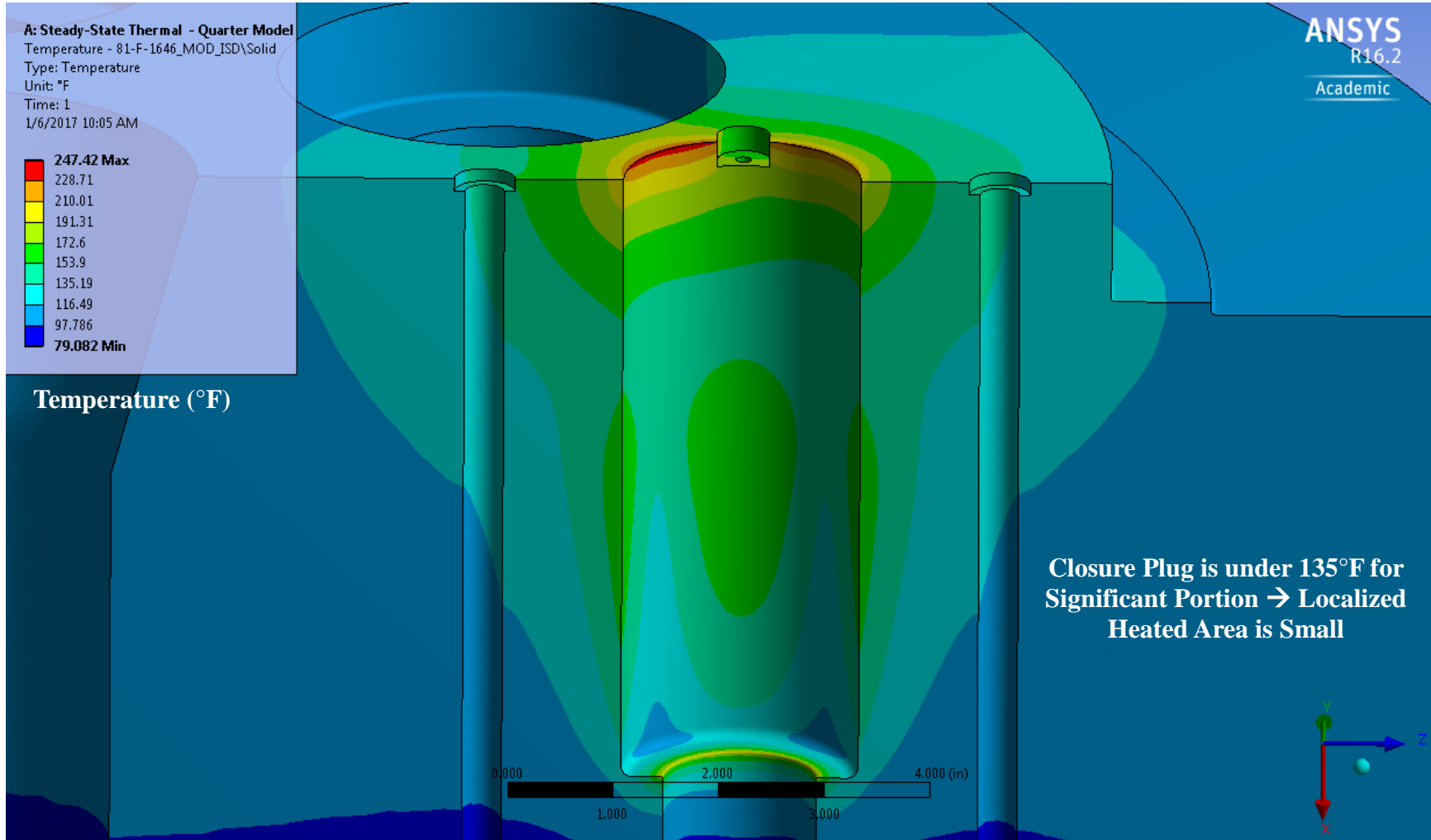
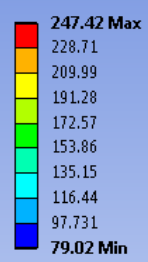
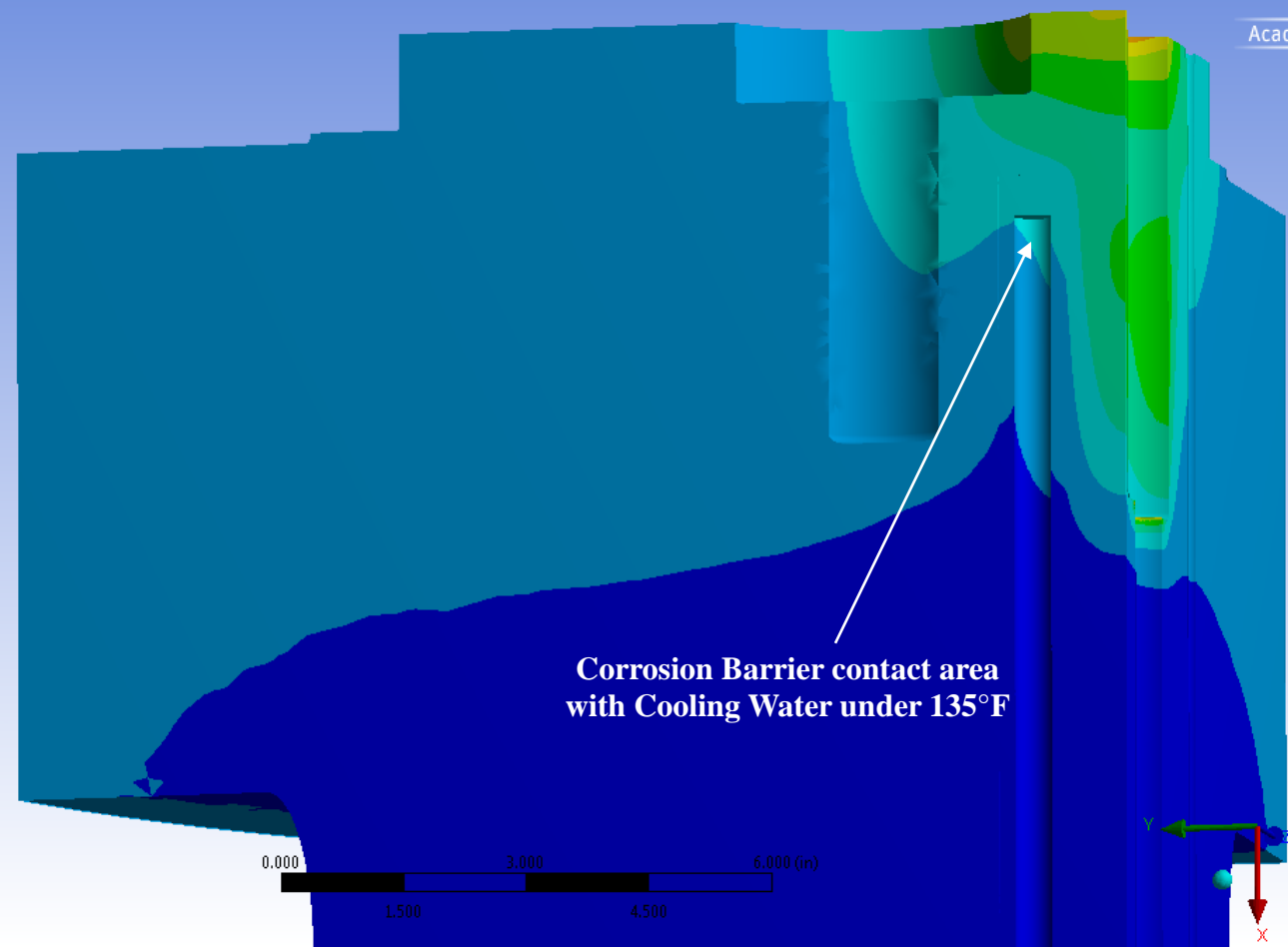


Figure 5.13: Vent Port in Closure Plug Temperature Results – Steady-State Thermal

A: Steady-State Thermal - Quarter Model  
Temperature - 81-F-1646\_MOD\_ISD\Solid1-COOLING\_PORT\_BARRIER\Solid1-COOLING\_PORT\_BARRIER\Solid1  
Type: Temperature  
Unit: °F  
Time: 1  
1/6/2017 10:21 AM



Temperature (°F)

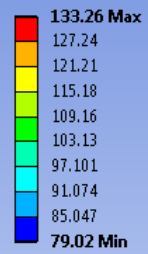


Corrosion Barrier contact area  
with Cooling Water under 135°F

Figure 5.14: Corrosion Barriers & Closure Plug Temperature Results Cross-Sectional View – Steady-State Thermal

**A: Steady-State Thermal - Quarter Model**

Temperature - COOLING\_PORT\_BARRIER\Solid1-COOLING\_PORT\_BARRIER\Solid1  
Type: Temperature  
Unit: °F  
Time: 1



**Temperature (°F)**

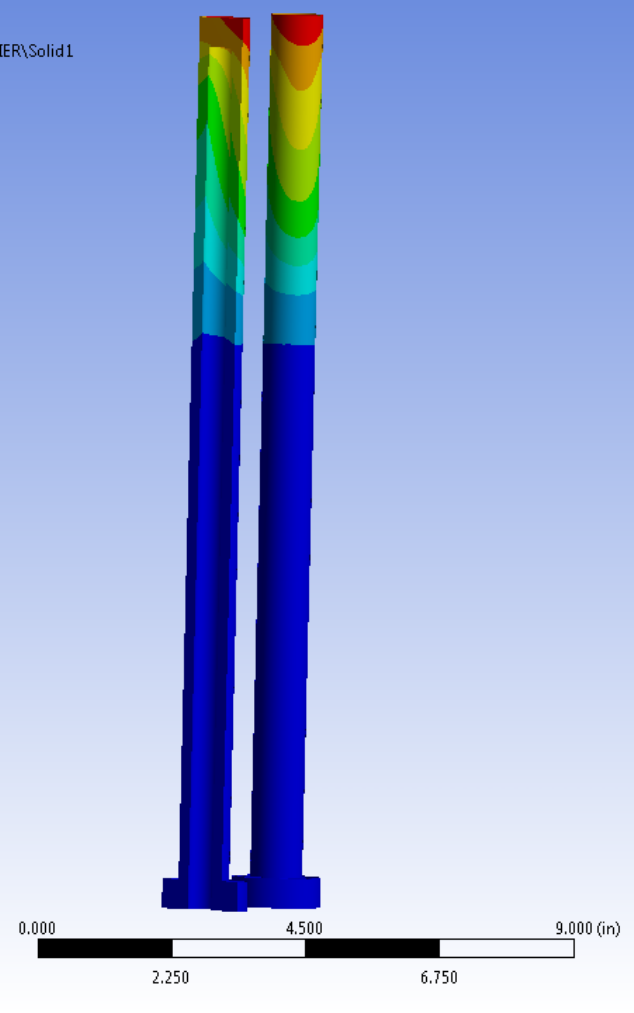
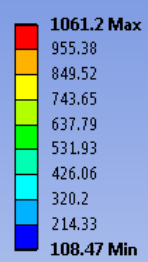
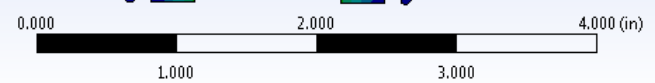
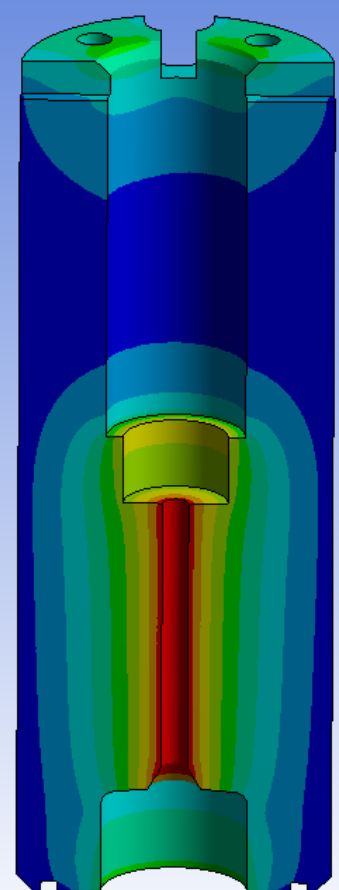


*Figure 5.15: Corrosion Barriers in Cooling Port Temperature Results Cross-Sectional View – Steady-State Thermal*

A: Steady-State Thermal - Quarter Model  
Temperature - SEAL\_HEAD\_JSD\Solid  
Type: Temperature  
Unit: °F  
Time: 1



Temperature (°F)



**Inconel 718**  
**Melting Range:**  
**2300°F – 2437°F**

**Inconel has Low Thermal Conductivity**  
↓  
**Slows Heating of Seal Head & Closure Plug**  
↓  
**Large Thermal Gradient**  
↓  
**Allows Water Cooling without reaching Boiling Point**

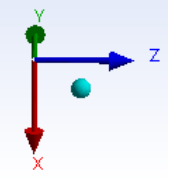


Figure 5.16: Seal Head Temperature Results – Steady-State Thermal

#### 5.4: Structural Analyses & Results – Closure Plug

The ANSYS Static Structural analysis was split for the Closure Plug and Seal Head. This section covers the analysis of the modified Closure Plug and Corrosion Barriers and includes a comparison to the current unmodified Closure Plug. The first step in this analysis was to establish the boundary conditions. The Closure Plug is secured to the Heater Vessel with the Heater Nut. For this analysis the Heater Nut was simulated with an elastic foundation stiffness feature available in ANSYS. The large female threaded opening at the center of the Closure Plug receives a male threaded Connector Pipe, and this connector pipe was modeled with a blow-off force applied on the associated threaded surface of the Closure Plug. The six ports in the Closure Plug which carry electrode heads assemblies (which carry electrical current into the Heater Vessel for heating the gas during a normal run) include a part called a Seal Ring, which was modeled using an effective bearing pressure. The Seal Head was similarly modeled with an effective bearing pressure which is simply a function of Heater Vessel pressure. Figure 5.17 shows the simplification of these boundary conditions to reduce computational time. More details can be found in Appendix A.7: Static Structural – Closure Plug Boundary Conditions.

The Heater gas pressure on the Closure Plug and the water pressure on the Corrosion Barriers were modeled with pressure boundary conditions. The thermal load was imported from the Steady State ANSYS analysis. A total of three analysis cases were completed for the Closure Plug. The first case was the current unmodified Closure Plug at 80°F and the results of this case were used for comparison to the next cases. Two cases were analyzed using the modified Closure Plug, one with thermal

loads applied to simulate a venting run and one with the Closure Plug at 80°F in order to simulate a nominal Tunnel run. Table 5.1 summarizes the mesh, convergence, boundary conditions, etc. used for each Static Structural analysis case for the Closure Plug.

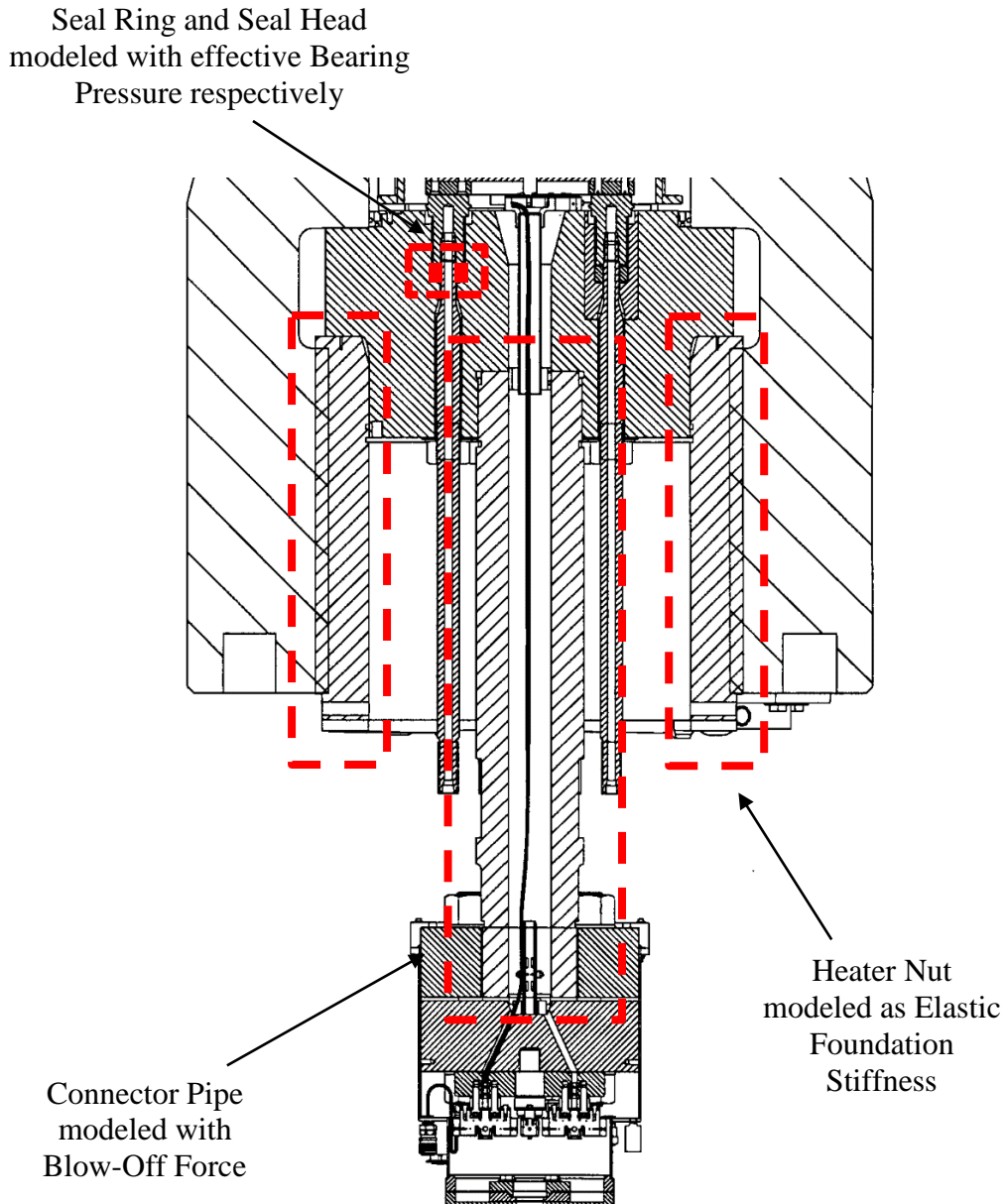


*Figure 5.17: Closure Plug – Boundary Condition Simplifications*

	<b>Case 1</b>	<b>Case 2</b>	<b>Case 3</b>
	<b>Current Closure Plug at 80°F</b>	<b>Modified Closure Plug with Thermal Load</b>	<b>Modified Closure Plug at 80°F</b>
<b><u>Boundary Conditions</u></b>	Fig. 5.18 to Fig. 5.20	Fig. 5.25 to Fig. 5.30	Fig. 5.25 to Fig. 5.29
Blow Off Force (Connector Pipe)	✓	✓	✓
Elastic Support (Heater Nut)	✓	✓	✓
Gas Pressure (27,000 psi)	✓	✓	✓
Seal Ring Bearing Pressure (2.409 times Gas Pressure)	✓	✓	✓
Seal Head Bearing Pressure (3.332 times Gas Pressure)	✗	✓	✓
Water Pressure (50 psi)	✗	✓	✓
Body Temperature (Imported from S.S. Thermal)	✗	✓	✗
<b><u>Mesh</u></b>			
Number of Nodes	3,024,804	2,452,491	3,551,479
Number of Elements	2,146,558	1,690,867	2,484,011
Element Types	Tetrahedral	Tetrahedral	Tetrahedral
Convergence	Adaptive von-Mises Stress & Safety Factor	Manual for von-Mises Stress (Adaptive not Supported with Imported Thermal Load)	Adaptive von-Mises Stress & Safety Factor

*Table 5.1: Structural Analyses Setup Summary – Closure Plug*

The current Closure Plug at 80°F (Case 1) boundary conditions are shown in Fig. 5.18 to Fig. 5.20. The current Closure Plug von-Mises Stress is shown in Fig. 5.21 and Fig. 5.22. A high stress area can be seen in the fillet area where the Closure Plug contacts the Heater Nut. Figure 5.23 and 5.24 shows that the current Closure Plug safety factor based on yield strength. Most of the current closure plug has a safety factor above 1.0. The only area that is below a safety factor of 1.0 is the fillet area, which has a minimum safety factor of 0.756. This area is designed with an elliptical fillet to counter these high stresses. Since the Closure Plug is subjected to high pressure cycles and experiences high stresses it has a risk mitigation plan that incorporates inspections, monitoring, fatigue studies, etc. to ensure it is still within safe design limits. The fillet area was not changed in this design, so the results from the current Closure Plug will be used as baseline comparison with the modified Closure Plug with thermal load (Case 2) and a modified Closure Plug at 80°F (Case 3).

The modified Closure Plug with thermal load (Case 2) boundary conditions are shown in Fig. 5.25 to Fig. 5.30. The von-Mises Stress is shown in Fig. 5.31 and Fig. 5.32. The same high stress area can be seen in the fillet area similar to the current Closure Plug. The safety factor shown in Fig. 5.33 and Fig. 5.34, is a better comparison to the current Closure Plug. The fillet area has a minimum safety factor of 0.762, compared to the current Closure Plug minimum safety factor of 0.756. The minor difference is due to the adaptive meshing used in Case 1 versus the manual meshing used in Case 2. An area of interest is where the material is removed by the vent port and cooling ports. The vent port area safety factor can be seen in Fig. 5.35,



it is calculated using material yield strength at 250°F. This is a conservative calculation since no part of the closure plug reached 250°F. The safety factor is lowered in that region since a large amount of material is removed, but the entire area has a safety factor greater 1.0 and most of the area is above a safety factor of 2.0. The cooling port area cross sectional view in Fig. 5.36, shows that the region is above a safety factor of 3.0. The Corrosion Barriers safety factor based on material yield strength is shown in Fig. 5.37 and is above a safety factor of 1.0.

The modified Closure Plug at 80°F (Case 3) boundary conditions are shown in Fig. 5.25 to Fig. 5.29. The safety factor results of this case are seen in Fig. 5.38 and Fig. 5.39. These results are indistinguishable to the results of the modified Closure Plug with thermal load (Case 2). This shows that that the driving factor is the gas pressure and not the thermal load, which is expected since the thermal gradient is mild in this location. A comparison of all three cases is shown in Fig. 5.40. The high stress in the fillet area is similar in all cases as expected. The removed material to make the new ports in Case 2 and 3 lowered the safety factor, but it is still above the material limits. These results indicate the planned modifications for the Closure Plug for this design are acceptable with the current Tunnel 9 operating conditions.

G: Static Structural - Quarter Model - Current CP  
Elastic Support  
Time: 1. s

- A Blow Off Force: 73048 lbf
- B Elastic Support: 9.9174e+005 lbf/in<sup>2</sup>

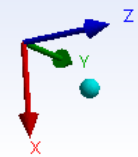
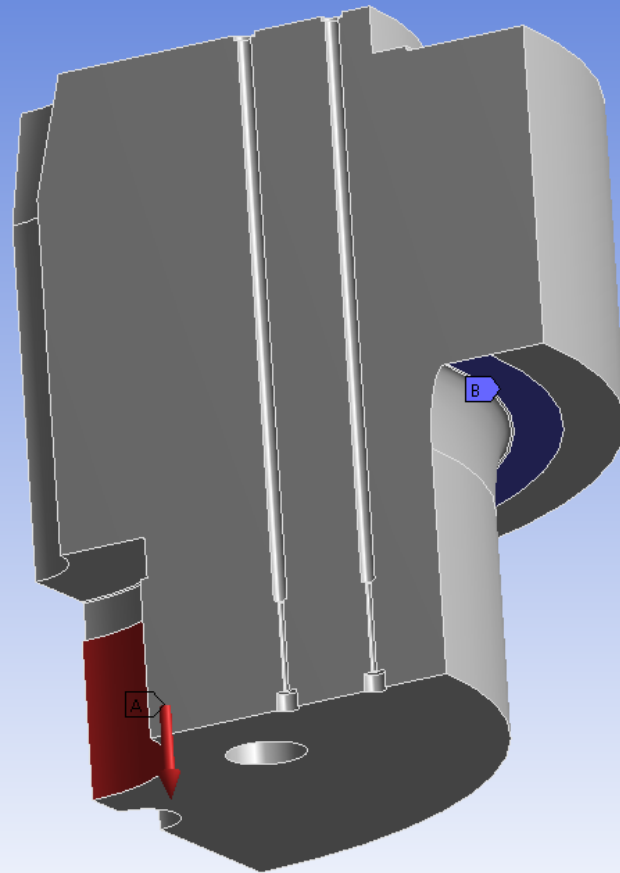


Figure 5.18: Current Closure Plug at 80°F (Case 1) – Blow Off Force & Elastic Support (B.C.s) – Static Structural

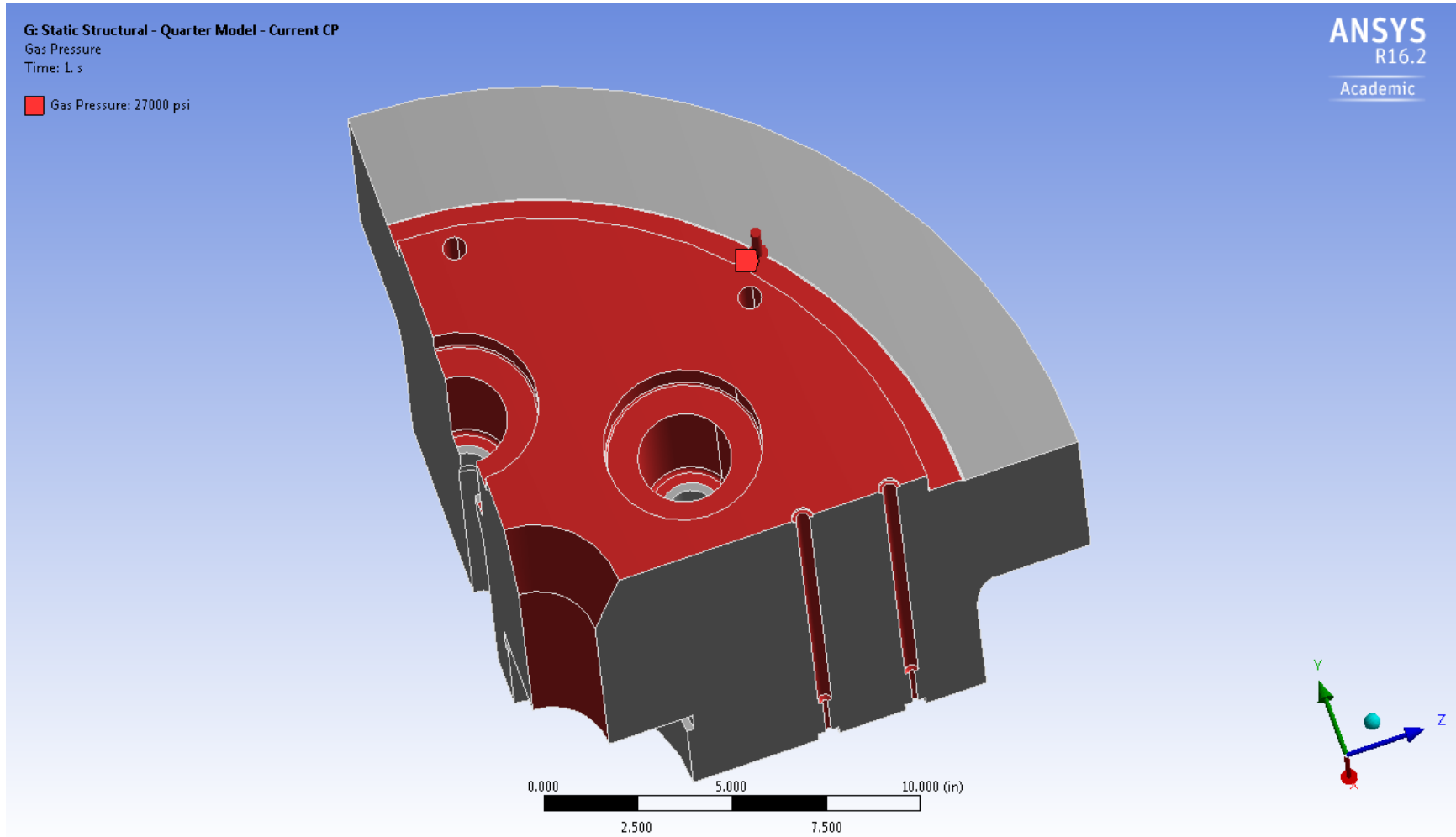
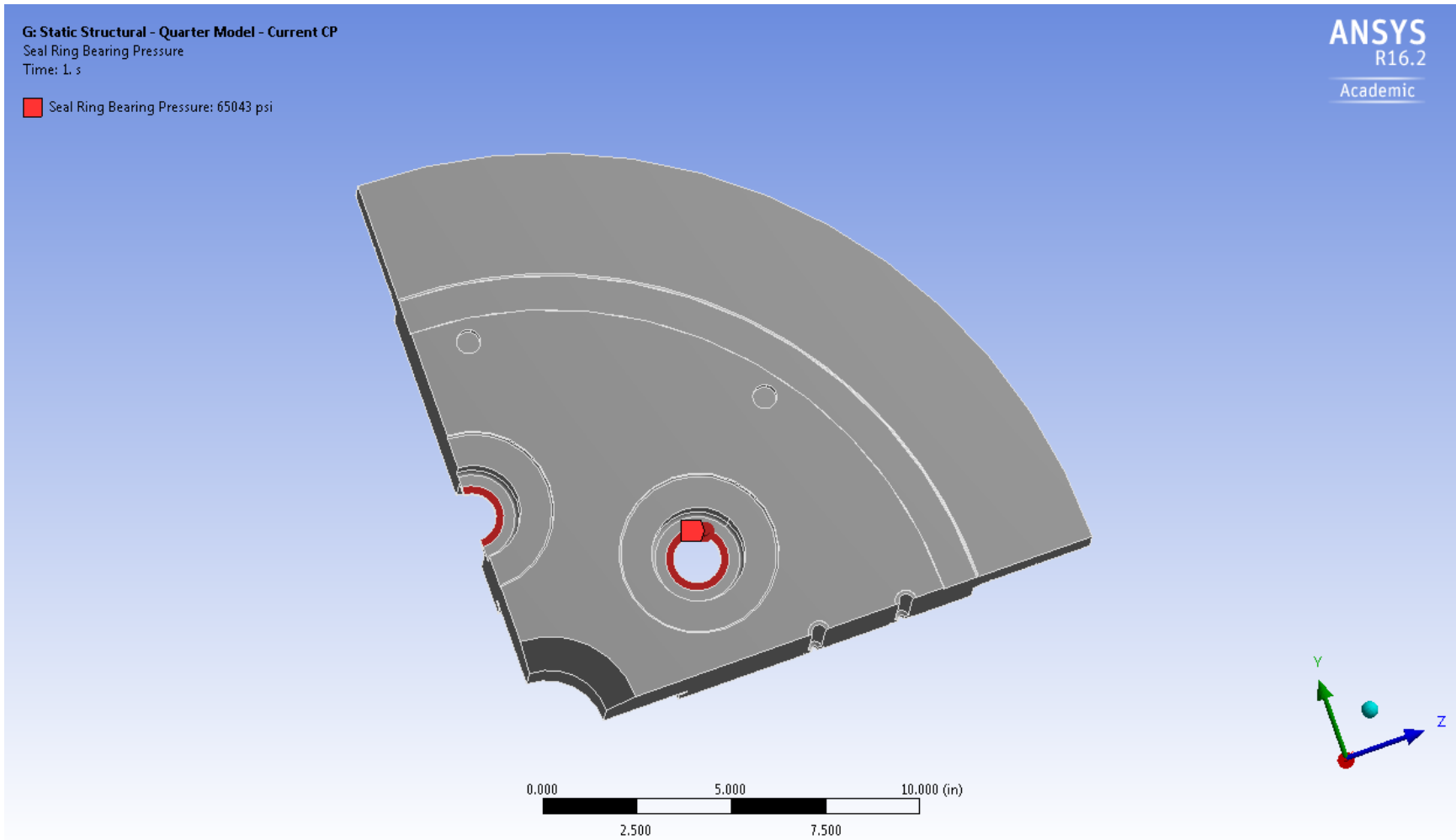
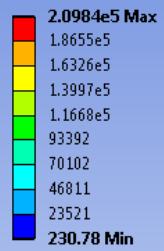


Figure 5.19: Current Closure Plug at 80°F (Case 1) – Gas Pressure (B.C.) – Static Structural



*Figure 5.20: Current Closure Plug at 80°F (Case 1) – Seal Ring Bearing Pressure (B.C.) – Static Structural*

G: Static Structural - Quarter Model - Current CP  
Equivalent Stress  
Type: Equivalent (von-Mises) Stress  
Unit: psi  
Time: 1



Von-Mises Stress (psi)

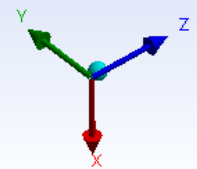
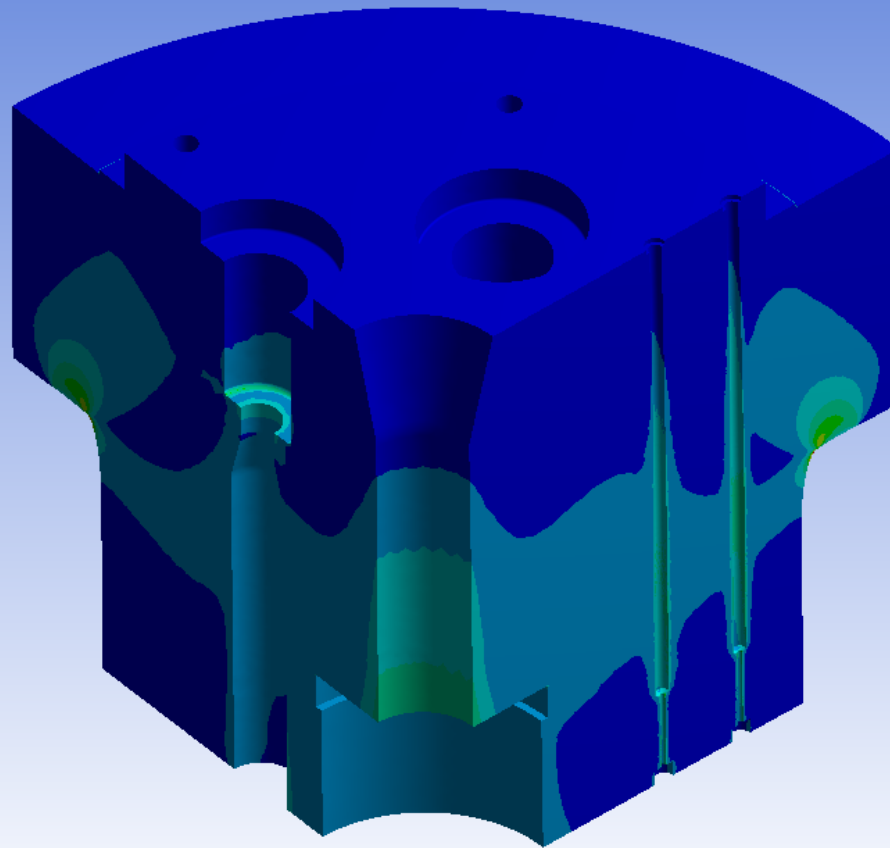
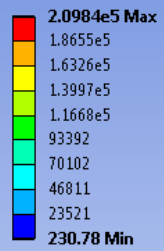


Figure 5.21: Current Closure Plug at 80°F (Case 1) – von-Mises Stress – Static Structural

G: Static Structural - Quarter Model - Current CP  
Equivalent Stress  
Type: Equivalent (von-Mises) Stress  
Unit: psi  
Time: 1



Von-Mises Stress (psi)

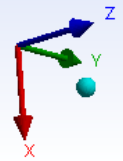
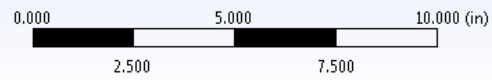
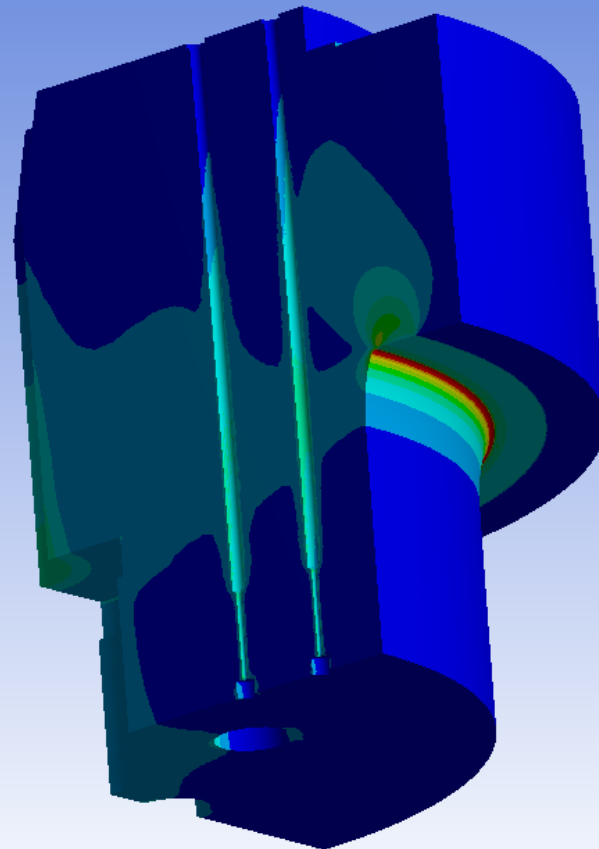
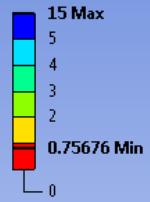


Figure 5.22: Current Closure Plug at 80°F (Case 1) Fillet Area View – von-Mises Stress – Static Structural

G: Static Structural - Quarter Model - Current CP  
Safety Factor - Room Temp. - YS  
Type: Safety Factor  
Time: 1



Safety Factor based on  
Yield Strength = 158.8 ksi

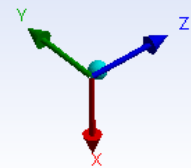
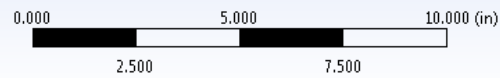
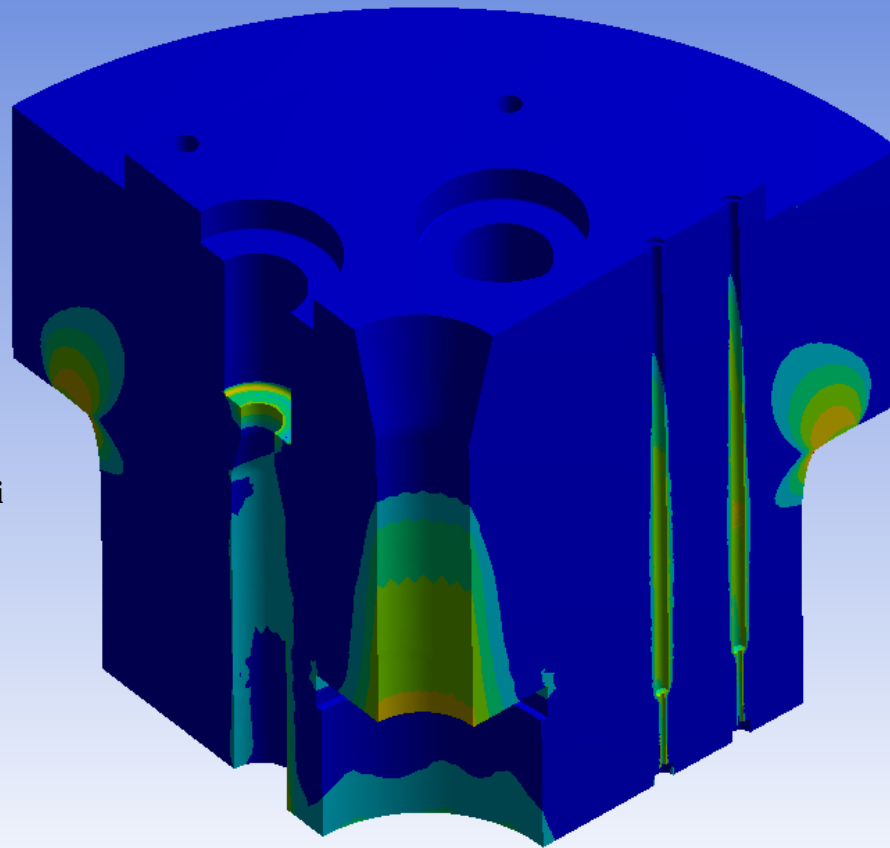
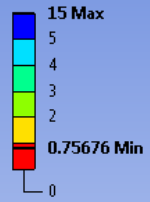
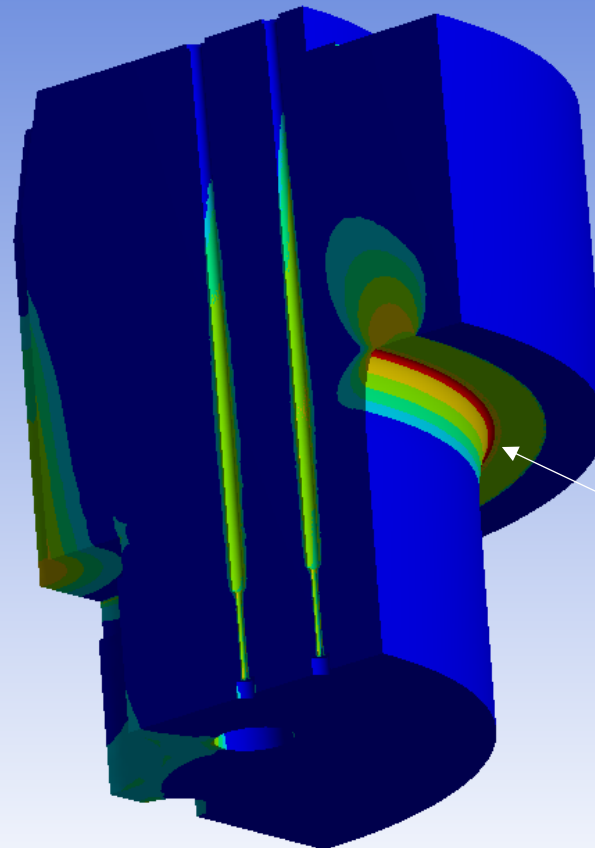


Figure 5.23: Current Closure Plug at 80°F (Case 1) – Safety Factor – Static Structural

G: Static Structural - Quarter Model - Current CP  
Safety Factor - Room Temp. - YS  
Type: Safety Factor  
Time: 1



Safety Factor based on  
Yield Strength = 158.8 ksi



Localized High Stress Area

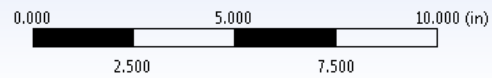
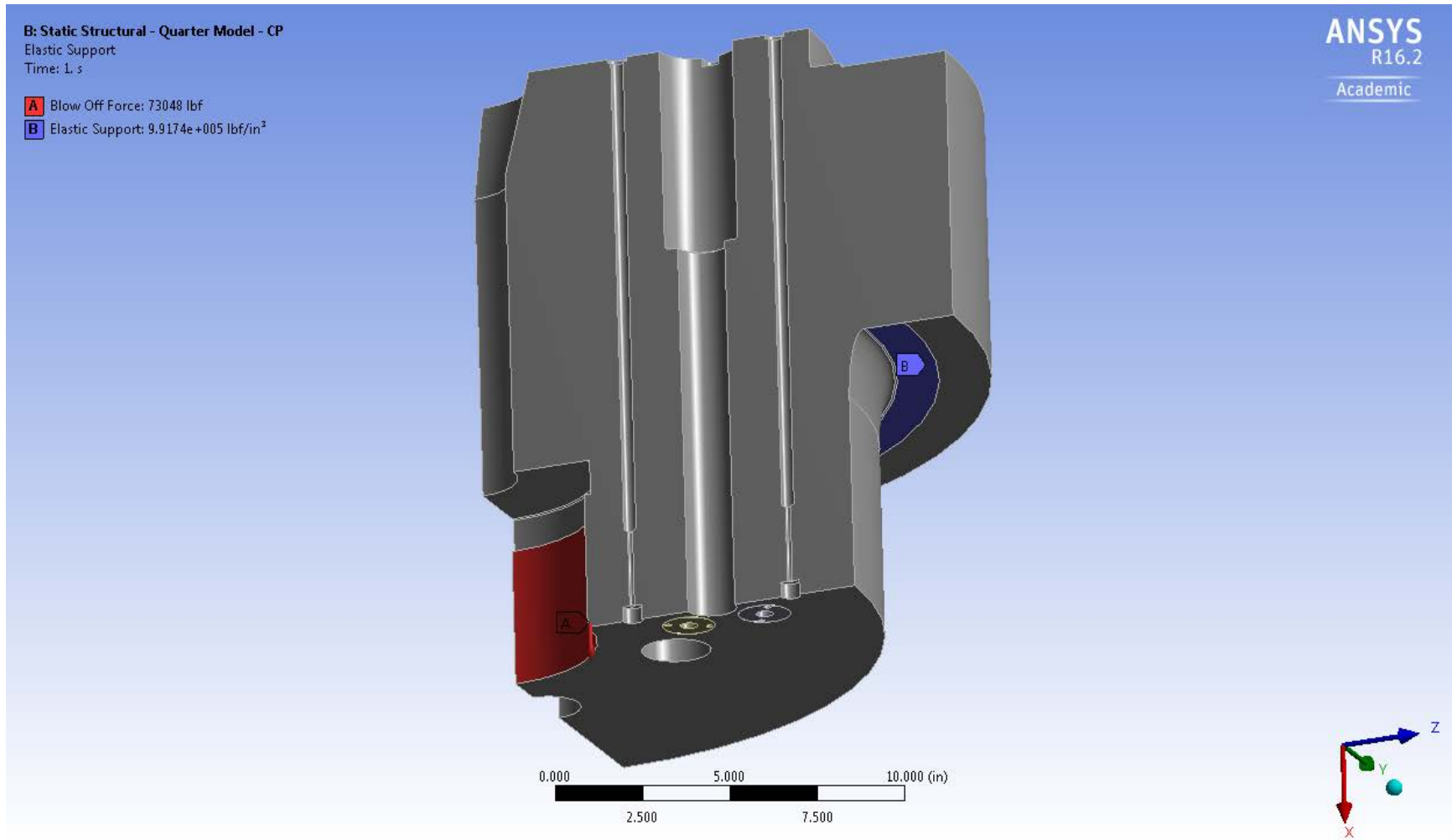


Figure 5.24: Current Closure Plug at 80°F (Case 1) Fillet Area View – Safety Factor – Static Structural





*Figure 5.25: Modified Closure Plug (Case 2 & Case 3) – Blow Off Force & Elastic Support (B.C.s) – Static Structural*

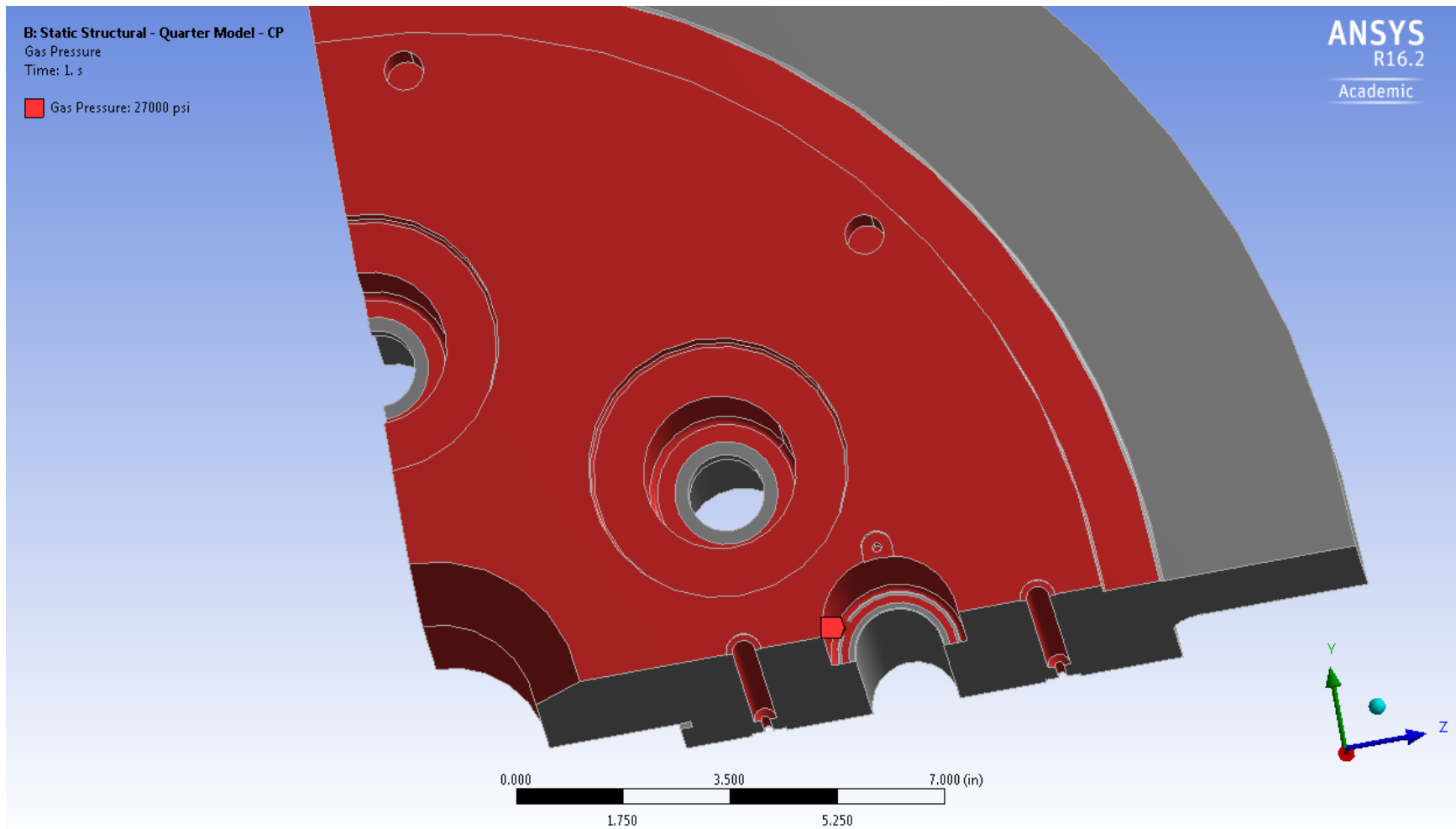
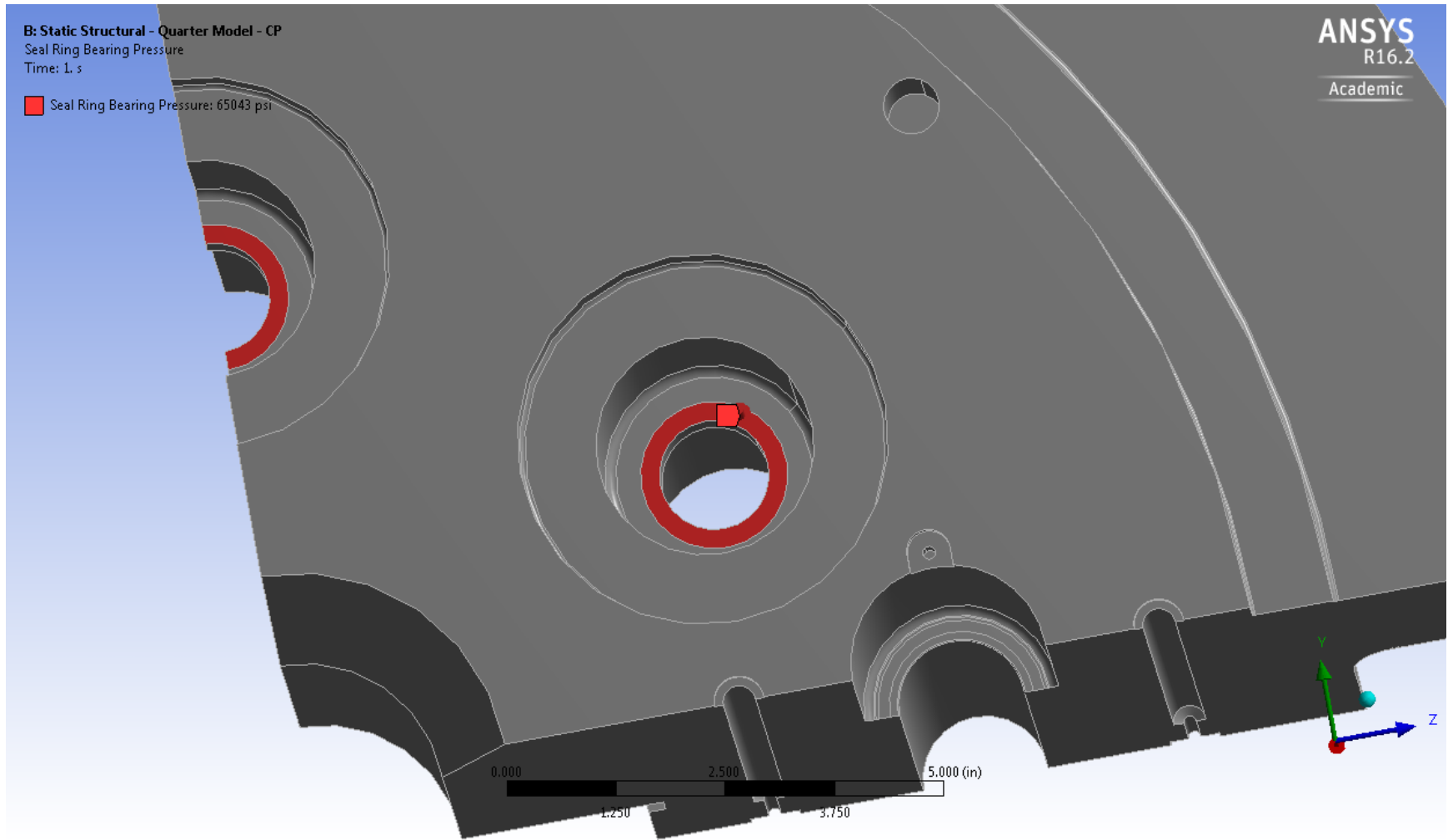
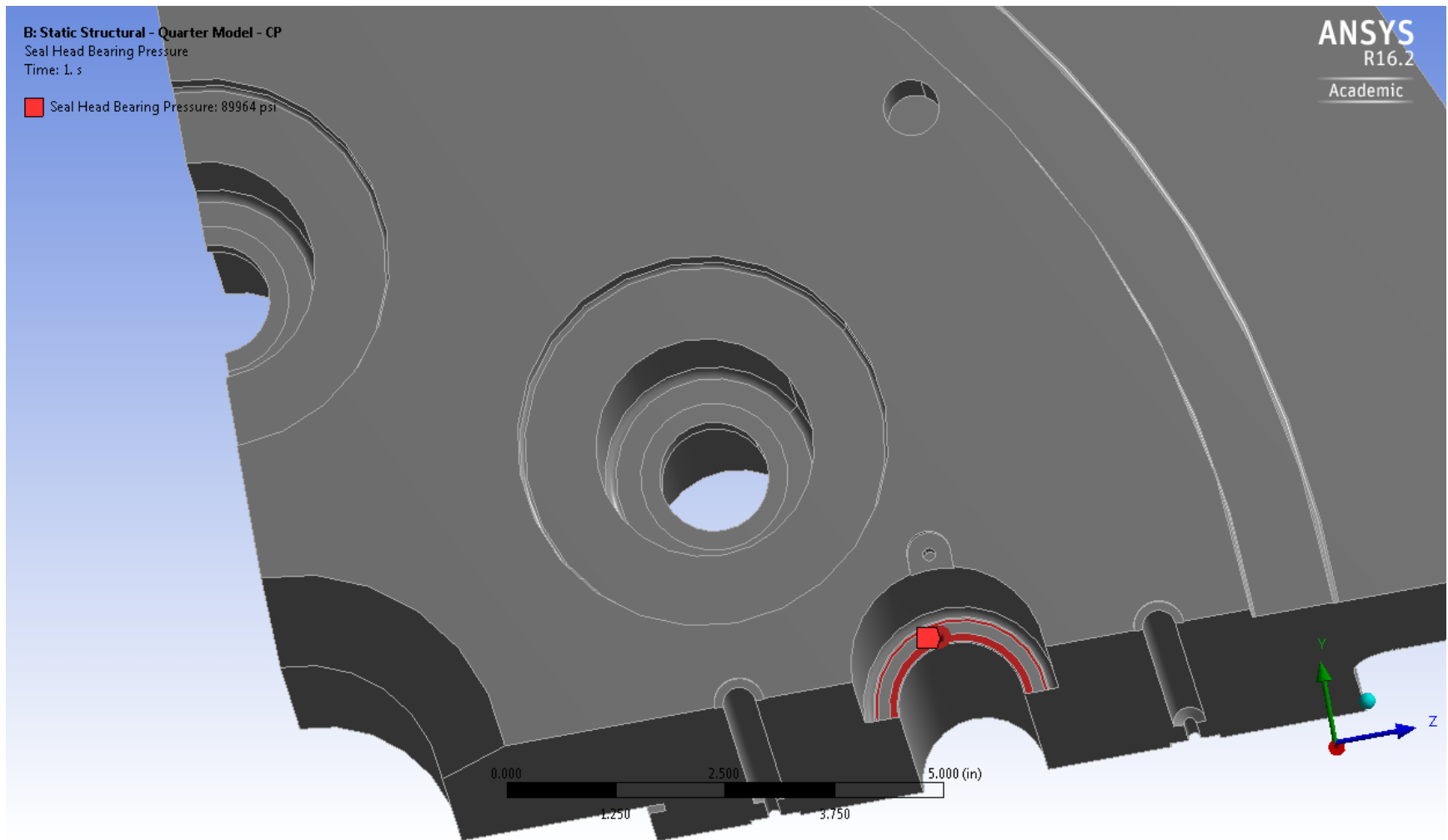


Figure 5.26: Modified Closure Plug (Case 2 & Case 3) – Gas Pressure (B.C.) – Static Structural



*Figure 5.27: Modified Closure Plug (Case 2 & Case 3) – Seal Ring Bearing Pressure (B.C.) – Static Structural*



*Figure 5.28: Modified Closure Plug (Case 2 & Case 3) – Seal Head Bearing Pressure (B.C.) – Static Structural*

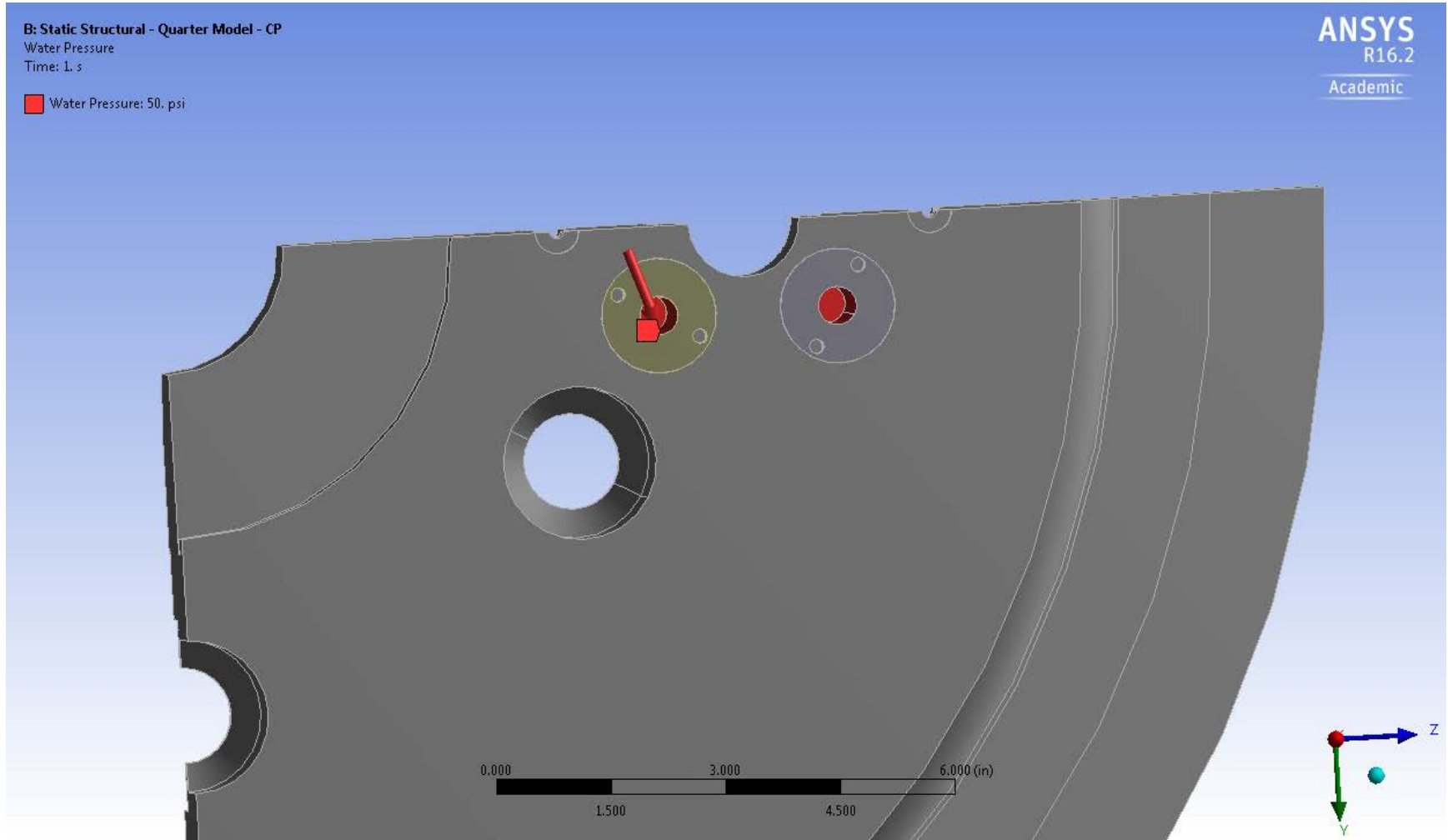
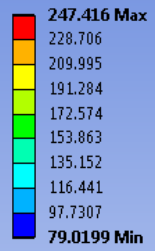


Figure 5.29: Modified Closure Plug (Case 2 & Case 3) – Water Pressure (B.C.) – Static Structural

B: Static Structural - Quarter Model - CP  
Imported Body Temperature  
Unit: °F



Temperature (°F)

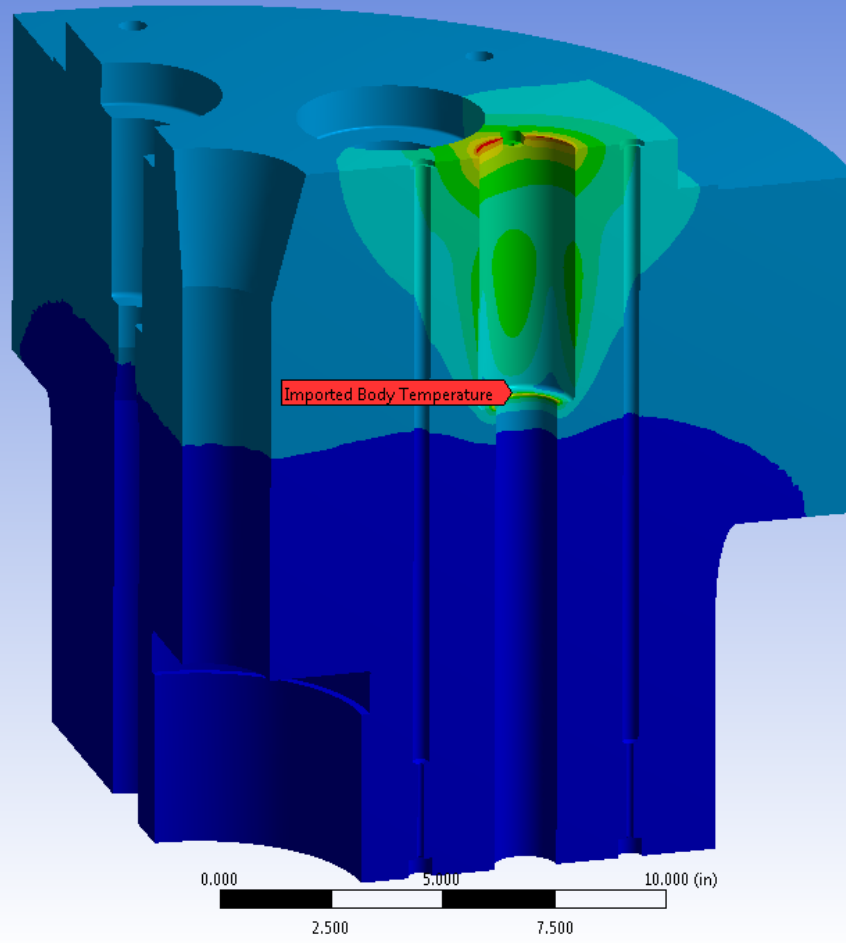


Figure 5.30: Modified Closure Plug with Thermal Load (Case 2) – Body Temp. (Imported S.S. Thermal) (B.C.) – Static Structural

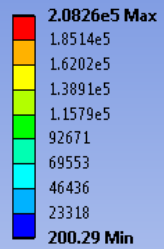
B: Static Structural - Quarter Model - CP

Equivalent (von-Mises) Stress - 81-F-1646\_MOD\_ISD\Solid

Type: Equivalent (von-Mises) Stress

Unit: psi

Time: 1



Von-Mises Stress (psi)

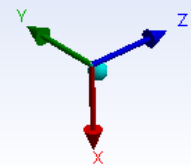
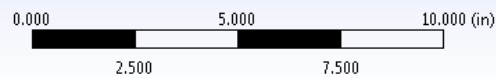
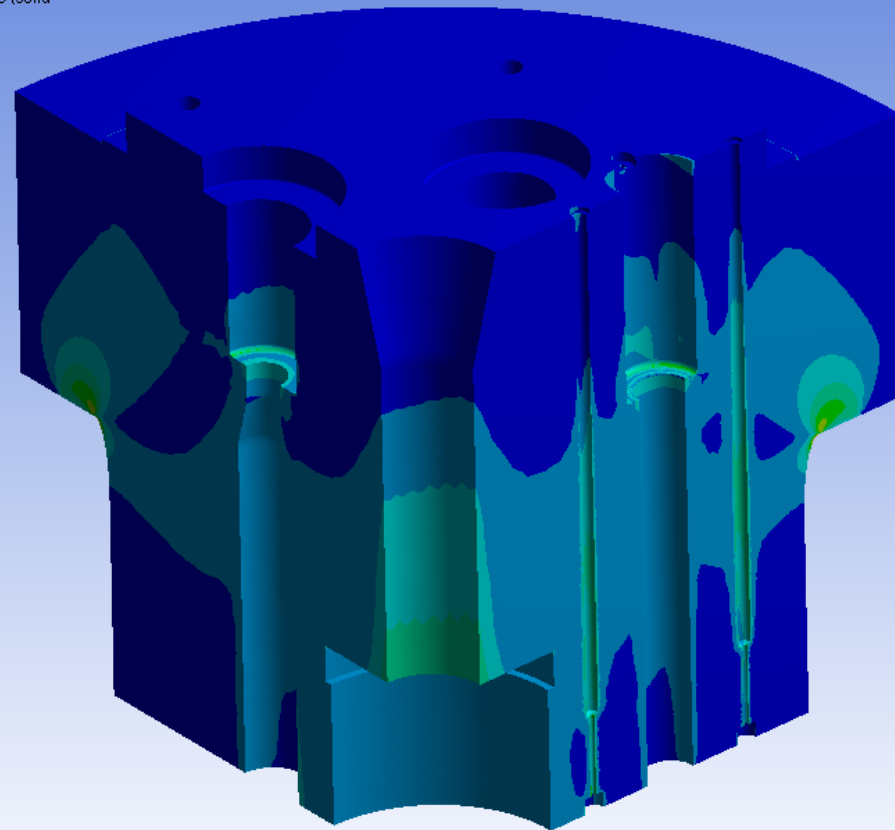
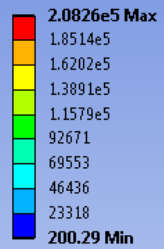


Figure 5.31: Modified Closure Plug with Thermal Load (Case 2) – von-Mises Stress – Static Structural

B: Static Structural - Quarter Model - CP  
Equivalent (von-Mises) Stress  
Type: Equivalent (von-Mises) Stress  
Unit: psi  
Time: 1



Von-Mises Stress (psi)

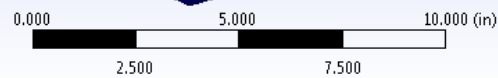
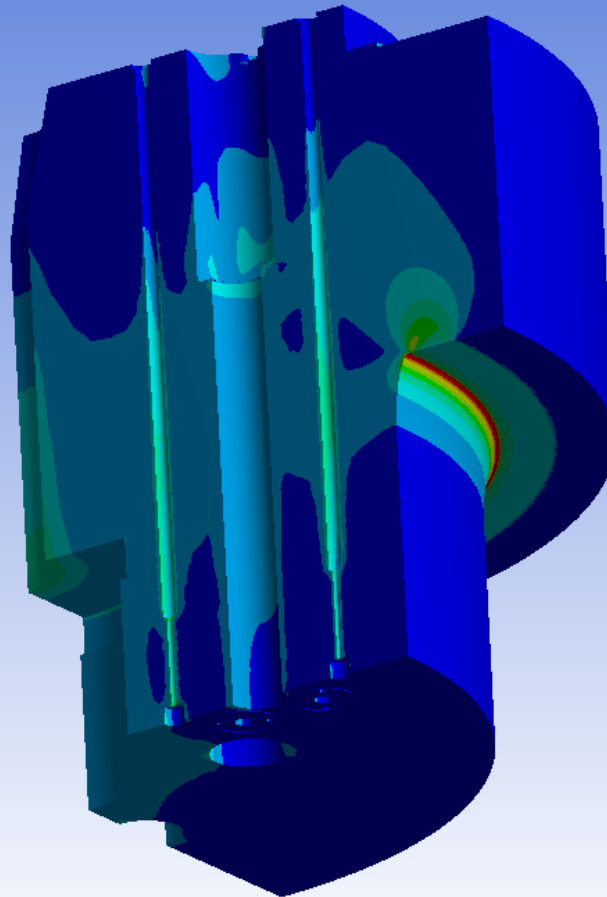
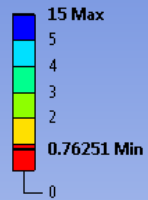


Figure 5.32: Modified Closure Plug with Thermal Load (Case 2) Fillet Area View – von-Mises Stress – Static Structural



B: Static Structural - Quarter Model - CP  
Safety Factor - 81-F-1646\_MOD\_ISD - Room Temp. - YS  
Type: Safety Factor  
Time: 1



**Safety Factor based on  
Yield Strength = 158.8 ksi**

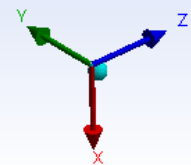
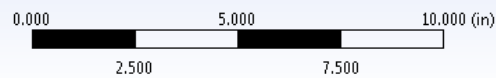
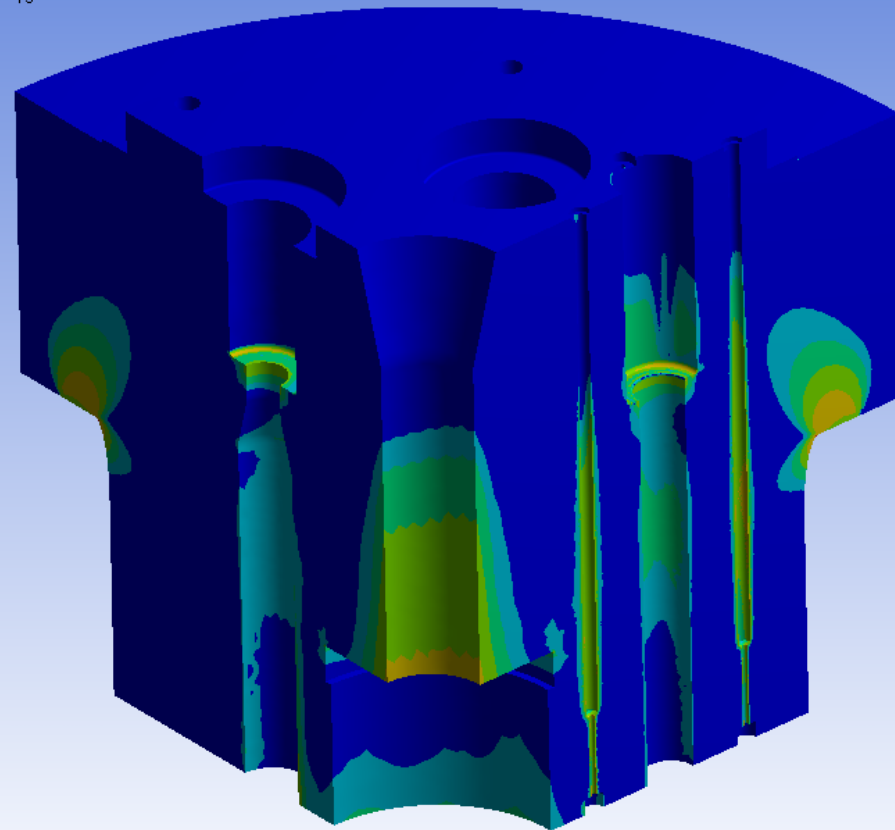
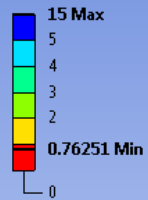
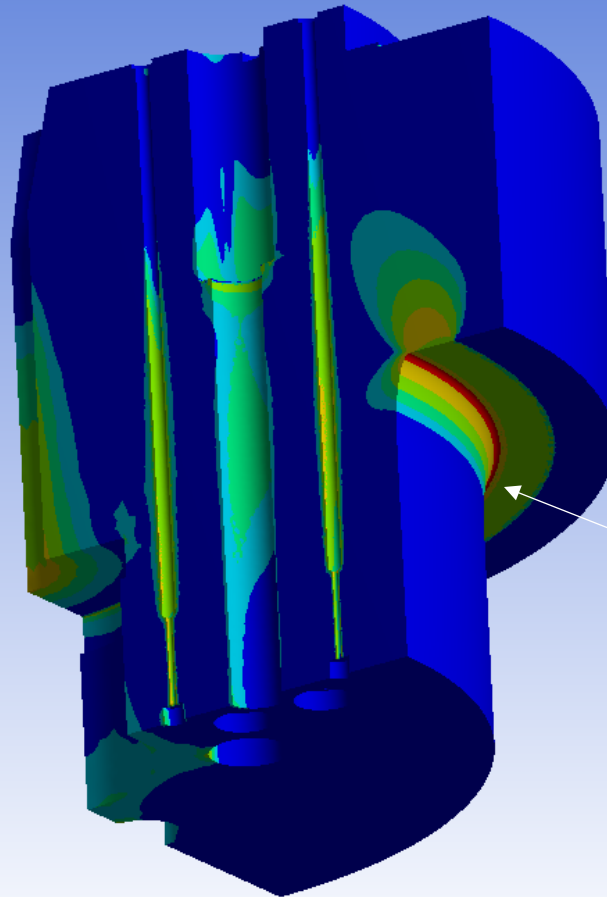


*Figure 5.33: Modified Closure Plug with Thermal Load (Case 2) – Safety Factor – Static Structural*

B: Static Structural - Quarter Model - CP  
Safety Factor - 81-F-1646\_MOD\_ISD - Room Temp. - YS  
Type: Safety Factor  
Time: 1



Safety Factor based on  
Yield Strength = 158.8 ksi



Similar to Case 1

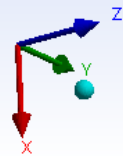
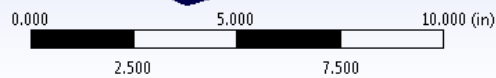


Figure 5.34: Modified Closure Plug with Thermal Load (Case 2) Fillet Area View – Safety Factor – Static Structural

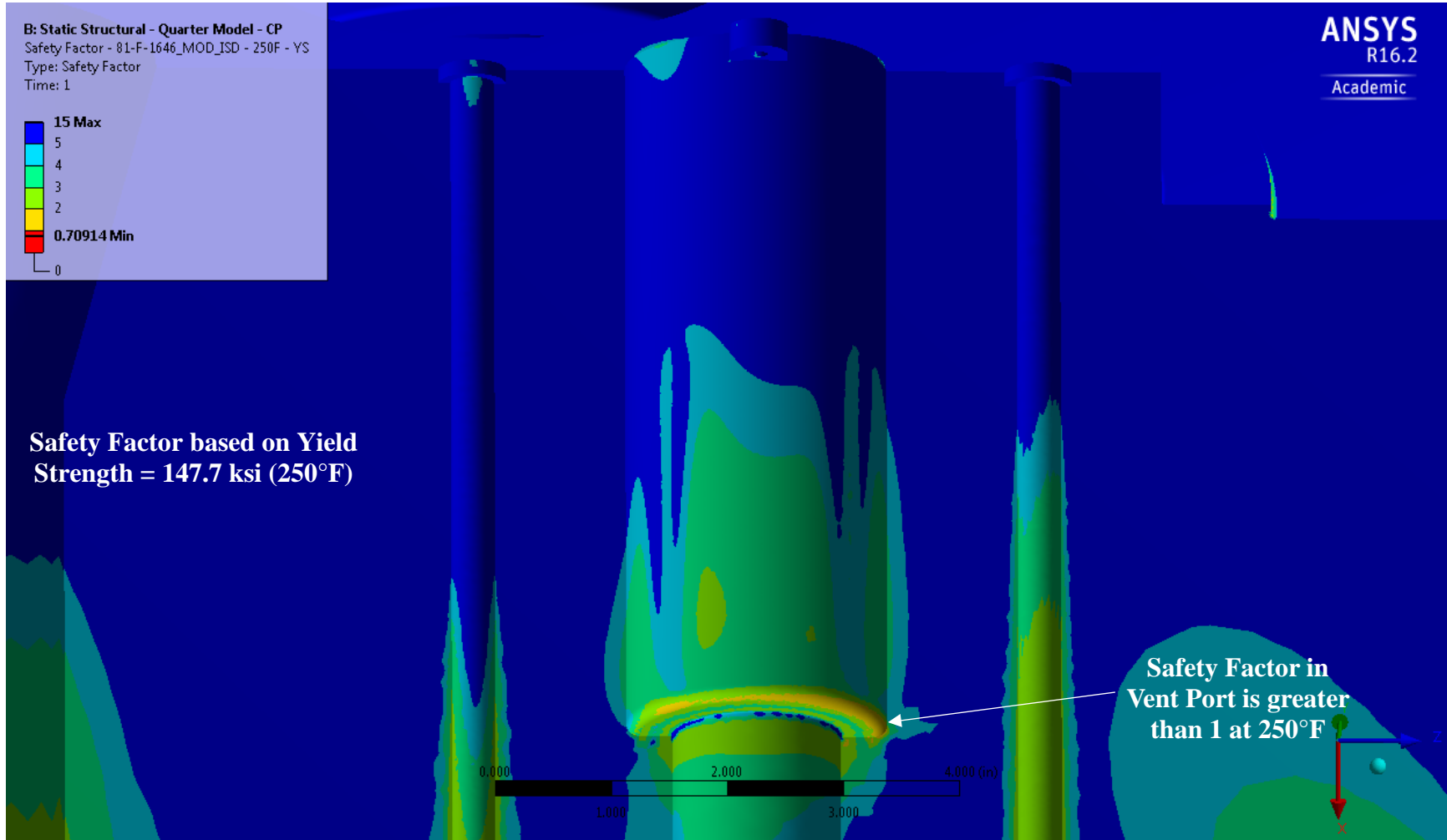
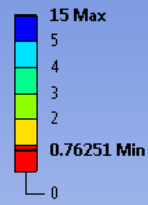
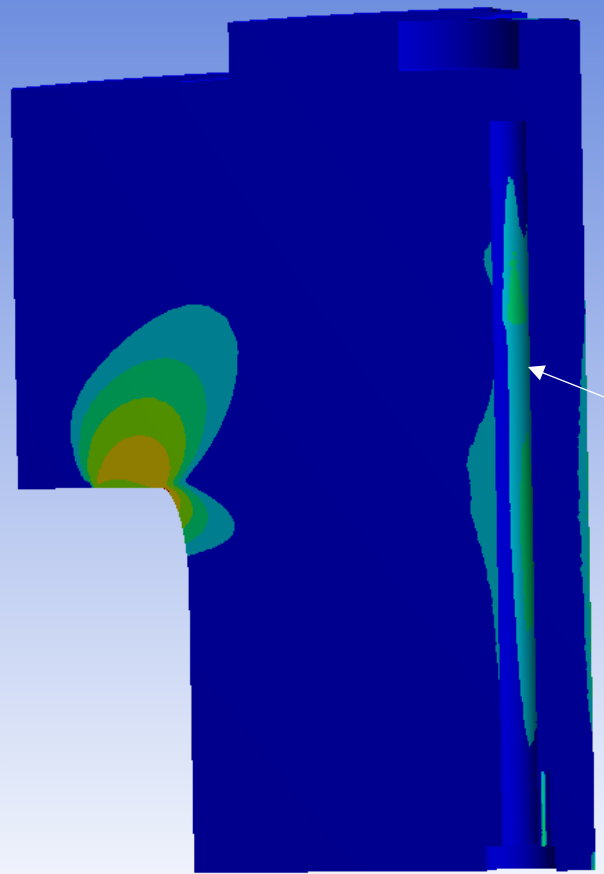


Figure 5.35: Modified Closure Plug with Thermal Load (Case 2) Vent Port View – Safety Factor at 250°F – Static Structural

B: Static Structural - Quarter Model - CP  
Safety Factor - 81-F-1646\_MOD\_ISD - Room Temp. - YS  
Type: Safety Factor  
Time: 1



Safety Factor based on  
Yield Strength = 158.8 ksi



Safety Factor in  
Cooling Port is  
greater than 3

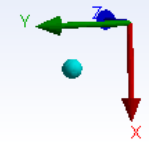
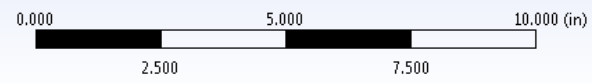


Figure 5.36: Modified Closure Plug with Thermal Load (Case 2) Cooling Port Cross Sect. View – Safety Factor – Static Structural

B: Static Structural - Quarter Model - CP  
Safety Factor - COOLING\_PORT\_BARRIER\Solid1-COOLING\_PORT\_BARRIER\Solid1  
Type: Safety Factor  
Time: 1



**Safety Factor based on  
Yield Strength = 69 ksi**

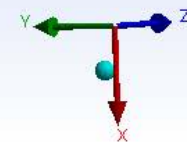
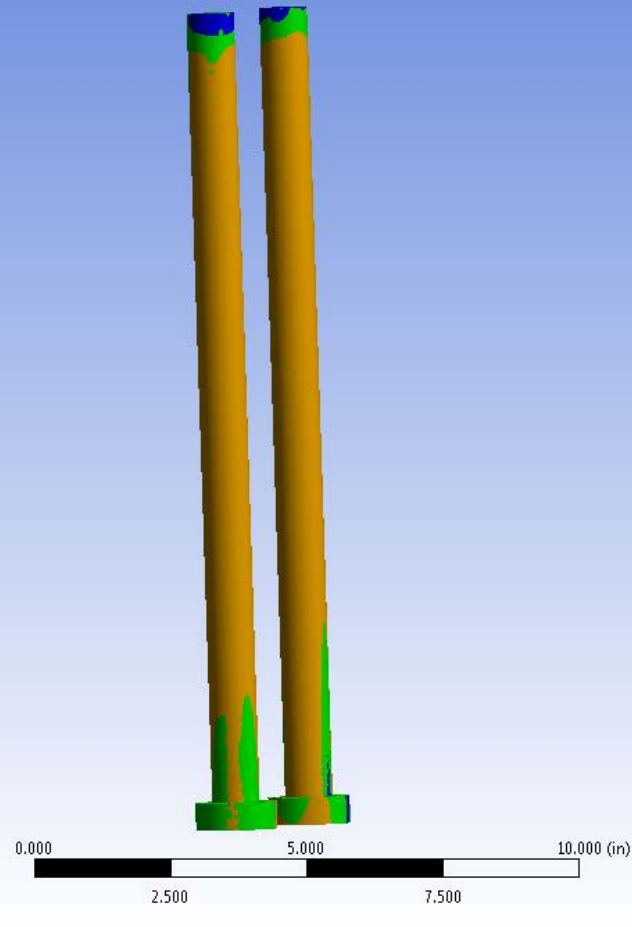
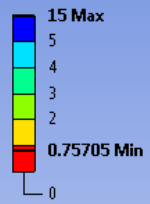
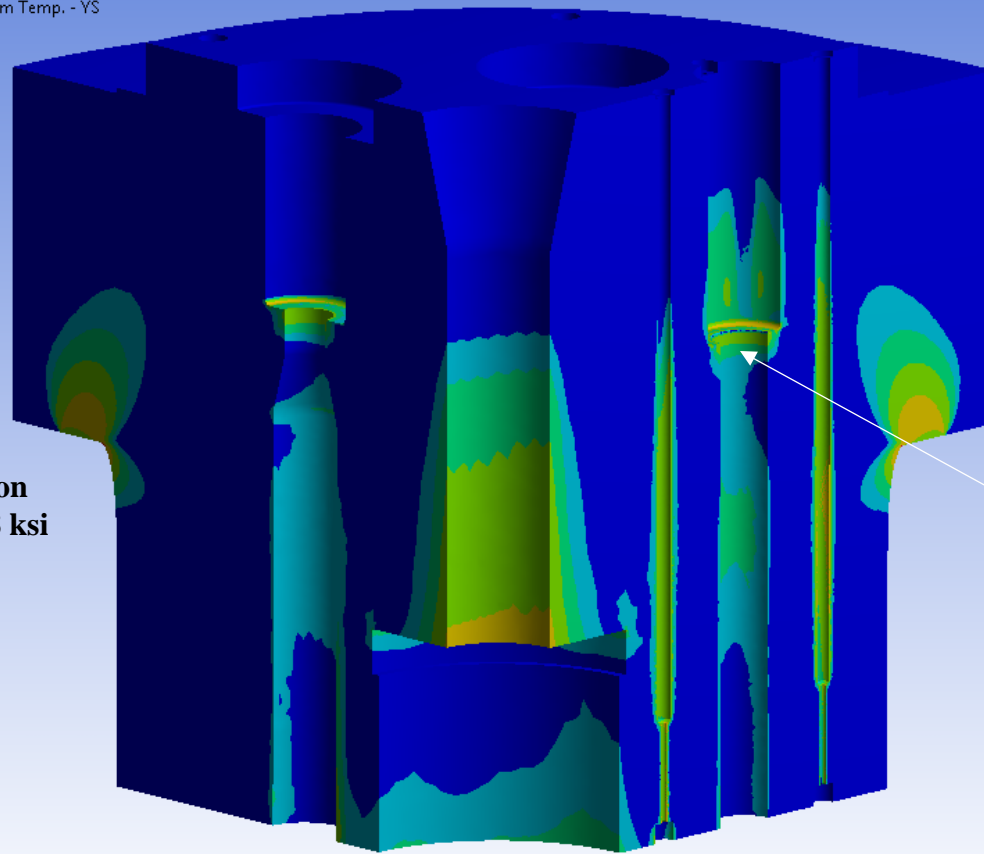


Figure 5.37: Modified Closure Plug with Thermal Load (Case 2) – Corrosion Barriers – Safety Factor – Static Structural

C: Static Structural - Quarter Model - CP - No Thermal Load  
Safety Factor - 81-F-1646\_MOD\_ISD - Room Temp. - YS  
Type: Safety Factor  
Time: 1  
1/9/2017 2:13 PM



Safety Factor based on  
Yield Strength = 158.8 ksi



Similar to Case 2

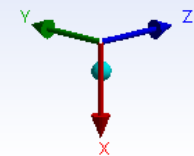
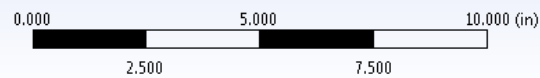
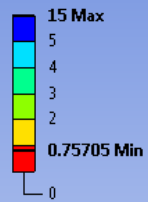
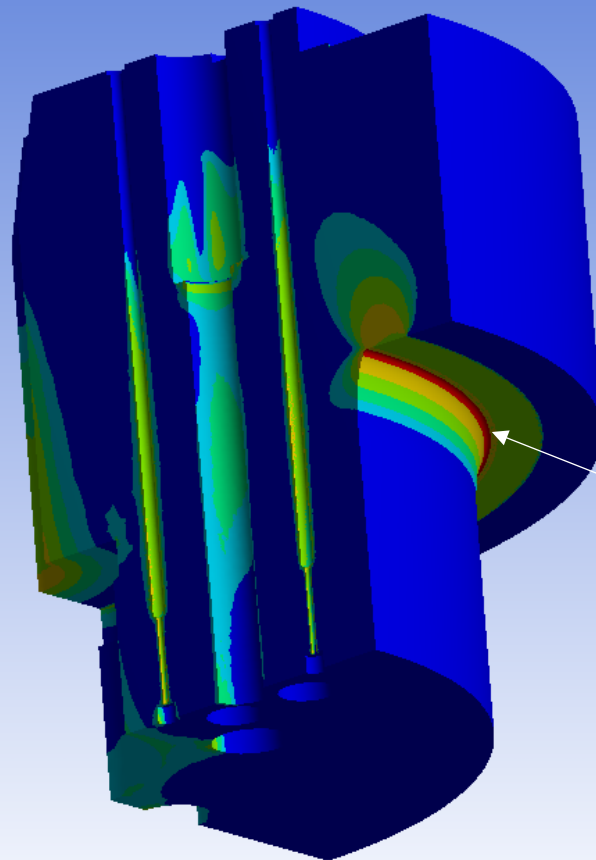


Figure 5.38: Modified Closure Plug at 80°F (Case 3) – Safety Factor – Static Structural

C: Static Structural - Quarter Model - CP - No Thermal Load  
Safety Factor - 81-F-1646\_MOD\_ISD - Room Temp. - YS  
Type: Safety Factor  
Time: 1  
1/9/2017 2:15 PM



Safety Factor based on  
Yield Strength = 158.8 ksi



Similar to Case 1 & 2

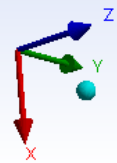
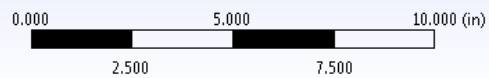
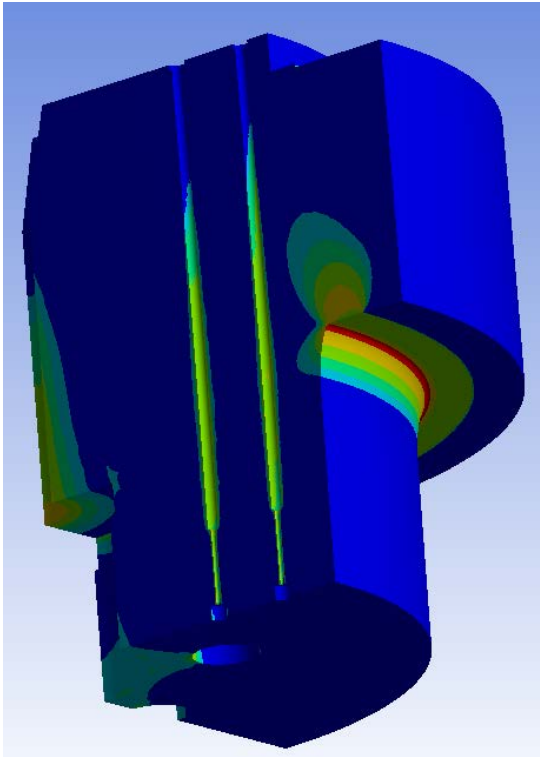


Figure 5.39: Modified Closure Plug at 80°F (Case 3) Fillet Area View – Safety Factor – Static Structural

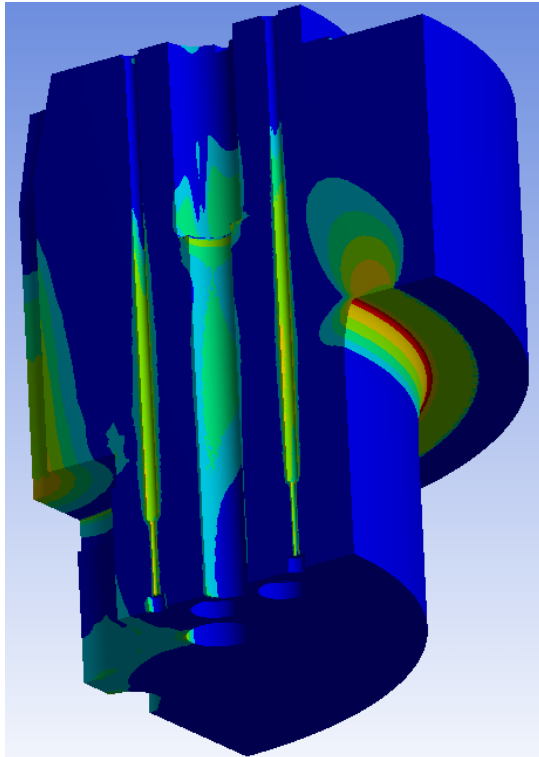
**Case 1  
Current Closure Plug  
at 80°F**

Minimum Safety Factor: 0.75676



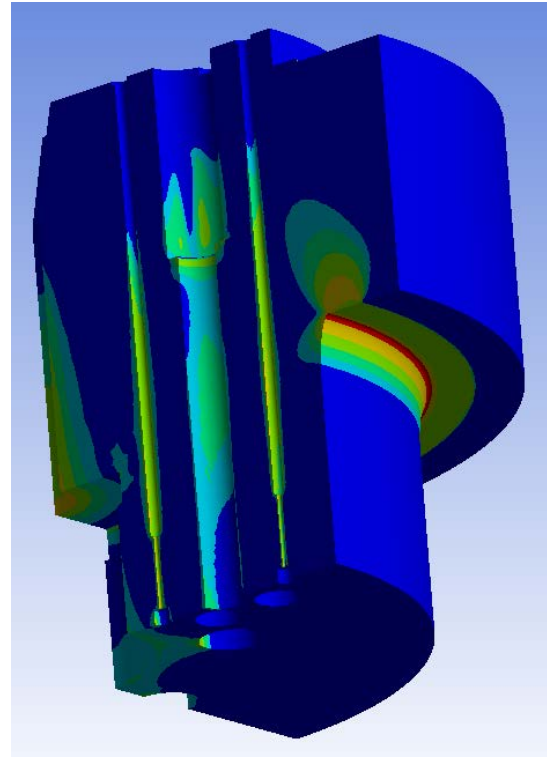
**Case 2  
Modified Closure Plug  
with Thermal Load**

Minimum Safety Factor: 0.76251



**Case 3  
Modified Closure Plug  
at 80°F**

Minimum Safety Factor: 0.75705



**Safety Factor based on Yield Strength = 158.8 ksi**

*Figure 5.40: Closure Plug Comparison – Safety Factor – Static Structural*



5.5: Structural Analyses & Results – Seal Head

This section covers the analysis of the Seal Head with two cases, one with thermal load (Case 1) to simulate a venting run and one at 80°F (Case 2) to simulate a nominal Tunnel run. The Seal Head with thermal load is an analysis for a venting scenario that is expected to be one time use part or sacrificial in use to save other systems of Tunnel 9. While the Seal Head at 80°F is a scenario the part will have to survive multiple run cycles. Table 5.2 summarizes the mesh, convergence, boundary conditions, etc. used for each Static Structural analysis case for the Seal Head.

	<b>Case 1</b>	<b>Case 2</b>
	<b>Seal Head with Thermal Load</b>	<b>Seal Head at 80°F</b>
<b><u>Boundary Conditions</u></b>	Fig. 5.41 to Fig. 5.44	Fig. 5.41 to Fig. 5.43
Frictionless Support (Seal Head Bearing Pressure)	✓	✓
Atmospheric Pressure (14.7 psi)	✓	✓
Gas Pressure (27,000 psi)	✓	✓
Body Temperature (Imported from S.S. Thermal)	✓	✗
<b><u>Mesh</u></b>		
Number of Nodes	1,216,507	2,171,252
Number of Elements	860,589	1,535,033
Element Types	Tetrahedral	Tetrahedral
Convergence	Manual for von-Mises Stress (Adaptive not Supported with Imported Thermal Load)	Adaptive von-Mises Stress & Safety Factor

*Table 5.2: Structural Analyses Setup Summary – Seal Head*

The Seal Head with thermal load (Case 1) boundary conditions are shown in Fig. 5.41 to Fig. 5.44. The von-Mises Stress, Minimum Principal Stress, Maximum Principal Stress are shown in Fig. 5.45, Fig. 5.46, and Fig. 5.47, respectively. The high stress area in the Seal Head is in the port, where gas is venting from. This is expected because large thermal gradients exist in the part at this location, which induce high thermal strains and stresses. The Principal Stresses show that most of the Seal Head is in compression. The other high stress area is the fillet in the female port for the high pressure fitting and piping, which is due to the gas pressure applying a shearing force to push that area out of the Seal Head. Since the Seal Head in Case 1 is considered a sacrificial part, the safety factor is based on the ultimate tensile strength. The safety factor based on ultimate tensile strength at room temperature is shown in Fig. 5.48. A more conservative calculation is safety factor based on ultimate tensile strength at 1200°F, which is shown in Fig. 5.49. This shows that high stress areas are below a safety factor of 1.0, but they are localized to areas that are in compression. The areas in compression should have higher strength than the bulk ultimate tensile strength used in the calculation. This makes it possible for the Seal Head to fail in a small localized area and not catastrophically fail which allows for sacrificial use.

The Seal Head at 80°F (Case 2) boundary conditions are shown in Fig. 5.41 to Fig. 5.43. The von-Mises Stress is shown in Fig. 5.50, and it is high in the fillet in the female port for the high pressure fitting. The safety factor is based on yield strength, since in this case the part will be cycled for multiple runs and is shown in Fig. 5.51 and Fig. 5.52. The safety factor is higher than 1.0 for the entire part, allowing it to be used for multiple runs during nominal Tunnel test runs.

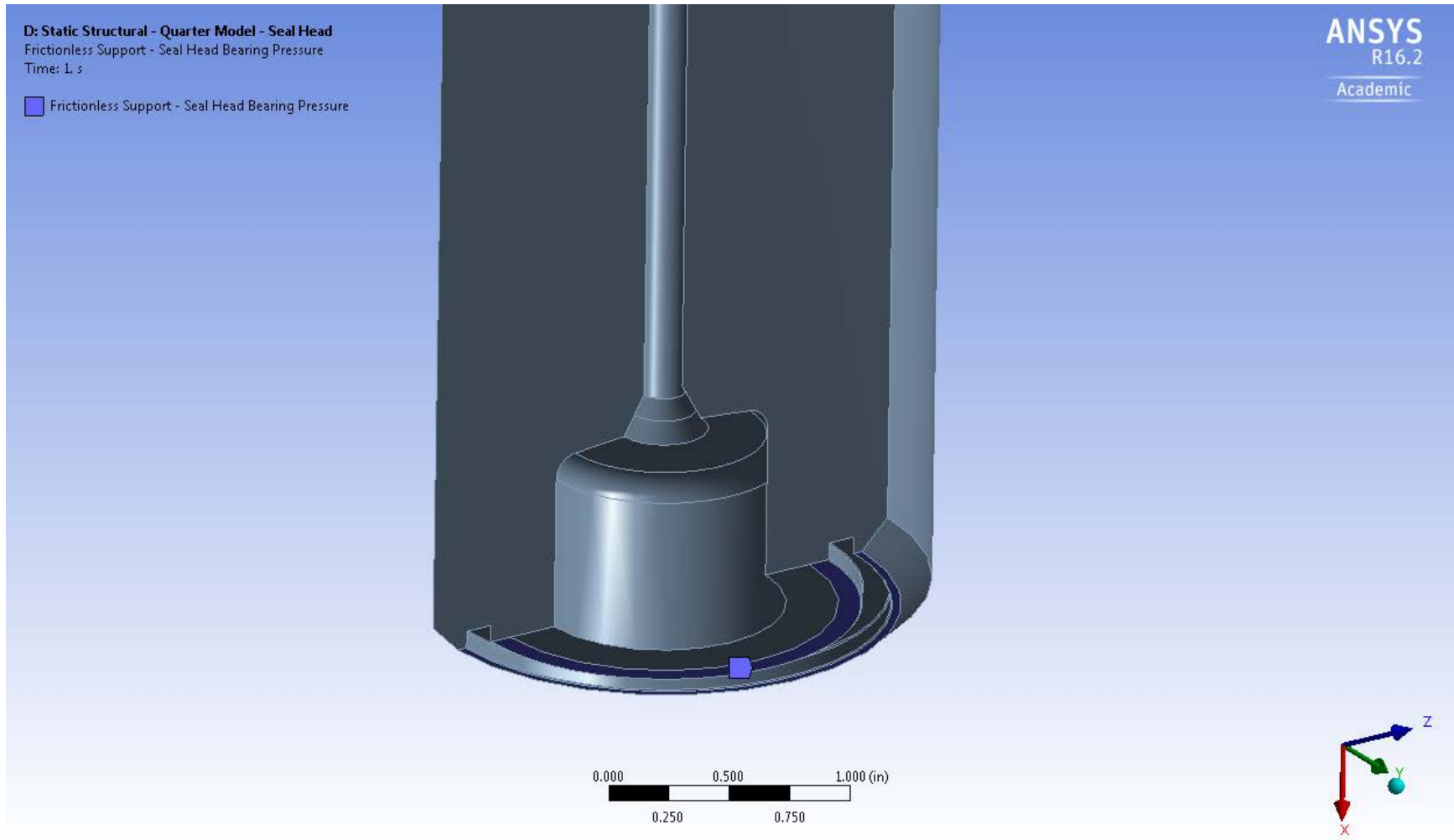


Figure 5.41: Seal Head (Case 1 & Case 2) – Frictionless Support - Seal Head Bearing Pressure (B.C.) – Static Structural

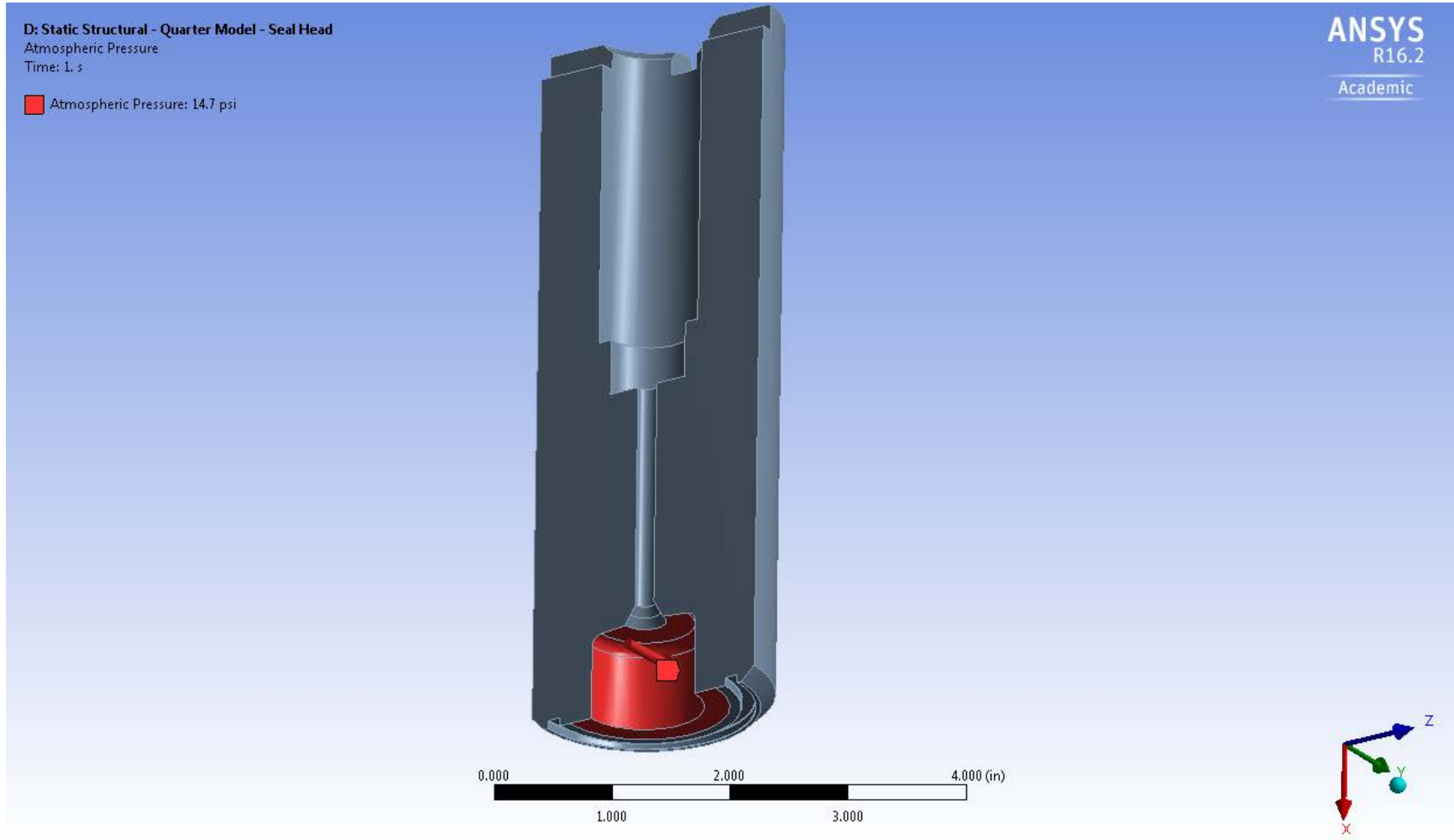


Figure 5.42: Seal Head (Case 1 & Case 2) – Atmospheric Pressure (B.C.) – Static Structural

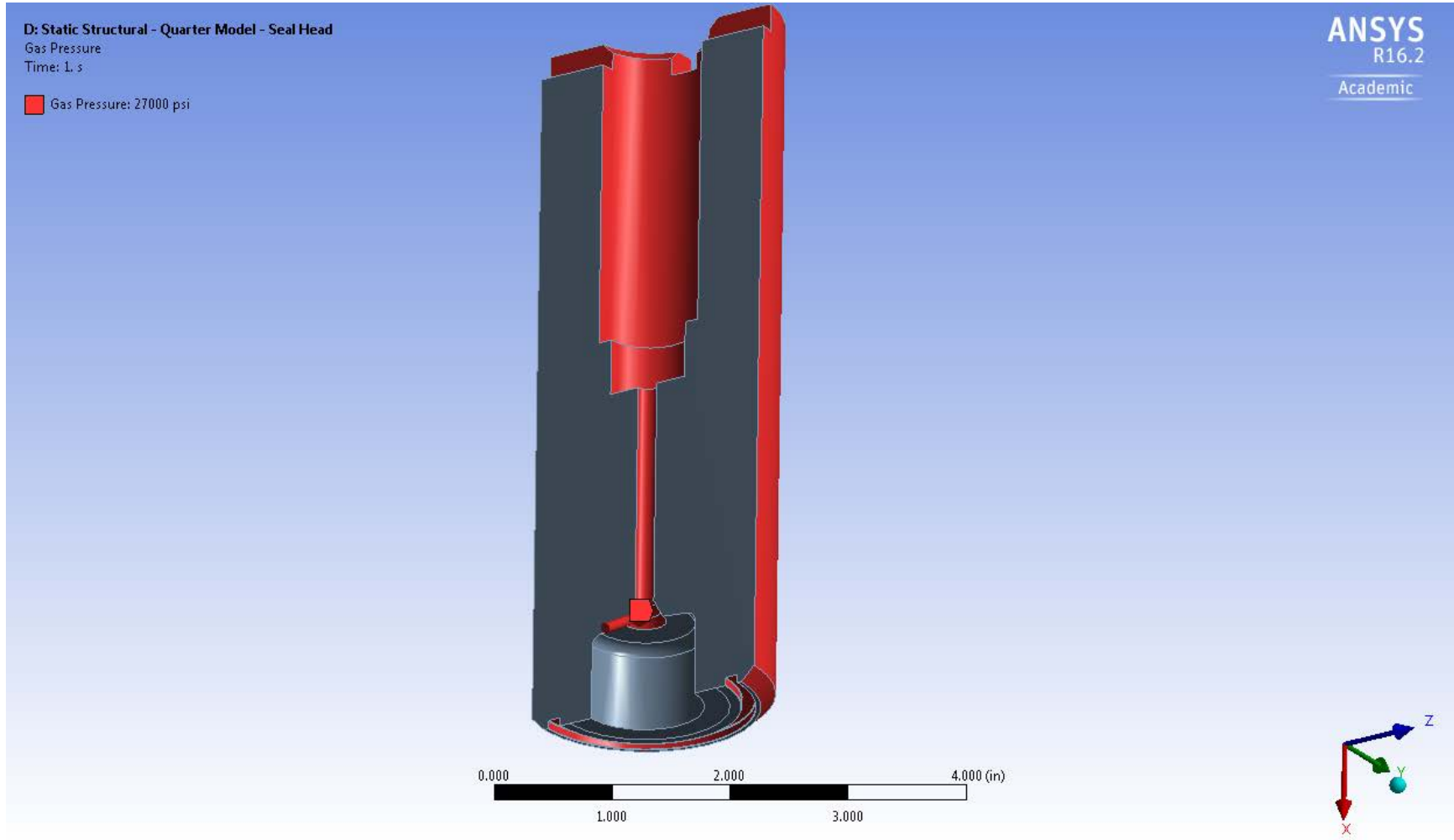
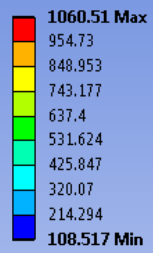


Figure 5.43: Seal Head (Case 1 & Case 2) – Gas Pressure (B.C.) – Static Structural

D: Static Structural - Quarter Model - Seal Head  
Imported Body Temperature  
Unit: °F



Temperature (°F)

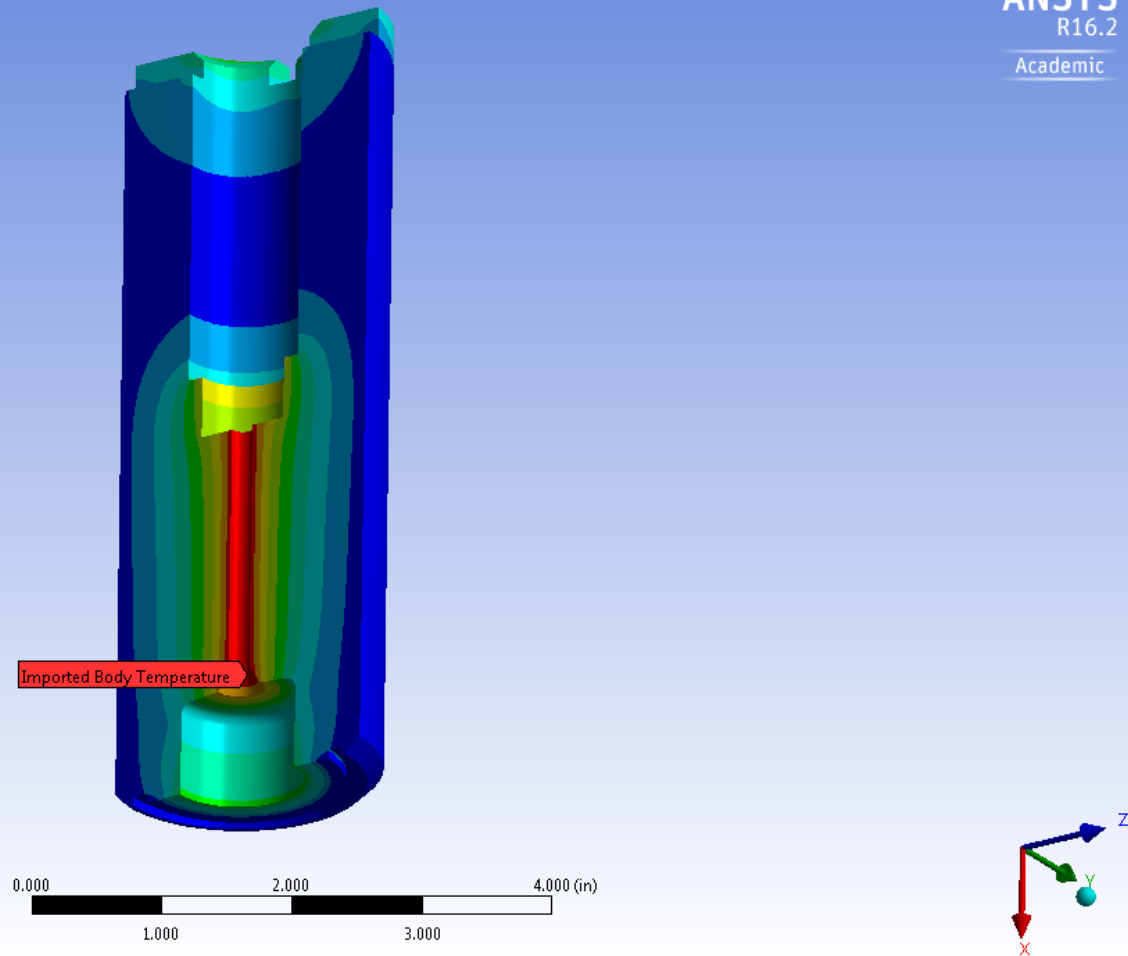
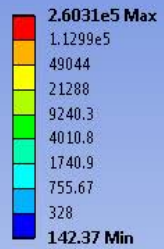


Figure 5.44: Seal Head with Thermal Load (Case 1) – Body Temperature (Imported S.S. Thermal) (B.C.) – Static Structural

D: Static Structural - Quarter Model - Seal Head

Equivalent (von-Mises) Stress  
Type: Equivalent (von-Mises) Stress  
Unit: psi  
Time: 1



Von-Mises Stress (psi)

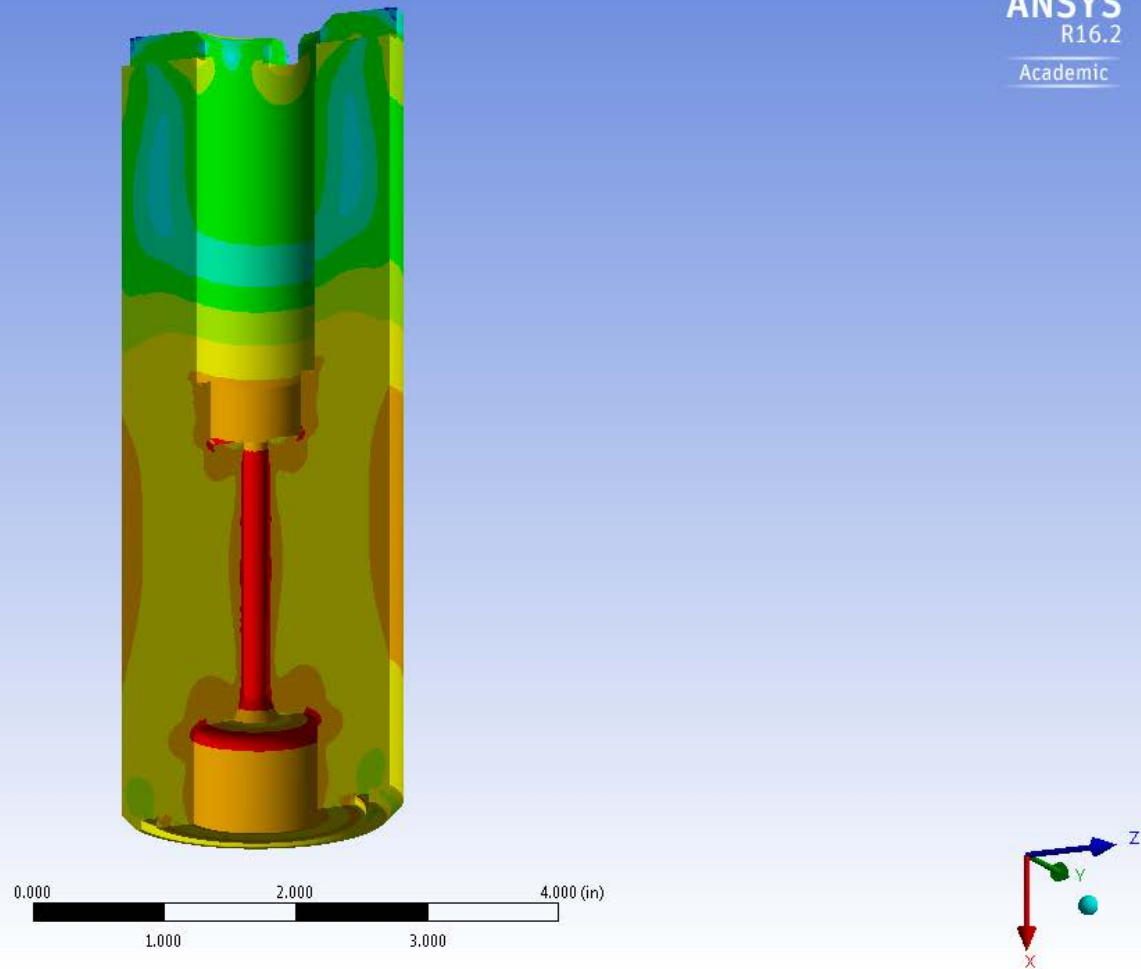


Figure 5.45: Seal Head with Thermal Load (Case 1) – von-Mises Stress – Static Structural

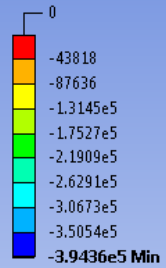
D: Static Structural - Quarter Model - Seal Head

Minimum Principal Stress

Type: Minimum Principal Stress

Unit: psi

Time: 1



**Minimum Principal  
Stress (psi)**

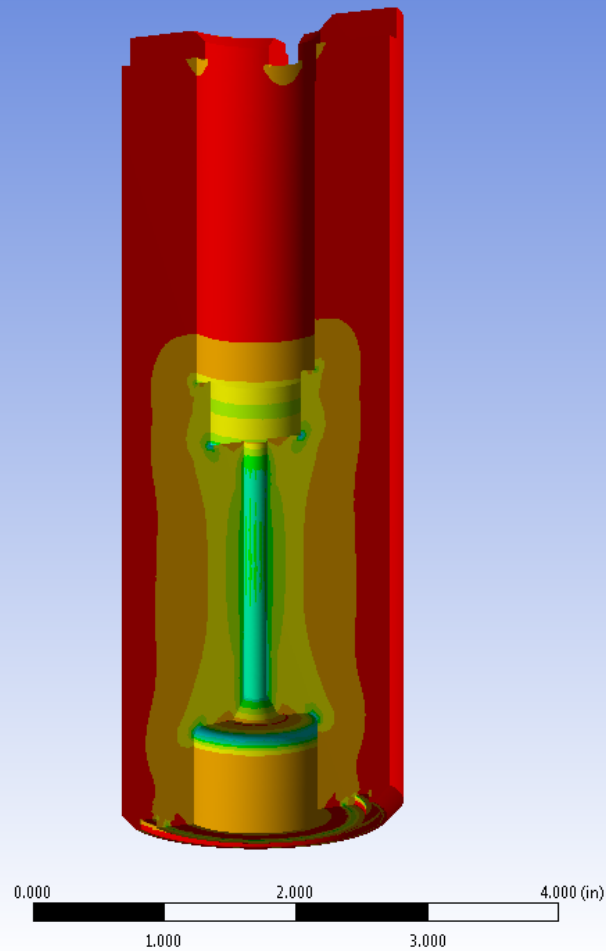


Figure 5.46: Seal Head with Thermal Load (Case 1) – Minimum Principal Stress – Static Structural



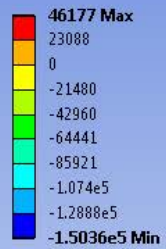
D: Static Structural - Quarter Model - Seal Head

Maximum Principal Stress

Type: Maximum Principal Stress

Unit: psi

Time: 1



Maximum Principal  
Stress (psi)

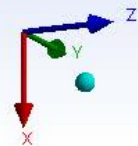
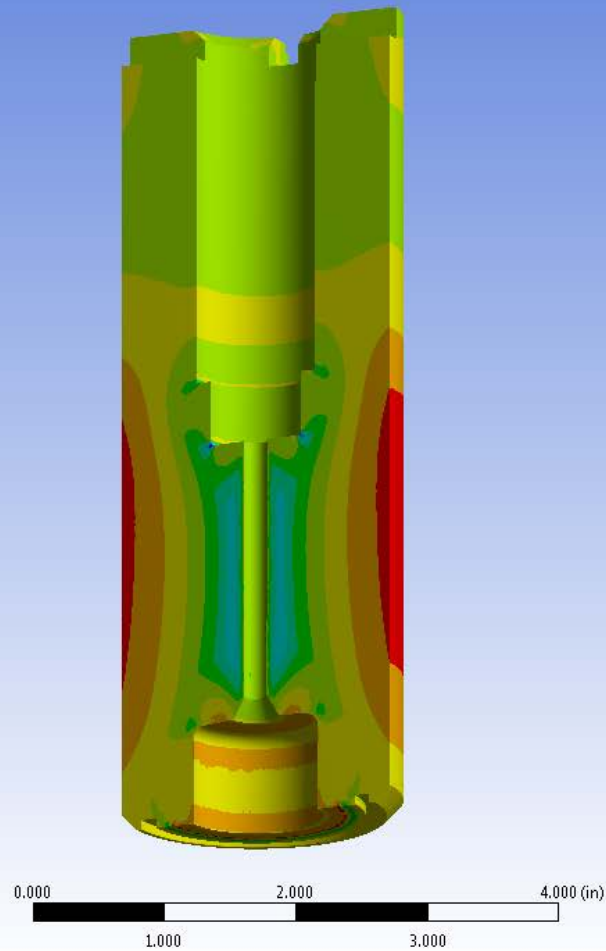
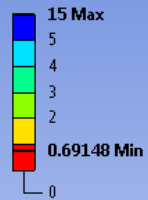


Figure 5.47: Seal Head with Thermal Load (Case 1) – Maximum Principal Stress – Static Structural

D: Static Structural - Quarter Model - Seal Head  
Safety Factor - Room Temp. - UTS  
Type: Safety Factor  
Time: 1



**Safety Factor based on Ultimate Tensile  
Strength = 180 ksi (Room Temp.)**

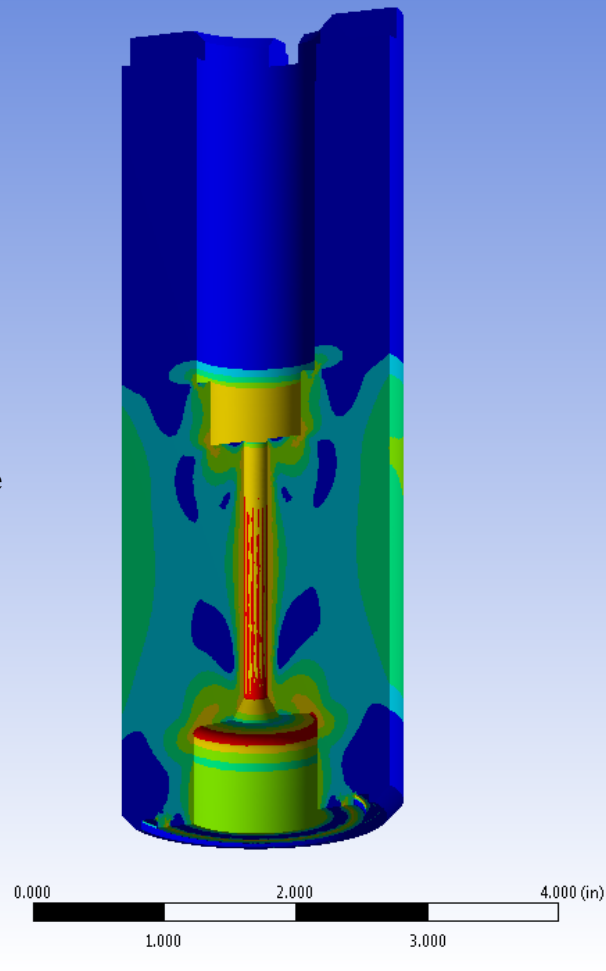
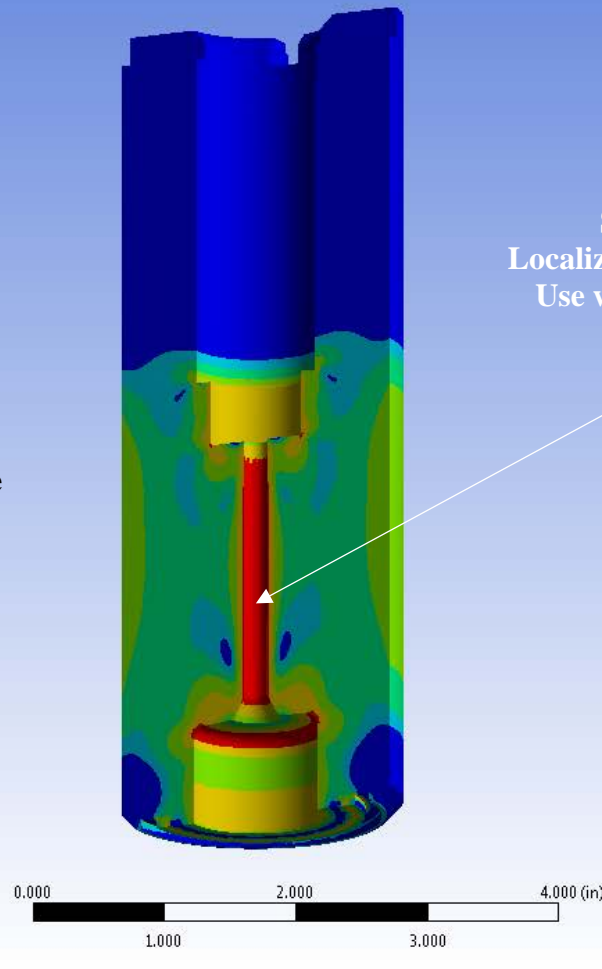


Figure 5.48: Seal Head with Thermal Load (Case 1) – Safety Factor – Static Structural

D: Static Structural - Quarter Model - Seal Head  
Safety Factor - 1200F - UTS  
Type: Safety Factor  
Time: 1



Safety Factor based on Ultimate Tensile  
Strength = 145 ksi (1200°F)



Safety Factor is below 1  
Localized which allows for Sacrificial  
Use without Catastrophic Failure

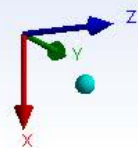
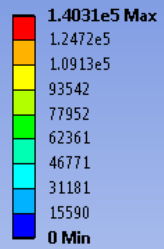


Figure 5.49: Seal Head with Thermal Load (Case 1) – Safety Factor at 1200°F – Static Structural

E: Static Structural - Quarter Model - Seal Head - No Thermal Load

Equivalent (von-Mises) Stress  
Type: Equivalent (von-Mises) Stress  
Unit: psi  
Time: 1



Von-Mises Stress (psi)

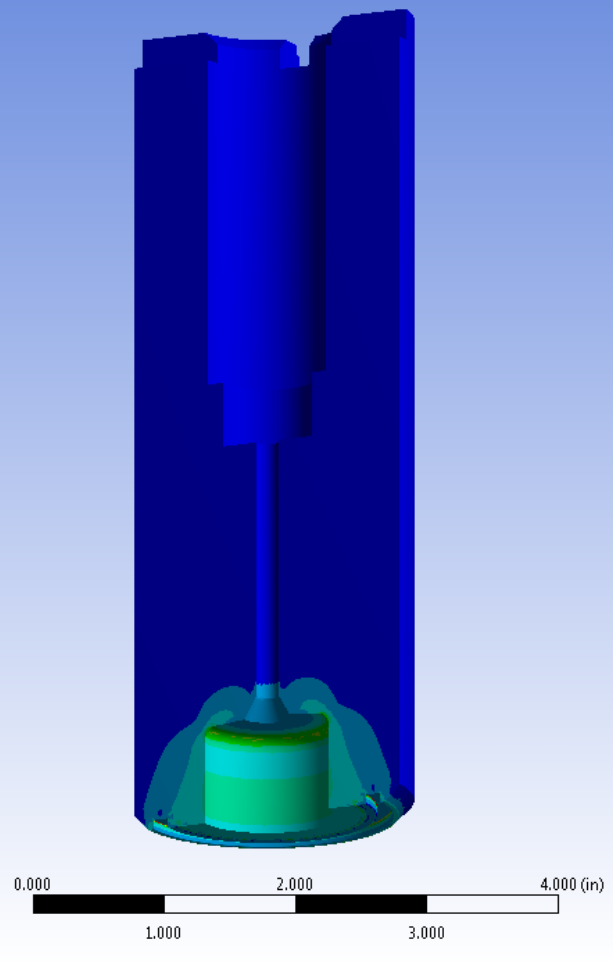
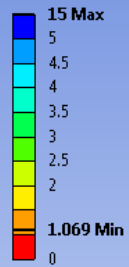
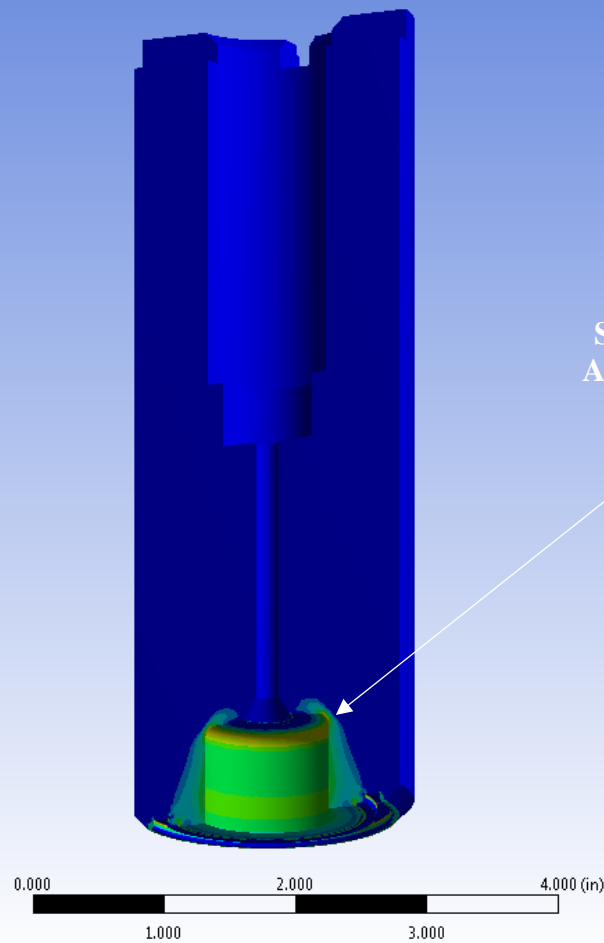


Figure 5.50: Seal Head at 80°F (Case 2) – von-Mises Stress – Static Structural

E: Static Structural - Quarter Model - Seal Head - No Thermal Load  
Safety Factor - Room Temp. - YS  
Type: Safety Factor  
Time: 1



**Safety Factor based on Yield  
Strength = 150 ksi (Room Temp.)**



Safety Factor in Fillet  
Area is greater than 1.5

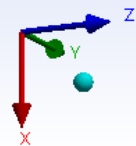


Figure 5.51: Seal Head at 80°F (Case 2) – Safety Factor – Static Structural

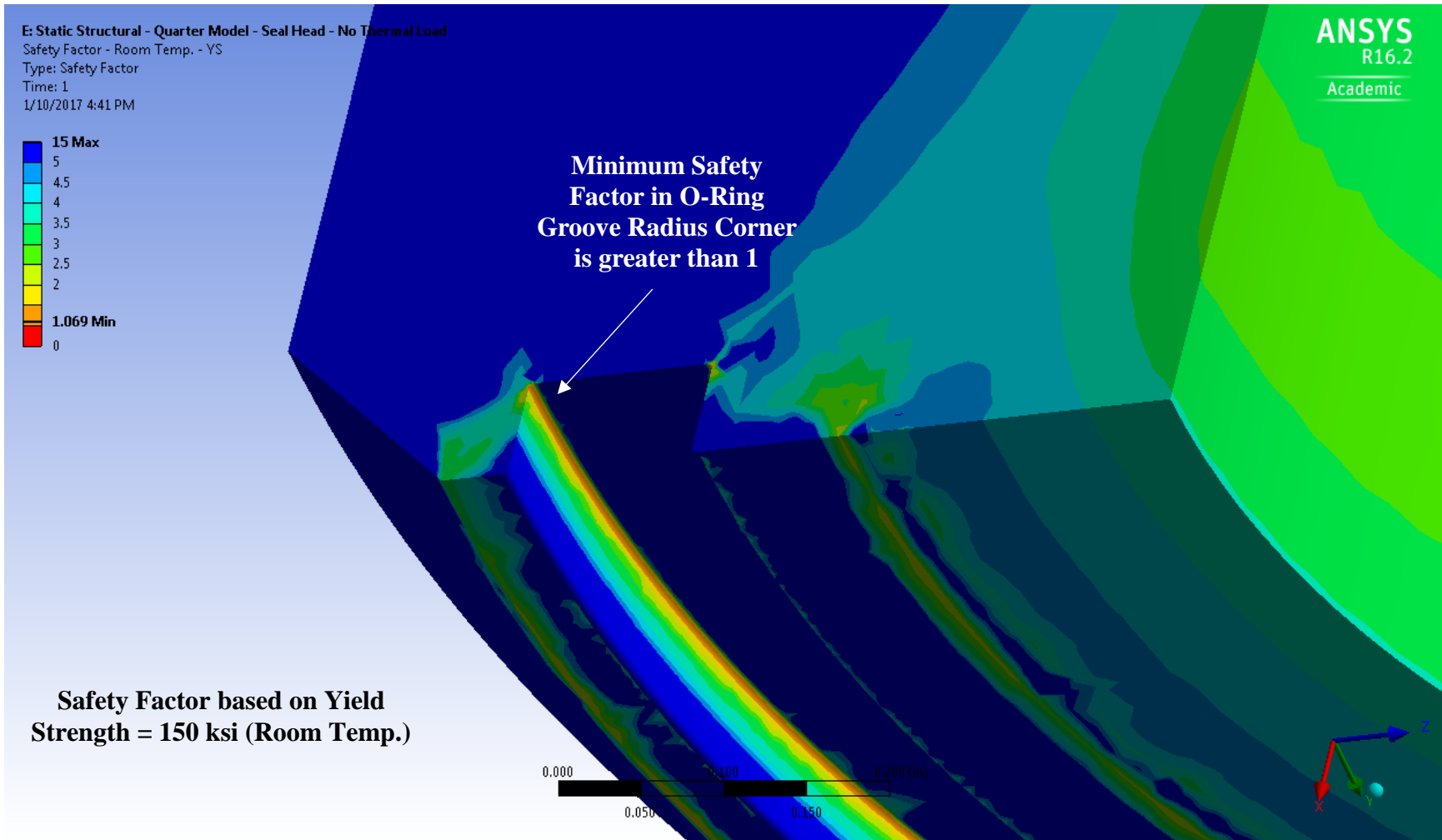


Figure 5.52: Seal Head at 80°F (Case 2) O-Ring Groove – Safety Factor – Static Structural

## 5.6: Summary

The design of a venting system that can handle hot gas at 3400°F and 27,000 psi leverages the ability to mix cold gas and hot gas prior to venting using the mixing Stand Pipe. The mixed gas is then vented through the Closure Plug. This is done by shielding the heating of critical parts such as the Closure Plug. The Closure Plug is shielded by the Seal Head, which is a sacrificial part. The other sacrificial parts are the high pressure and high temperature piping and valves that are connected to the Closure Plug. The design with sacrificial parts allows to save other Tunnel 9 systems in case of an emergency, while only replacing a few parts. The Closure Plug is also actively cooled with water to stay under the 300°F limit. The changes to the Closure Plug compared to the current Closure Plug shows that the planned modifications are within design limits and are capable of running at the harshest Tunnel 9 gas conditions of 3400°F and 27,000 psi. The Seal Head will also be capable of surviving multiple nominal Tunnel 9 run conditions. The Seal Head only becomes a sacrificial part once it is subjected to a venting scenario, after which it is intended to be inspected and replaced if needed.

## Chapter 6: Conclusions, and Future Research

### 6.1: Summary of Findings

- By instrumenting critical locations and leveraging passive cooling, it is possible to vent a nitrogen batch Heater Vessel at 1550°F and 22,000 psi
- Thermal stratification in the Heater Vessel is very localized and transition from cold gas to hot gas occurs in a short distance
- Venting a nitrogen batch Heater Vessel at 3400°F and 27,000 psi through the Bottom Closure Plug appears feasible using the proposed vent system using sacrificial parts

### 6.2: Conclusions

The Heater Vessel at AEDC Hypervelocity Wind Tunnel No. 9 requires the capability to vent nitrogen gas up to 3400°F and 27,000 psi to mitigate risk of hot gas being held or trapped in the Heater Vessel. It was demonstrated that the Tunnel 9 Heater Vessel has the ability to vent nitrogen gas back through the inlet path for gas up to 1550°F and 22,000 psi. This was accomplished by instrumenting critical locations and leveraging passive cooling during the Heater Venting Test. This is possible due to the existence of two thermally distinct gas regions in the pressurized Heater Vessel, one region of cold gas under 300°F and the other region the Heater core which contains the hot gas. This hot gas region was further studied in the Heater Thermal Stratification Test to measure the thermal gradient in this region by instrumenting the Heater core with thermocouples. The results from this test demonstrated that the thermal gradient happens in small region in lower part of the



Heater core. In the transition region, gas temperatures rapidly increase from 300°F to 3400°F gas in about 2 feet of height. Since the transition zone is small, it can be considered all at 3400°F to give the worst case scenario. The gas volume in the Heater Vessel was then treated as cold gas at 300°F (31% of the volume) and hot gas at 3400°F (69% of the volume). This information was used to design a gas venting system through the bottom Closure Plug of the Heater Vessel. The venting system leverages the ability to mix cold gas and hot gas in order to cool the gas prior to venting. It is vented through sacrificial parts shielding the heating of critical parts such as the Closure Plug and other Heater Vessel parts from thermal damage. The venting system is also actively cooled with water to ensure it does not exceed 300°F rated limit of the Closure Plug. The modifications to Closure Plug are within design limits and are capable of running at the harshest Tunnel 9 condition of 3400°F and 27,000 psi. The new venting system will provide a safe way to vent hot gas from the Heater Vessel and save Tunnel 9 systems in case of an emergency.

### 6.3: Research Contributions

The design of the vent system has the potential to improve the safety of Tunnel 9. If an emergency were to occur, which made it necessary to vent hot gas, the proposed system can avoid the loss of multi-million dollar systems to thousands of dollar in sacrificial parts, which would need to be replaced. The design and materials can also be applied to other high temperature and high pressure applications in many other fields that may need similar systems.

#### 6.4: Suggestions for Future Research

The proposed vent system design is a good platform to continue building on. For future testing of the design it is recommended that thermocouples be used in the testing of the parts. Proposed thermocouple locations for testing are on the commercial piping and valves used in the vent path. Also the high pressure piping between the Driver Manifold and bottom of the Closure Plug. The temperature entering the Corrosion Barriers from the city water manifold and the water exiting after use need to be monitored. In the high pressure environment the entrance for hot gas and cold gas sections on Stand Pipe need to be instrumented with thermocouples. The surface of Closure Plug near vent port also needs to be monitored.

Future work includes adding the capability to meter the orifices on the Stand Pipe entrances of hot gas and cold gas. The design of the Stand Pipe also needs to be verified that it will not interfere with other Heater Vessel parts near the bottom of the Closure Plug. It is expected that some modifications to the Heater Base will be needed. The Seal Head tolerances need evaluated to account for thermal expansion, so Seal Head can slip in and out the vent port in the Closure Plug for ease of assembly and replacement. The O-ring gland size on the Seal Head needs to be finalized, and possibly changed to lower stress in the parts. A plastic structural analysis of Seal Head needs to be completed to better understand the complete failure mechanism of the sacrificial part. The city water used for cooling needs to have a manifold designed to ensure an equal flow rate for all eight cooling ports. A transient thermal analysis for the case with no cooling water needs to be completed to see the effect of venting

with a malfunctioning cooling system. The effect of using water cooling jackets on the commercial piping also could be further researched.

## Appendices

### A.1: Stand Pipe Mixing Calculations

The Stand Pipe mixing was calculated in two ways. The Stand Pipe mixing calculation based on temperature ratio is shown in Table A.1. The Stand Pipe mixing calculation based on density and conservation of mass is shown in Table A.2. The density method accounts for large difference in densities, which shows that higher density cold gas cools the lower density hot gas with about 50% cold gas and 50% hot gas mix. The density method is based on the gas pressure, but does not account for the pressure drop in the Heater Vessel, which will change the mixing ratio as gas is vented. While the temperature method results in 75% cold gas and 25% hot gas mix. The temperature based method was used in this design since it is conservative compared to the density based method.

<b><u>Stand Pipe Mixing based on Temperature</u></b>	
<b>Hot Gas Ratio in Piping Mix</b>	<b>0.25</b>
<b>Cold Gas Ratio in Piping Mix</b>	<b>0.75</b>
Mixed Temperature in Piping [deg F]	1075
Hot Gas Temperature [deg F]	3400
Cold Gas Temperature [deg F]	300
ID of Mixed Section [in]	0.1875
Area of Mixed Section [in <sup>2</sup> ]	0.027611654
Area of Hot Gas Section [in <sup>2</sup> ]	0.006902914
Area of Cold Gas Section [in <sup>2</sup> ]	0.020708741
<b>ID of Hot Gas Section [in]</b>	<b>0.09375</b>
<b>ID of Cold Gas Section [in]</b>	<b>0.162379763</b>

*Table A.1: Stand Pipe Mixing Calculation based on Temperature*

<b><u>Stand Pipe Mixing based on Density</u></b>	
Hot Gas Ratio in Piping Mix	0.4973619
Cold Gas Ratio in Piping Mix	0.5026381
Pressure [psi]	27000
Mixed Temperature in Piping [deg F]	1075
Hot Gas Temperature [deg F]	3400
Cold Gas Temperature [deg F]	300
Mixed Gas Density [lbm/in <sup>3</sup> ]	0.015079861
Hot Gas Density [lbm/in <sup>3</sup> ]	0.008021071
Cold Gas Density [lbm/in <sup>3</sup> ]	0.022064555
ID of Mixed Section [in]	0.1875
Area of Mixed Section [in <sup>2</sup> ]	0.027611654
Area of Hot Gas Section [in <sup>2</sup> ]	0.013732985
Area of Cold Gas Section [in <sup>2</sup> ]	0.013878669
Mixed Gas Mass [lbm]	0.00041638
Hot Gas Mass [lbm]	0.000110153
Cold Gas Mass [lbm]	0.000306227
*Assume Length of 1 in	
Mass Conservation	
Mixed Gas Mass – (Hot Gas Mass + Cold Gas Mass) $\approx$ 0	8.65475E-15
ID of Hot Gas Section [in]	0.132232293
ID of Cold Gas Section [in]	0.132931827

*Table A.2: Stand Pipe Mixing Calculation based on Density*

*A.2: Additional Views of Design*

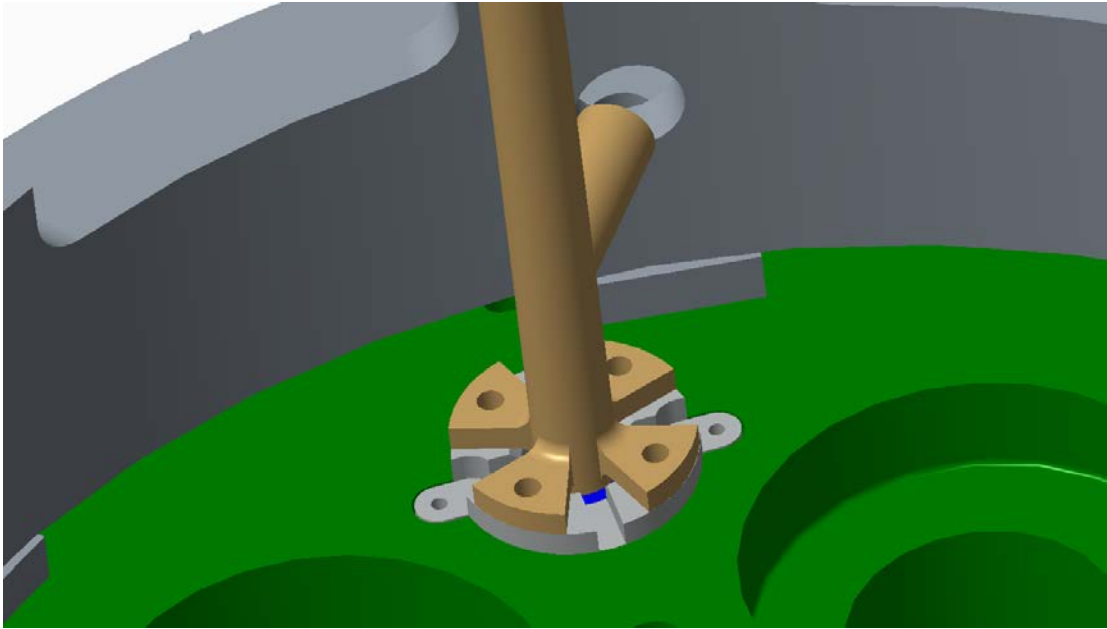


*Figure A.1: Close-Up of Modified Clouse Plug with Stand Pipe, Seal Head, and Hold  
Down Plates*

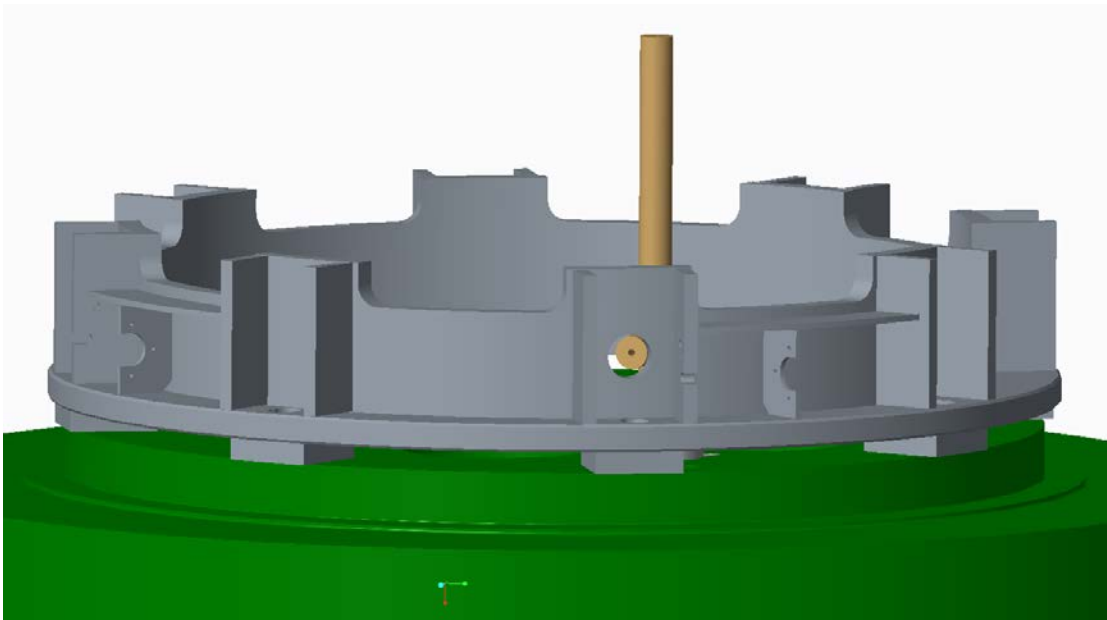


*Figure A.2: View of Modified Clouse Plug from Outside of Spool*

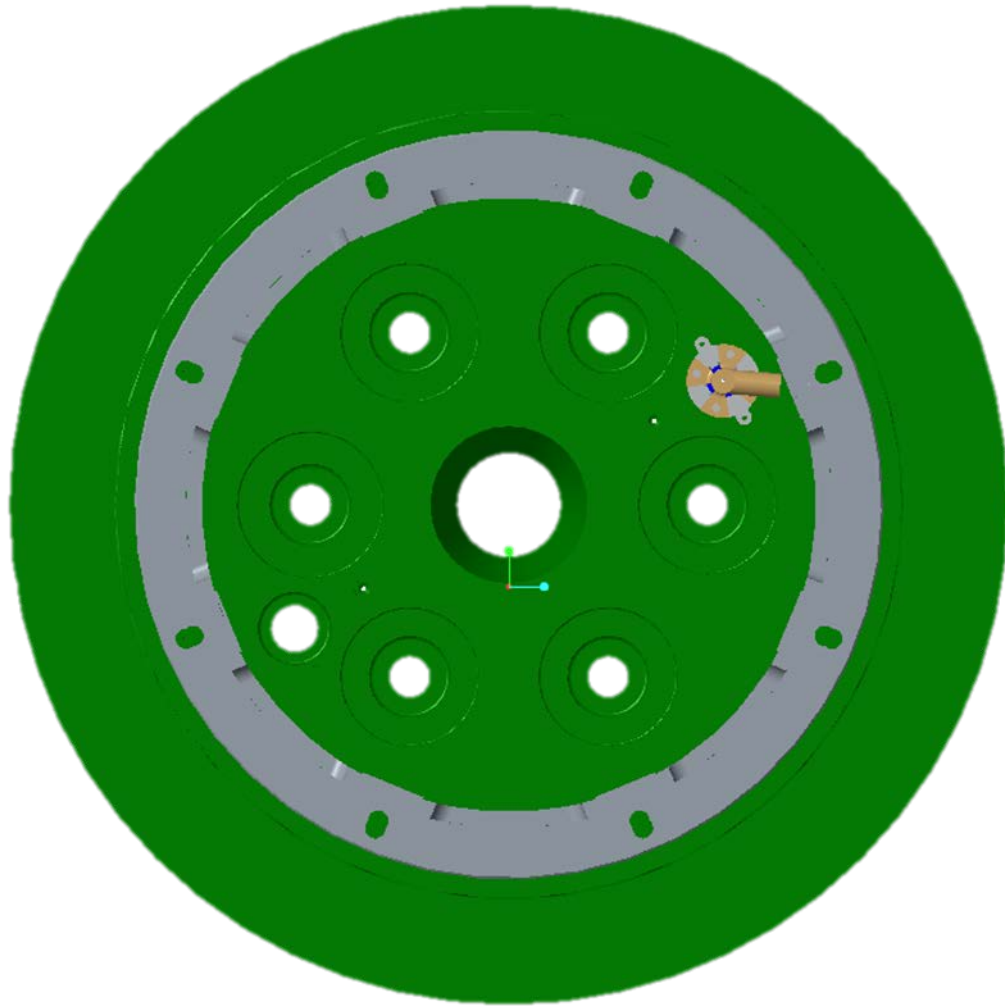


*Figure A.3: Top View of Modified Clouse Plug with Stand Pipe and Seal Head*

*A.3: Material Properties*

<b>AISI 4340 &amp; ASTM A723 Alloy Steel</b>				
Temperature (F)	Density (lbm in <sup>-3</sup> )			
70	0.284			
Temperature (F)	Coefficient of Thermal Expansion (F <sup>-1</sup> )			
68	6.83E-06			
482	7.61E-06			
932	8.06E-06			
Temperature (F)	Young's Modulus (psi)	Poisson's Ratio	Bulk Modulus (psi)	Shear Modulus (psi)
70	29700000	0.29	23571428.57	11511627.91
Temperature (F)	Tensile Yield Strength (psi)			
70	158800			
Temperature (F)	Tensile Ultimate Strength (psi)			
70	168100			
Temperature (F)	Thermal Conductivity (BTU s <sup>-1</sup> in <sup>-1</sup> F <sup>-1</sup> )			
70	0.000595174			
Temperature (F)	Specific Heat (BTU lbm <sup>-1</sup> F <sup>-1</sup> )			
70	0.114			

\* Properties from AISI and ASTM (UTS & YS from National Forge Data)

*Table A.3: AISI 4340 Alloy Steel – Material Properties*



<b>C-103 Niobium</b>				
Temperature (F)	Density (lbm in <sup>-3</sup> )			
70	0.32			
Temperature (F)	Coefficient of Thermal Expansion (F <sup>-1</sup> )			
70	3.80E-06			
200	3.80E-06			
400	3.90E-06			
600	3.90E-06			
800	4.00E-06			
1000	4.00E-06			
1200	4.10E-06			
1400	4.10E-06			
1600	4.20E-06			
1800	4.30E-06			
2000	4.40E-06			
2200	4.50E-06			
Temperature (F)	Young's Modulus (psi)	Poisson's Ratio	Bulk Modulus (psi)	Shear Modulus (psi)
68	13053391.27	0.38	18129710.1	4729489.591
2192	9282411.571	0.38	12892238.29	3363192.598
Temperature (F)	Tensile Yield Strength (psi)			
1200	27000			
Temperature (F)	Tensile Ultimate Strength (psi)			
1200	46000			
Temperature (F)	Thermal Conductivity (BTU s <sup>-1</sup> in <sup>-1</sup> F <sup>-1</sup> )			
70	0.000509259			
1600	0.000509259			
2035	0.000543981			
2380	0.000597222			
Temperature (F)	Specific Heat (BTU lbm <sup>-1</sup> F <sup>-1</sup> )			
70	0.082			

\* Properties from ATI Wah Chang

*Table A.4: C-103 Niobium – Material Properties*

<b>Glidcop AL-60 (UNS C15760)</b>				
Temperature (F)	Density (lbm in <sup>-3</sup> )			
70	0.318			
Temperature (F)	Coefficient of Thermal Expansion (F <sup>-1</sup> )			
70	9.20E-06			
300	9.20E-06			
Temperature (F)	Young's Modulus (psi)	Poisson's Ratio	Bulk Modulus (psi)	Shear Modulus (psi)
70	19000000	0.34	19791666.67	7089552.239
Temperature (F)	Tensile Yield Strength (psi)			
70	69000			
Temperature (F)	Tensile Ultimate Strength (psi)			
70	72000			
Temperature (F)	Thermal Conductivity (BTU s <sup>-1</sup> in <sup>-1</sup> F <sup>-1</sup> )			
68	0.004305556			
Temperature (F)	Specific Heat (BTU lbm <sup>-1</sup> F <sup>-1</sup> )			
70	0.092			

\* Properties from North American Höganäs High Alloys LLC

*Table A.5: Glidcop AL-60 (UNS C15760) – Material Properties*

<b>Inconel 625</b>				
Temperature (F)	Density (lbm in <sup>-3</sup> )			
70	0.305			
Temperature (F)	Coefficient of Thermal Expansion (F <sup>-1</sup> )			
70	7.10E-06			
200	7.10E-06			
400	7.30E-06			
600	7.40E-06			
800	7.60E-06			
1000	7.80E-06			
1200	8.20E-06			
1400	8.50E-06			
1600	8.80E-06			
1700	9.00E-06			
Temperature (F)	Young's Modulus (psi)	Poisson's Ratio	Bulk Modulus (psi)	Shear Modulus (psi)
70	30100000	0.278	22597597.6	11776212.83
200	29600000	0.28	22424242.42	11562500
400	28700000	0.286	22352024.92	11158631.42
600	27800000	0.29	22063492.06	10775193.8
800	26900000	0.295	21869918.7	10386100.39
1000	25900000	0.305	22136752.14	9923371.648
1200	24700000	0.321	22998137.8	9348978.047
1400	23300000	0.34	24270833.33	8694029.851
1600	21400000	0.336	21747967.48	8008982.036
Temperature (F)	Tensile Yield Strength (psi)			
70	60000			
Temperature (F)	Tensile Ultimate Strength (psi)			
70	120000			
Temperature (F)	Thermal Conductivity (BTU s <sup>-1</sup> in <sup>-1</sup> F <sup>-1</sup> )			
0	0.000123047			
69.8	0.000131072			
100.4	0.000135084			
199.4	0.000144447			
399.2	0.000167184			
600.8	0.000188583			
800.6	0.000209983			
1000.4	0.000234057			
1200.2	0.000254119			
1400	0.000278194			

1599.8	0.000304943			
1799.6	0.000337042			
Temperature (F)	Specific Heat (BTU lbm <sup>-1</sup> F <sup>-1</sup> )			
0	0.096			
70	0.098			
200	0.102			
400	0.109			
600	0.115			
800	0.122			
1200	0.135			
1400	0.141			
1600	0.148			
1800	0.154			
2000	0.16			

\* Properties from Special Metals Corporation

*Table A.6: Inconel 625 – Material Properties*

<b>Inconel 718</b>				
Temperature (F)	Density (lbm in <sup>-3</sup> )			
70	0.297			
Temperature (F)	Coefficient of Thermal Expansion (F <sup>-1</sup> )			
70	7.31E-06			
200	7.31E-06			
400	7.53E-06			
600	7.74E-06			
800	7.97E-06			
1000	8.09E-06			
1200	8.39E-06			
1400	8.91E-06			
Temperature (F)	Young's Modulus (psi)	Poisson's Ratio	Bulk Modulus (psi)	Shear Modulus (psi)
70	29000000	0.294642857	23536231.88	11200000
100	28800000	0.285714286	22400000	11200000
200	28400000	0.290909091	22637681.16	11000000
300	28000000	0.28440367	21645390.07	10900000
400	27600000	0.277777778	20700000	10800000
500	27100000	0.278301887	20373049.65	10600000
600	26700000	0.271428571	19468750	10500000
700	26200000	0.27184466	19139007.09	10300000
800	25800000	0.277227723	19302222.22	10100000
900	25300000	0.277777778	18975000	9900000
1000	24800000	0.278350515	18648062.02	9700000
1100	24200000	0.273684211	17821705.43	9500000
1200	23700000	0.288043478	18635897.44	9200000
1300	23000000	0.292134831	18441441.44	8900000
1400	22300000	0.311764706	19744791.67	8500000
1500	21300000	0.314814815	19170000	8100000
1600	20200000	0.328947368	19682051.28	7600000
1700	18800000	0.323943662	17797333.33	7100000
1800	17400000	0.338461538	17952380.95	6500000
1900	15900000	0.370689655	20493333.33	5800000
2000	14300000	0.401960784	24310000	5100000
Temperature (F)	Tensile Yield Strength (psi)			
70	150000			
Temperature (F)	Tensile Ultimate Strength (psi)			
70	180000			

Temperature (F)	Thermal Conductivity (BTU s <sup>-1</sup> in <sup>-1</sup> F <sup>-1</sup> )			
70	0.000152392			
200	0.000167824			
400	0.000192901			
600	0.000216049			
800	0.000239198			
1000	0.000262346			
1200	0.000285494			
1400	0.000310571			
1600	0.000333719			
1800	0.000358796			
2000	0.000383873			
Temperature (F)	Specific Heat (BTU lbm <sup>-1</sup> F <sup>-1</sup> )			
70	0.104			

\* Properties from Special Metals Corporation

*Table A.7: Inconel 718 – Material Properties*

<b>Nitrogen (Thermal Conductivity)</b>			
Temperature (F)	Density (lbm in <sup>-3</sup> )	Temperature (F)	Thermal Conductivity (BTU s <sup>-1</sup> in <sup>-1</sup> F <sup>-1</sup> )
0	0.026281521	0	1.75E-06
200	0.022530786	200	1.41E-06
400	0.019739591	400	1.26E-06
600	0.017593991	600	1.20E-06
800	0.015896008	800	1.18E-06
1000	0.014517752	1000	1.18E-06
1200	0.013374685	1200	1.20E-06
1400	0.012409725	1400	1.23E-06
1600	0.011582771	1600	1.27E-06
1800	0.010864561	1800	1.31E-06
2000	0.010234862	2000	1.35E-06
2200	0.009677056	2200	1.40E-06
2400	0.009179584	2400	1.45E-06
2600	0.008732328	2600	1.50E-06
2800	0.008328063	2800	1.55E-06
3000	0.007960649	3000	1.60E-06
Temperature (F)	Specific Heat (BTU lbm <sup>-1</sup> F <sup>-1</sup> )		
35.33	0.248159911		
80.33	0.248398756		
125.33	0.248398756		
170.33	0.248637601		
215.33	0.248876446		
260.33	0.249354136		
350.33	0.250548361		
440.33	0.252220275		
530.33	0.25436988		
620.33	0.25675833		
710.33	0.259385624		
800.33	0.262251764		
890.33	0.265117903		
980.33	0.267984043		
1070.33	0.270850182		
1160.33	0.273716322		
1250.33	0.276343616		
1340.33	0.278732066		
1430.33	0.281120515		
1520.33	0.283508965		
1610.33	0.285658569		
1700.33	0.287569329		
1790.33	0.289480089		

\* Properties from NIST REFPROP

Table A.8: Nitrogen (Thermal Conductivity) – Material Properties

A.4: Choked Flow Equation and Heat Transfer Correlations

$\dot{m} = \frac{p_0 A^*}{\sqrt{T_0}} \sqrt{\frac{\gamma}{R} \left( \frac{2}{\gamma + 1} \right)^{(\gamma+1)/(\gamma-1)}}$	Choked Flow Equation [3]
$f = (0.79 \ln(Re) - 1.64)^{-2}$	Petukhov Correlation [4]
$Nu = \frac{\left(\frac{f}{8}\right) (Re - 1000) Pr}{1 + 12.7 \left(\frac{f}{8}\right)^{1/2} (Pr^{2/3} - 1)}$	Gnielinski Correlation [4]
$Nu = 0.023 Re^{4/5} Pr^n$ <p><math>n = 0.3</math> for gas cooling      <math>n = 0.4</math> for gas heating</p>	Dittus-Boelter Correlation [4]
$Nu = 0.027 Re^{4/5} Pr^{1/3} \left( \frac{\mu}{\mu_w} \right)^{0.14}$ <p><math>\mu =</math> gas viscosity at bulk fluid temperature  <math>\mu_w =</math> gas viscosity at wall temperature</p>	Sieder-Tate Correlation [4]

Table A.9: Choked Flow Equation and Heat Transfer Correlations



A.5: Gas Heating Convective Heat Transfer Coefficient Calculation

<u>Reservoir Conditions</u>	
Pressure [psi]	2.700E+04
Temperature [deg F]	1.075E+03
Pressure [MPa]	1.862E+02
Temperature [deg K]	8.526E+02
Pressure [Pa]	1.862E+08
Density [kg/m <sup>3</sup> ]	4.174E+02
Enthalpy (hr) [kJ/kg]	1.061E+03
Enthalpy (hr) [J/kg]	1.061E+06
Gamma (cp/cv)	1.373E+00
Thermal Cond. [mW/m-K]	9.293E+01
Thermal Cond. [W/m-K]	9.293E-02
Viscosity [ $\mu$ Pa-s]	5.318E+01
Viscosity [Pa-s]	5.318E-05
Prandtl (Pr #)	7.022E-01
R [J/K-kg]	2.968E+02

<u>Choked Throat (Valve)</u>	
Number of Valves	2
Diameter [in]	<b>7.800E-02</b>
Diameter [m]	1.981E-03
Area [m <sup>2</sup> ]	3.083E-06
Total Area [m <sup>2</sup> ]	6.166E-06

<u>Flow Rates</u>	
Total Mass Flow Rate [kg/s]	1.552E+00
Mass Flow Rate Per Valve [kg/s]	7.760E-01
Mass Flow Rate Per Valve [lbm/s]	1.711E+00

<u>Wall Properties</u>	
Temperature [deg F]	1.000E+02
Temperature [deg K]	3.109E+02
Viscosity [ $\mu$ Pa-s]	7.719E+01
Viscosity [Pa-s]	7.719E-05

Properties from NIST REFPROP

**60VM9081(HT) - 0.078" Orifice (Inco 625 - 1100F Limit - 29.8 ksi Limit)**

<b>Pipe Conditions</b>	
Outer Diameter [in]	0.5625
Inner Diameter [in]	0.1875
Inner Diameter [m]	0.0047625
Hydraulic Diameter [m]	0.0047625
Area [m <sup>2</sup> ]	1.78139E-05
Velocity Per Piping System [m/s]	104.3558764

<b>Heat Transfer (Smooth Tubes)</b>							
Reynolds (Re #)	3.901E+06						
Darcy Friction Factor (Smooth Tubes Correlation - Petukhov)	9.336E-03						
Nusselt (Nu #) Gnielinski	3.516E+03	>	Convective Heat Transfer Coefficient (h) [W/m <sup>2</sup> -K]	6.860E+04	>	Convective Heat Transfer Coefficient (h) [BTU/s-in <sup>2</sup> -F]	2.331E-02
Nusselt (Nu #) Dittus-Boelter (n = 0.3 for Cooling of N <sub>2</sub> )	3.878E+03	>	Convective Heat Transfer Coefficient (h) [W/m <sup>2</sup> -K]	7.566E+04	>	Convective Heat Transfer Coefficient (h) [BTU/s-in <sup>2</sup> -F]	2.570E-02
Nusselt (Nu #) Sieder-Tate	4.270E+03	>	Convective Heat Transfer Coefficient (h) [W/m <sup>2</sup> -K]	8.332E+04	>	<b>Convective Heat Transfer Coefficient (h) [BTU/s-in<sup>2</sup>-F]</b>	<b>2.831E-02</b>

\*Used highest value for worst case scenario

Table A.10: Gas Heating Convective Heat Transfer Coefficient Calculation

A.6: Water Cooling Convective Heat Transfer Coefficient Calculation

<b>Cooling Ports (Water)</b>	
Inner Diameter [in]	3.750E-01
Outer Diameter [in]	5.000E-01
Inner Diameter [m]	9.525E-03
Outer Diameter [m]	1.270E-02
Hydraulic Diameter [m]	3.175E-03
Area of Annulus [m <sup>2</sup> ]	5.542E-05
Total Volumetric Flow Rate of City Water [Gallons per Minute]	10
Total Volumetric Flow Rate of City Water [m <sup>3</sup> per Second]	6.309E-04
Number of Cooling Ports	8
Volumetric Flow Rate of City Water per Cooling Port [m <sup>3</sup> per Second]	7.886E-05
Velocity in Annulus [m/s]	1.423E+00
Pressure [psi]	50
Temperature [deg F]	78
Pressure [MPa]	3.447E-01
Temperature [deg K]	2.987E+02
Density [kg/m <sup>3</sup> ]	9.970E+02
Thermal Cond. [mW/m-K]	6.076E+02
Thermal Cond. [W/m-K]	6.076E-01
Viscosity [ $\mu$ Pa-s]	8.788E+02
Viscosity [Pa-s]	8.788E-04
Prandtl (Pr #)	6.047E+00

Properties from NIST REFPROP

<b>Heat Transfer (Smooth Tubes)</b>							
Reynolds (Re #)	5.126E+03						
Darcy Friction Factor (Smooth Tubes Correlation - Petukhov)	3.832E-02						
Nusselt (Nu #) Gnielinski	3.933E+01	>	Convective Heat Transfer Coefficient (h) [W/m <sup>2</sup> -K]	7.526E+03	>	<b>Convective Heat Transfer Coefficient (h) [BTU/s-in<sup>2</sup>-F]</b>	<b>2.557E-03</b>

\*Use Gnielinski due to Re range

Table A.11: Water Cooling Convective Heat Transfer Coefficient Calculation

*A.7: Static Structural – Closure Plug Boundary Conditions*

<b><u>Blow-Off Force</u></b>	
Pressure Load (PSI)	27000
Diameter of Connector Pipe End Plate (in <sup>2</sup> )	3.712
Area of Connector Pipe (in <sup>2</sup> )	1.082E+01
Total Blow-Off Load on CP (lbf)	2.922E+05
<b>Blow-Off Load on Quarter Model CP (lbf)</b>	<b>7.305E+04</b>
<b><u>Gas Pressure</u></b>	
Pressure Load (PSI)	27000
Heater Closure Plug Outer Diameter (in)	24
Heater Closure Plug Inner Diameter (in)	3.188
Area on Top of Closure Plug (in <sup>2</sup> )	4.444E+02
Force Acting on Top of Closure Plug (lbf)	1.200E+07
<b><u>Elastic Foundation Stiffness</u></b>	
Total Force on Closure Plug (lbf)	1.229E+07
Heater Nut Outer Diameter (in)	27.5
Heater Nut Inner Diameter (in)	25.1
Contact Area between Nut & Closure Plug (in <sup>2</sup> )	9.915E+01
Expected Displacement ( $x_{efs}$ ) (in)	0.125
<b>Elastic Foundation Stiffness (EFS) (lbf/in<sup>3</sup>)</b>	<b>9.917E+05</b>
$EFS = \frac{Total\ Force}{(Expected\ Displacement)(Contact\ Area)}$	

*Table A.12: Blow-Off Force and Elastic Foundation Stiffness Calculation*

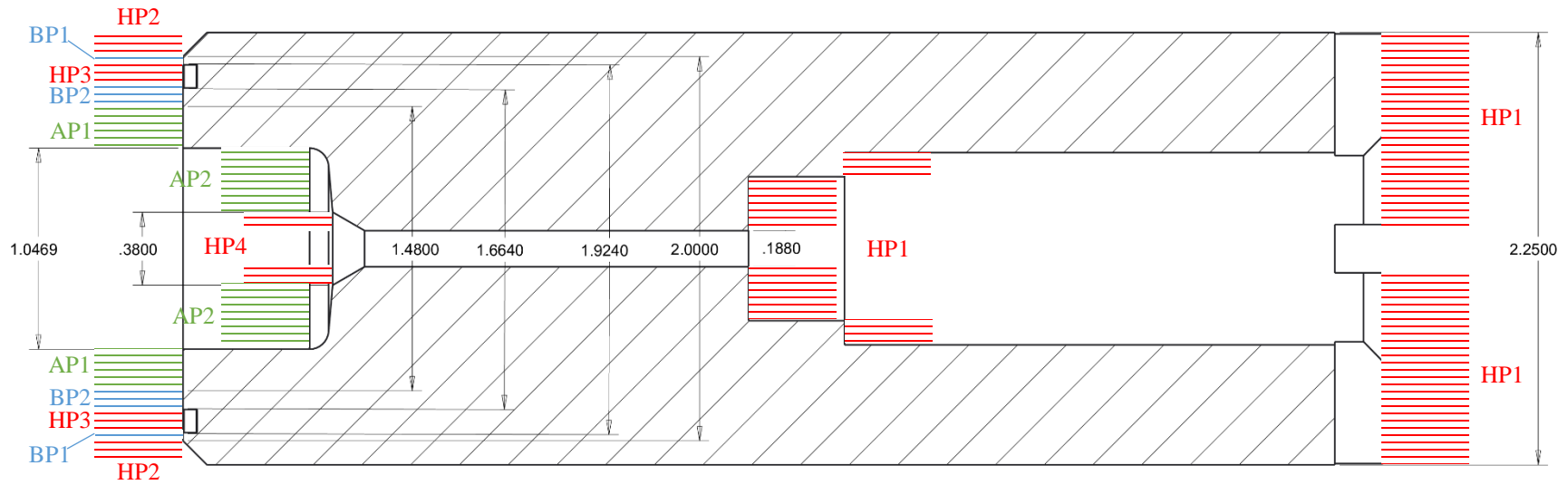


Figure A.4: Seal Head Bearing Pressure Diagram

Heater Pressure (psi)	27000			
Heater Pressure 1 (HP1) Area (in <sup>2</sup> )	3.9483			
Heater Pressure 2 (HP2) Area (in <sup>2</sup> )	0.8345			
Heater Pressure 3 (HP3) Area (in <sup>2</sup> )	0.7327			
Heater Pressure 4 (HP4) Area (in <sup>2</sup> )	0.08565			
Atmospheric Pressure 1 (AP1) Area (in <sup>2</sup> )	0.8596			
Atmospheric Pressure 2 (AP2) Area (in <sup>2</sup> )	0.7473			
Bearing Pressure 1 (BP1) Area (in <sup>2</sup> )	0.2342	→	$\Sigma Forces = 0$	
Bearing Pressure 2 (BP2) Area (in <sup>2</sup> )	0.4543		Bearing Pressure (psi)	89975.55
			Pressure Ratio (Bearing Pressure/Heater Pressure)	3.3324

Table A.13: Seal Head Bearing Pressure Calculation

## Bibliography

- [1] J. F. Lafferty *et al.*, "The hypervelocity wind tunnel no. 9; continued excellence through improvement and modernization," *53rd AIAA Aerospace Sciences Meeting*, Jan. 2015.
- [2] H. V. Atkinson and S. Davies, "Fundamental aspects of hot isostatic pressing: An overview," *Metallurgical and Materials Transactions A*, vol. 31, no. 12, pp. 2981–3000, Dec. 2000.
- [3] Anderson, J. D., 2011, *Fundamentals of Aerodynamics*, 5th ed., McGraw-Hill, New York, NY.
- [4] Bergman, T. L., Lavine, A.S., Incropera, F.P., and Dewitt, D.P., 2011, *Fundamentals of Heat and Mass Transfer*, 7th ed., John Wiley & Sons Inc., Hoboken, NJ.